A Comparative Study on Physiological Responses to Drought in Wild *Vitis* Species

By

MIRIAM KALTENBACH

THESIS

Submitted in partial satisfaction of the requirements for the degree of

MASTER OF SCIENCE

in

Viticulture and Enology

in the

OFFICE OF GRADUATE STUDIES

of the

UNIVERSITY OF CALIFORNIA

DAVIS

Approved:

_____

Elisabeth J Forrestel, Chair

_____

Andrew J McElrone

_____

Luis Diaz-Garcia

Committee in Charge

2023

CONTENTS

LIST OF FIGURES

LIST OF TABLES

List of Supplementary Tables

ABSTRACT

Context and purpose of the study:

Crossings of three wild *Vitis* species are commonly used worldwide as rootstocks in grape production. Disease resistance and vigor are among the most important factors for their selection. With climate change resulting in increasing water limitations, finding rootstocks conferring increased tolerance to drought will be of great importance as well. Therefore, identifying *Vitis* species with improved drought tolerance, and incorporating them into breeding programs could contribute to more resilient rootstocks under water-limiting conditions. Furthermore, these species will serve as valuable resources for increasing the genetic variation of the current rootstocks available. Investigating the leaf physiology of these species is pivotal, potentially offering valuable insights into their adaptive mechanisms under drought stress. We hypothesized that species native to drier habitats would exhibit a superior physiological performance under drought stress.

Materials and methods:

The root and canopy physiological characteristics, and the anatomical and biochemical bases of photosynthetic capacity of nine North American wild *Vitis* species across a wide latitudinal range (New England through Mexico) under two soil moisture treatments (controlled dry down (20–40% w/w 'drought') and maintained irrigated (70–90% w/w 'control')), were evaluated using a whole-plant experimental approach. We investigated the links between leaf structural diversity and physiological features that enhance photosynthetic capacity under controlled, non-stressed conditions and whether these relationships are upheld under prolonged water stress. Experiments were performed in a greenhouse under ambient atmospheric conditions using clonal and non-grafted saplings. Physiological parameters measured throughout the experiment included midday and predawn leaf water potentials, leaf gas exchange, root and leaf biomass, and spectral measurements. Additionally, X-ray imaging of plant tissues was performed at a single time point mid-experiment, and manual segmentation was used to prepare images for auto-segmentation using machine learning algorithms. Linear regression models were used to describe the relationships between anatomical and physiological variables, and their associations with biogeoclimatic variables.

Results and discussion:

Our data shows the impact of drought treatment and indicated differential responses to drought stress across species. Furthermore, structural differences that drive photosynthetic responses were observed. Elucidating canopy traits associated with improved performance under drought conditions could facilitate the rapid screening of germplasms to develop drought-tolerant rootstocks in the future.

Keywords: *Vitis*, grapevines, water-use efficiency, water stress, drought tolerance

ACKNOWLEDGMENTS

I express my sincere gratitude to Dr. Elisabeth Forrestel, my advisor. Her belief in my capabilities pushed me beyond my expectations, enabling me to complete this thesis.

I would also like to express my appreciation to Dr. Andrew McElrone and Dr. Luis Diaz-Garcia for their valuable advice, encouragement, and constructive critiques, which significantly improved this work.

I am thankful to Dr. Mina Momayyezi's meticulous mentorship and the dedicated assistance provided by the members of the Forrestel and McElrone labs, who supported me through my research.

I am deeply indebted to my incredible family and friends (back home and in the US) and Dr. Heymann, whose unwavering support has been the bedrock of my accomplishments. This journey and my time at UC Davis would not have been possible without their support.

Finally, I would like to thank the Graduate Group of the Department of Viticulture and Enology and my classmates for making this time special.

1 | INTRODUCTION

Grapevine is among one of the most important horticultural crops worldwide, and most wine-growing regions are located in the Mediterranean climate, which is characterized by dry and hot summers. As water enables vines to maintain essential physiological processes, and limited water availability can negatively affect vine health and yield, it is considered a key limiting factor in agriculture (Serra et al., 2014; Tomás et al., 2014b). Generally, *Vitis vinifera*, subsp. *vinifera*,, the most renowned and planted species, is considered relatively heat and drought-tolerant (Serrano et al., 2022), however, the majority of vineyards, especially in Europe, are not irrigated and water resources are becoming increasingly limited (Costa et al., 2016). Drought stress triggers various physiological and biochemical reactions in plants. There are many strategies that vines can develop to deal with drought. However, most grapevines appear to avoid water stress through adaptive mechanisms (Chaves et al., 2010). From an agronomic perspective, adaptation should be understood as the capacity to uphold both yield and fruit ripening when faced with water limitations (Serra et al., 2014). Hence, in the context of viticulture, drought tolerance should encompass the dual capability of sustaining productivity during the present growing season, preventing adverse carry-over effects, and potentially the mortality caused by drought over multiple seasons (Gambetta et al., 2020). Climate change exacerbates water scarcity issues and further increases the risk of more severe and frequent droughts increases (Schultz, 2000; IPCC, 2022). As the wine industry faces these challenges, it is important to further increase the resilience of vineyards by finding multiple strategies to adapt to a changing climate. A potential approach would be to further explore the genetic diversity of the genus *Vitis* and gain a better understanding of the mechanisms underlying plant responses to drought (Serra et al., 2014). It is crucial to understand and investigate the potential of drought tolerance in existing *Vitis* species because increased drought tolerance aligns with sustainable vineyard practices by reducing water consumption and reliance on irrigation. With increased climate variability and unpredictable and irregular rainfall patterns, drought-tolerant species can provide a buffer against fluctuations in water availability, enabling vines to withstand drought periods and recover more efficiently when water becomes available. *Vitis* species that are more drought-tolerant possess complex traits that allow them to use water more efficiently and adapt to drought conditions through comprehensive changes in their physiological, biochemical, and genetic characteristics (Larcher, 2003). Since the North American pest phylloxera *(Daktulosphaira vitifoliae)* was imported into Europe and destroyed own-rooted *V. vinifera*, wild *Vitis* species have

been used as rootstocks because they are mostly resistant to these insects. Today, these rootstocks are not only selected based on their pest resistance, but also on other characteristics such as their adaptation to soil chemistry, vigor, rooting depth, and increased interest in their tolerance to abiotic soil-borne problems such as drought or salinity (Dry, 2007; Granett et al., 1983). They are considered key elements in the adaptation to climate change (Serra et al., 2014). More than 80% of vineyards worldwide are planted on rootstocks of North American species or interspecific hybrids of *Vitis* species that combine desirable characteristics (Ollat et al., 2016). Keller (2010) claimed that the genetic background of these rootstocks is very limited, as it is estimated that 90% of the parentage of rootstocks worldwide originates from less ten different rootstock cultivars. In a study conducted by Riaz et al. (2019), it was revealed that 39% of the examined rootstocks could be traced back to only three accessions of three grape species. Having mostly *Vitis riparia*, *Vitis rupestris*, and *Vitis berlandieri* in our toolbox is minimal, and it is important to expand this and investigate the traits that North American *Vitis* species offer even further. These species have unique characteristics and traits that make them valuable resources for improving the grapevine cultivation and sustainability. Although many studies have focused on drought tolerance among grapevine genotypes of *Vitis vinifera* and characterized key agronomic indicators, such as fruit quality, yield or growth under drought conditions (Gambetta et al., 2020), only limited research has been conducted on the potential of wild *Vitis* species, and knowledge about the mechanisms of drought is still very scarce (Ollat et al., 2023). North American species of *Vitis* originate from distinct native ecosystems. While most grow close to a permanent water source, some grow in dry and rocky zones. Unfortunately, limited research has been conducted on the ecological attributes of these habitats. Specific environmental conditions and the behavior of *Vitis* species in their habitat have not been adequately documented during plant collection (Pap et al., 2015; Arnold and Schnitzler, 2020). When studying biogeographical parameters and describing the environmental characteristics of three *Vitis* species (*V. berlandieri*, *V. rupestris*, and *V. riparia*), Morano and Walker (1995) found that their specific habitats reflect their adaptation to environmental conditions as they grow across diverse climates, including regions with hot and dry summers, cold winters, and variable precipitation patterns. The ability of these species to thrive in such environments highlights their potential to impart climate resilience to cultivated grapevines (Padgett-Johnson et al., 2003). As up to 28 species are native to the eastern and southwestern US and Mexico (Kikkert et al., 2001), they offer a rich source of genetic diversity. Therefore, Ollat et al. (2023) emphasized the significant potential of identifying adapted genotypes and favorable alleles in challenging environments.

Natural selection, with its extensive testing of gene combinations under various environmental pressures, has played a role in shaping wild species that have long occupied local niches with adaptive improvements that are not comparable to any testing in plant breeding programs (Lasky et al., 2012; Cortés and López-Hernández, 2021). These distinct environmental forces, driven by different climatic conditions, may have contributed to the adaptation of the insular subpopulations (Blois et al., 2023). Typically, adaptation is linked to multiple traits, such as morphological, physiological, anatomical, and biochemical characteristics in a specific environment (Ollat et al., 2023).

This study focused on the physiological and morphological responses to drought and the anatomical adaptation strategies of North American *Vitis* to identify species with higher drought tolerance. The nine species were selected based on their geographical distribution, as they distribute over a wide latitudinal range from New England to Mexico, capturing variations in climate, including temperature, rainfall patterns, and water availability. Historical climate data from the original collection sites of georeferenced germplasm accessions can be used to investigate local adaptations to abiotic stresses and environments (Cortés and López-Hernández, 2021; Briscoe Runquist et al., 2020). Representation of various native climatic conditions offers diverse responses to drought stress. We hypothesized that species native to drier habitats would exhibit a superior physiological performance under drought stress. In addition, the nine selected species exhibited significant genetic variability. By studying species with diverse genetic backgrounds, the next step is to gain insights into the genetic basis of drought tolerance and to identify potential sources of resilience for breeding programs (Blois et al., 2023). Lastly, the selected species have been previously used for rootstock breeding; therefore, it is important to investigate the physiological responses to drought and anatomical adaptation strategies under water-limiting conditions.

2 | MATERIALS AND METHODS

TABLE 1 List of traits and variables used

Variable	Definition	Unit
A_n	Net assimilation rate	μmol CO_2 m^{-2} s^{-1}
A_{max}	Maximum assimilation rate at saturating CO_2	μmol CO_2 m^{-2} s^{-1}
C_i	Intercellular airspace CO_2 concentration	μmol mol s^{-1}
C_i^*	Intercellular CO_2 photocompensation point	μmol mol s^{-1}
E	Transpiration rate	mmol m^{-2} s^{-1}
g_m	Mesophyll conductance	mol CO_2 m^{-2} s^{-1}
g_s	Stomatal conductance	mol m^{-2} s^{-1}
J_{max}	Maximum rate of electron transport	
L_{leaf}	Leaf thickness	μmol
L_{mes}	Mesophyll thickness	μmol
$SA_{pa\text{-}cell}/SA_{mes\text{-}cell}$	Ratio of palisade cell surface area to total mesophyll cell surface area	m^2 m^{-2}
$SA_{sp\text{-}cell}/SA_{mes\text{-}cell}$	Ratio of spongy cell surface area to total mesophyll cell surface area	m^2 m^{-2}
$SA_{pa\text{-}cell+sp\text{-}cell}/SA_{mes\text{-}cell}$	Ratio of palisade and spongy cell surface area to total mesophyll cell surface area	m^2 m^{-2}
T_{leaf}	Leaf temperature	°C
TPU	Rate of triose phosphate use	
V_{cmax}	Maximum carboxylation rate at saturating CO_2	
$V_{pa\text{-}cell}/V_{mes\text{-}cell}$	Ratio of palisade cell volume to total mesophyll cell volume	m^3 m^{-3}
$V_{sp\text{-}cell}/V_{mes\text{-}cell}$	Ratio of spongy cell volume to total mesophyll cell volume	m^3 m^{-3}
$V_{sp\text{-}cell}/V_{pa\text{-}cell}$	Ratio of spongy cell volume to palisade cell volume	m^3 m^{-3}
WUE_i	Intrinsic water use efficiency (A_n/g_s)	μmol CO_2 mol^{-1} H_2O
WUE_{inst}	Instantaneous water use efficiency (A_n/E)	μmol CO_2 mol^{-1} H_2O
Ψ_{MD}	Midday leaf water potential	MPa
Ψ_{PD}	Predawn leaf water potential	MPa
R_d	Dark respiration	μmol m^{-2} s^{-1}
θ_{IAS}	Mesophyll porosity	m^3 m^{-3}

2.1 | Plant materials and growth conditions

Ten cuttings per accession (n = 90 total) of the nine *Vitis* species listed in Table 2 were taken from the University of California Breeding Collection. After soaking the basal node of each cutting in auxin root solution (Earth Science Products), it was stored for 21 days in a tray with vermiculite in a mist room. When roots were initiated, the cuttings were planted in 7.5 L pots containing a 1:1 sand-to-peat mix with vermiculite at the bottom as the growth substrate. The clonal and non-grafted saplings were grown at the Core Greenhouses Complex at the University of California, Davis, under supplemental lighting (minimum photosynthetic active radiation (PAR) = 400 μmol m^2s^{-1}) for a 14-hour photoperiod, with a maximum temperature of 30°C during the day and 25°C during the night. Over 35 days, plants were watered with Hoagland's solution to establish the plants. Subsequently, the method of Bartlett et al. (2021) was used to perform a controlled dry-down during an experimental period of four weeks. All pots were equally treated during the establishment period. To reach the target weight of 80% of the saturated pot weight plus half of the pot evapotranspiration, the pots were weighed, and water was applied three times per week to reach an average soil water content of approximately 80% of the saturated pot weight between the waterings. Water was added until drainage was visible to determine the saturated weight per pot. The pot was weighed once the drainage stopped and excessive water was lost.

The difference in pot weights between watering days was set as the plant evapotranspiration (E_{plant}) and was measured using the pot-saturated weight at the start of both periods.

After the establishment period, a randomized complete block design was used to assign five vines per accession to one of the two watering treatments. The watering treatment during the establishment period was continued for well-watered plants, whereas the remaining half of the vines were exposed to water stress. These plants were re-watered to 40% of the saturated pot mass, in addition to half of the pot evapotranspiration under the new watering treatment. Each block was equipped with an empty reference pot to account for soil evaporation. New E_{plant} values were calculated after withholding water from the vines for 14 days in the controlled dry-down until the pots reached 20-40% of the saturated pot mass. As shown in Figure 2, the treatments were conducted for an additional 26 days.

2.2 | Photosynthesis measurements

The major measurements were taken three times during the experiment. At the end of the establishment period (8 weeks after the cuttings were taken), 2 weeks after the beginning of the two different treatments, when leaves for segmentation were also collected, and at the end of the experiment, immediately before harvesting for biomass. Photosynthetic measurements, such as the net assimilation rate (A_n) (see Table 1 for symbol definitions), stomatal conductance (g_s), and intercellular airspace CO_2 concentration (C_i), were obtained from the youngest fully expanded leaves between 11am and 1pm using a LICOR-6800 gas exchange system. The ambient chamber CO_2 (C_a) was set to 400 μmol mol^{-1} with a fan speed of 10,000rpm, leaf temperature was maintained at 25°C, and all measurements were performed under a photosynthetic photon flux density (PPFD) of 1400 μmol $m^{-2}s^{-1}$. The intrinsic water use efficiency (WUE_i) was calculated using A/g_s and instantaneous water use efficiency (WUE_{inst}) was calculated using A/E in four replications per accession and treatment (Hatfield and Dold, 2019).

2.3 | CO_2 response curves

A-C_i curves were constructed for three representative individuals of each species and treatment to obtain a better understanding of differences in photosynthetic responses among the accessions. The sample CO_2 concentrations were 400, 50, 80, 100, 150, 200, 250, 400, 500, 600, 700, 800, 900, 1200, 1400 μmol $m^{-2}s^{-1}$ and PPFD was at 1200 μmol $m^{-2}s^{-1}$. To estimate the rate of photosynthetic electron transport (J), the maximum assimilation rate at saturating CO_2 (V_{cmax}) allowed for RuBisCO, and dark respiration (R_d), the photosynthetic model by Sharkey (2016) was used to fit the A-C_i curves.

2.4 | Water potential measurements

A pressure chamber was used to measure the leaf water potentials. predawn leaf water potential (Ψ_{PD}) was measured between 4 am and 6 am before sunrise and midday leaf water potential (Ψ_{MD}) was measured between 11 am and 1 pm. Leaves similar to those used for gas exchange measurements were chosen from each accession in 3 replications. The leaves were covered with a plastic bag for 10-15 to allow equilibration, and petioles were then cut using a razor blade and placed inside the pressure chamber. The gasket pressure was slowly increased until a water meniscus began to form, and a balanced pressure was reached and recorded.

2.5 | Vegetative growth

At the end of the experiment, most plants were harvested for root and canopy biomasses. The primary shoots were cut 5 cm above the soil line and, together with the lateral shoots, weighed for fresh canopy biomass. Roots were carefully extracted from the pot, filtered through a mesh sieve, and then rinsed in a container of water to eliminate any attached soil particles. The root biomass was quantified by weighing.

2.6 | X-ray micro computed tomography imaging, segmentation, and mesophyll traits

The leaves used for gas exchange measurements were collected for scanning. The leaves were bagged and kept cool until scanning at the Lawrence Berkeley National Laboratory (LBNL) Advanced Light Source (ALS) on the day of collection. A 5 mm wide and 10 mm long segment was carefully extracted from the central area of each plant's leaf lamina, and the same region where the A-C_i curves were recorded, which was then sandwiched between two pieces of Kapton tape (ULINE) to prevent moisture loss during X-ray scanning. The prepared samples were positioned within the tip of a pipette and subjected to continuous tomography scanning at 21 keV for a duration of 15 minutes, utilizing a 10× objective lens with a pixel resolution of 0.65 µm and then reconstructed as described by Rippner et al. (2022). As four replicates (leaves) were stacked above each other during the imaging, the grid was cropped, and 500 consecutive slices from the reconstructed 1000-image stack of each replicate were selected for further analysis using ImageJ. The stacks were changed from 32 to 8 bit greyscale and prepared for segmentation. Whole leave, adaxial and abaxial epidermis, whole mesophyll, palisade mesophyll, spongy mesophyll bundle sheath extensions, and veins were manually segmented following Théroux-Rancourt et al. (2020). The airspace within the leaf was segmented by thresholding between the minimum and maximum grayscale values and then manually cleaned.

Representative hand-labeled slices were then used to train and test for auto-segmentation using machine learning algorithms (Rippner et al., 2022).The algorithm was trained individually according to species and treatment (n=24 each).

Leaf and mesophyll traits

The same six slices were used to manually measure the leaf thickness (L_{leaf}) and mesophyll thickness (L_{mes}).

As described by Théroux-Rancourt et al. (2017), Mesophyll porosity (θ_{IAS}) was calculated by determining the intercellular airspace (V_{IAS}) volume as a proportion of the total mesophyll volume ($V_{\text{mes-cell}}$). The spongy cell volume to

total mesophyll cell volume ($V_{sp\text{-}cell}$/ $V_{mes\text{-}cell}$), palisade cell volume to total mesophyll cell volume ($V_{pa\text{-}cell}$/ $V_{mes\text{-}cell}$) and spongy cell volume to palisade cell volume ($V_{sp\text{-}cell}$/ $V_{pa\text{-}cell}$) ratio were calculated as described by Momayyezi et al. (2022a), and the palisade cell surface area to total mesophyll cell surface area ($SA_{pa\text{-}cell}$/ $SA_{mes\text{-}cell}$), spongy cell surface area to total mesophyll cell surface area ($SA_{sp\text{-}cell}$/ $SA_{mes\text{-}cell}$) and palisade and spongy cell surface area to total mesophyll cell surface area ($SA_{pa\text{-}cell+sp\text{-}cell}$/ $SA_{mes\text{-}cell}$).

2.7 | Climate data for accessions' native habitats

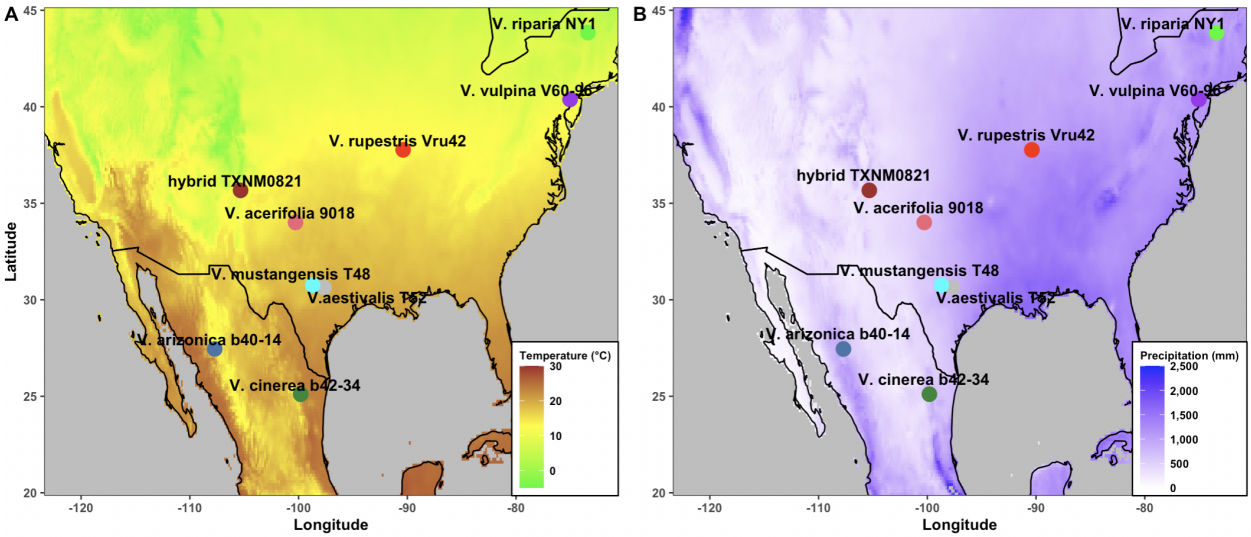

FIGURE 1 Geographic distribution map for 9 *Vitis* accessions with (A) mean annual temperature and (B) annual precipitation climate data for North America.

TABLE 2 *Vitis* species and genotypes used in the study, coordinates of collection location, and climate data of their native habitat.

Species	Genotype	Lat	Long	T (°C)	P (mm)	T CV (°C/100)	T_{CQ} (°C)
V. acerifolia	9018	34.00830	-100.28200	16.5	565	853.6	5.2
V. aestivalis	T52	30.63270	-97.67720	19.2	837	705.0	9.8
V. arizonica	b40-14	27.45250	-107.71200	15.5	891	438.6	9.9
V. cinerea	b42-34	25.10855	-99.80620	22.1	849	516.0	15.1
V. mustangensis	T48	30.75920	-98.70030	18.8	701	720.9	9.1
V. riparia	NY1	43.84172	-73.38702	7.2	919	996.8	-6.3
hybrid (*V. riparia* x *V. arizonica*)	TXNM0821	35.66890	-105.33610	6.7	526	667.1	-1.5
V. rupestris	Vru42	37.76774	-90.38350	12.4	1105	892.4	0.4
V. vulpina	V60-96	40.38058	-75.03229	10.7	1172	877.0	-0.8

T, Annual Mean Temperature; P, Annual Precipitation; TCV, Temperature Seasonality; T_{CQ}, Mean Temperature of Coldest Quarter.

The coordinates of the native habitat of each accession were extracted from the breeding collections of the University of California. For each habitat, bioclimatic variables, such as annual mean temperature (AMT), annual precipitation (P), and temperature seasonality (TCV), were obtained from the WorldClim dataset, as shown in Table 2 and Figure 1 (Fick and Hijmans, 2017).

2.8 | Statistics

RStudio (RStudio Team, 2020) was used to analyze the data and generate figures and tables (see Kaltenbach (2023) for repository). Analysis of variance with the main factors "species" and "treatment" was performed to determine the p-values for each physiological and anatomical trait. To perform post-hoc analysis, Tukey's HSD was employed for all pair-wise comparisons. Statistically significant results of the treatment are indicated by * on the figures for α <0.05. Pearson's correlation coefficients of the mean values for the parameters per species separated by treatment were used to investigate relationships between biogeoclimatic variables and physiological and morphological parameters.

3 | RESULTS

This study examined various *Vitis* species and genotypes within their native habitats, focusing on their climatic characteristics. The results revealed substantial climate variability among these genotypes, with latitude (Lat) playing a significant role in influencing ecological and physiological responses. annual mean temperature exhibited a broad range, with the highest recorded in *V. cinerea* (b42-34) (22.1°C) and the lowest recorded in *V. riparia* (NY1) (7.2°C). annual precipitation showed marked differences, with the greatest precipitation occurring in *V. rupestris* (Vru42) (1105 mm) and *V. vulpina* (V60-96), which experiences relatively high rainfall (1172 mm). *V. acerifolia* (9018), which receives approximately 565 mm of rainfall annually, and the hybrid (TXNM0821) which receives 526 mm of rainfall had the lowest precipitation across the species. temperature seasonality varied significantly across genotypes, and latitude appeared to influence this parameter, particularly in *V. riparia* (NY1), which had the highest seasonality (996.8). The mean temperature of the coldest quarter (T_{CQ}) ranged from a peak of 15.1°C in *V. cinerea* (b42-34) to a low of -6.3°C in *V. riparia* (NY1).

3.1 | Soil moisture and plant water relationships

Drought treatment

The control and drought conditions imposed during the potted vine dry-down experiment were evaluated using soil moisture and physiological measurements. Drought treatments led to a significant decrease in pot water content across all species, although there was some variation among species and over time. (see Figure 2). The soil moisture of the control ranged from 65% to 95% at all times, with the majority of the days being above 75% . The drought-treated pots had water contents between 5% and 30% after the beginning of the 14-day dry-down period. Most of the time, stressed plants had a soil moisture content between 20% and 30%, as expected in the experimental design.

Water potentials

Cell expansion and plant growth rely directly on turgor pressure, which is one of the earliest indicators of water stress in plants. Measurements of vine water status (Ψ_{MD} and Ψ_{PD}) indicated the impact of drought treatment in terms of water stress, as the majority of the species demonstrated a notable decrease during the later phases of the experiment (Figures 3 & 4). Even under controlled conditions, Ψ_{MD} showed differences across the species, with *V. vulpina* (V60-96) and the

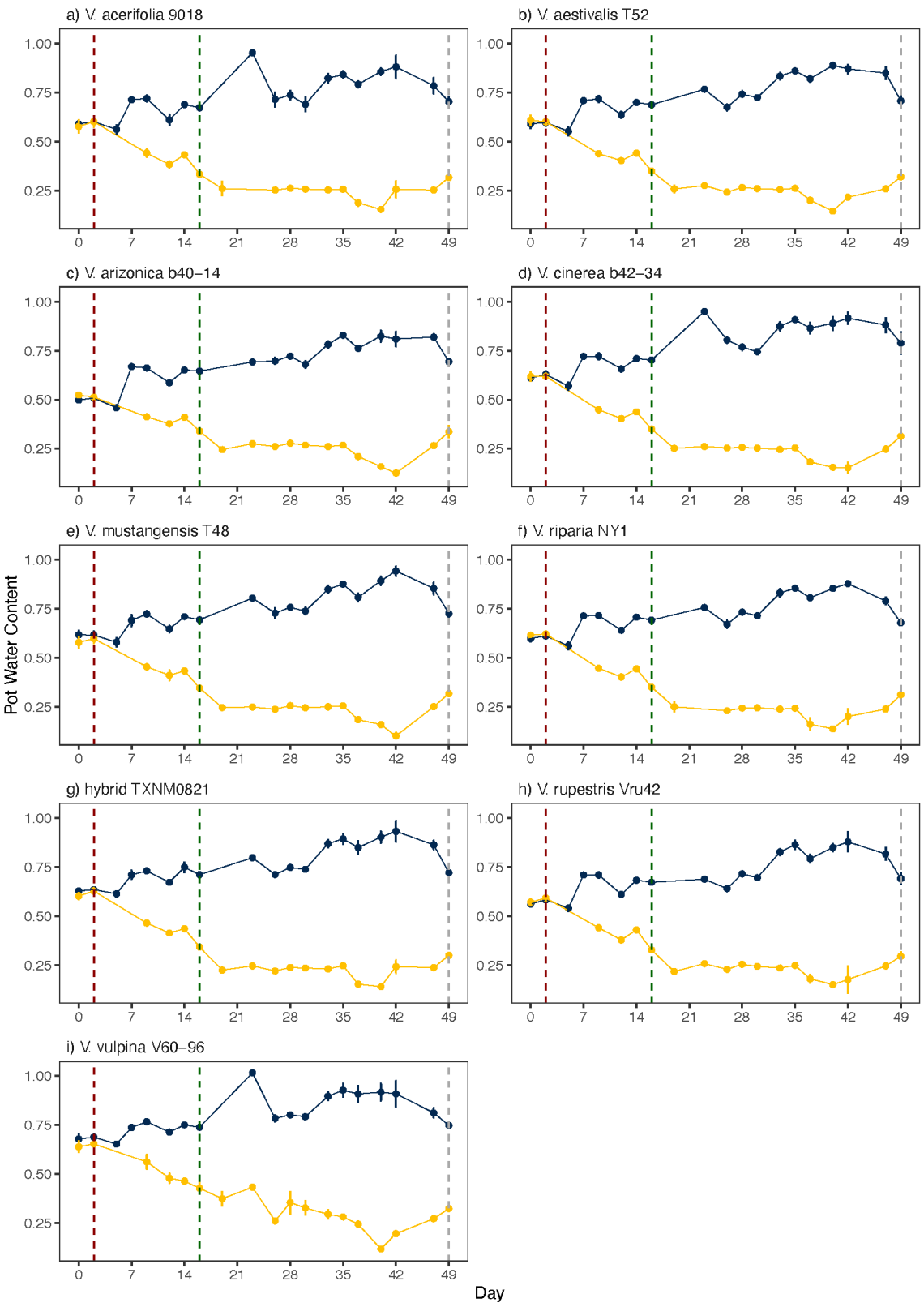

FIGURE 2 Pot water contents (i.e., pot weights normalized by saturated pot weights) over the experimental period for each of the 9 *Vitis* accessions. Blue points represent well-watered plants and yellow points represent water-stressed plants. Dashed lines mark major measurement dates, red indicates the beginning of the drought treatment (day 2), green indicates when leaves were taken for segmentation (day 16), and grey represents the end of the experiment (day 49). Well-watered plants were watered to 80% of the saturated pot weight, and water-stressed plants to 20-30% of the saturated weight. Error bars show standard errors. N = 5.

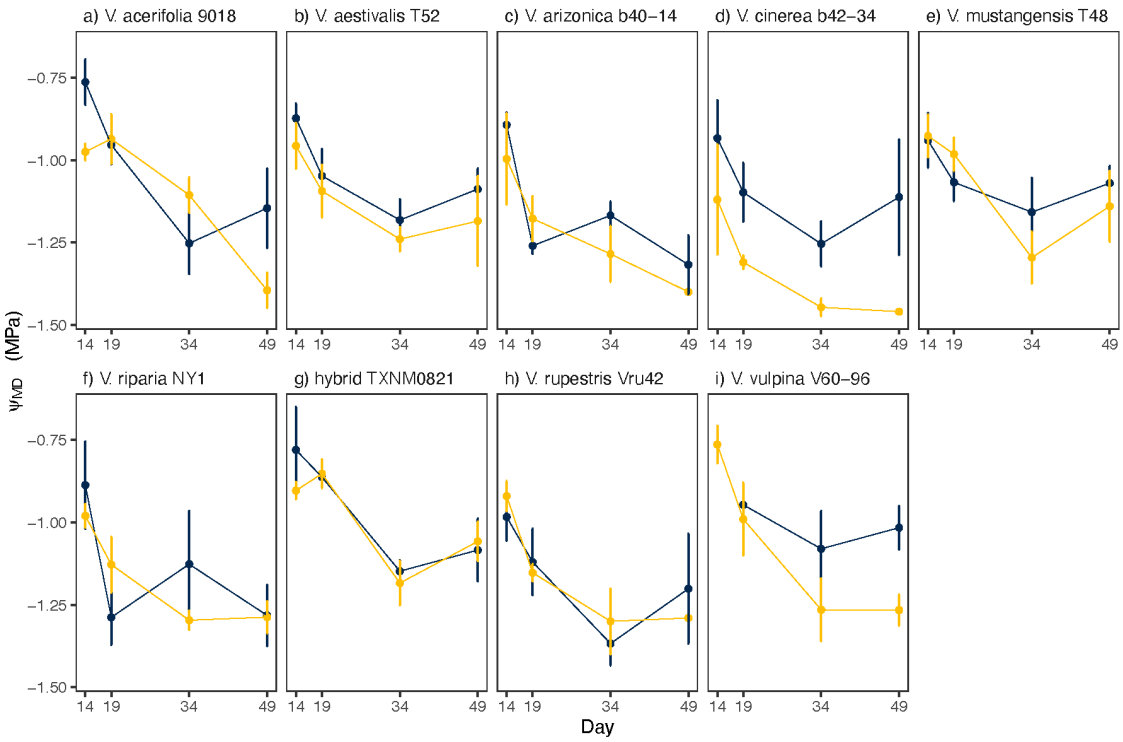

FIGURE 3 Midday leaf water potential (Ψ_{MD}, bar) over time of 9 *Vitis* accessions under well-watered (blue) and water-stressed (yellow) treatments. N = 4 (±SE). Day 14 marks the beginning of the drought treatment.

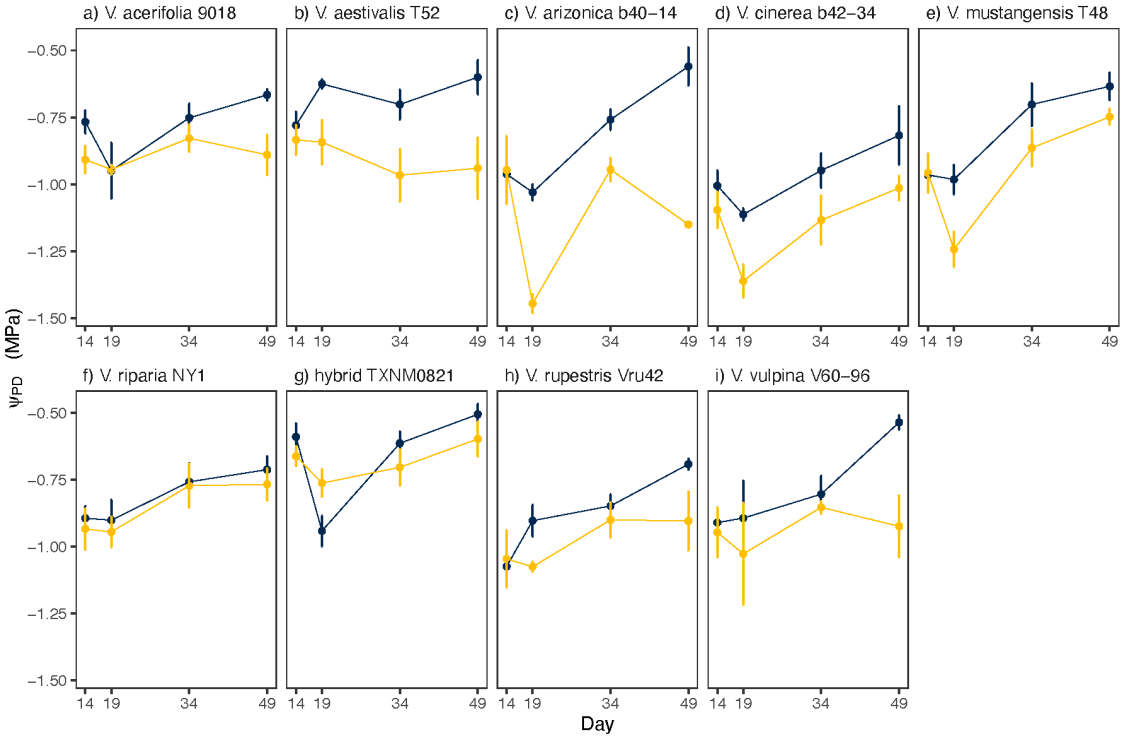

FIGURE 4 Predawn leaf water potential (Ψ_{PD}, bar) over time of 9 *Vitis* accessions under well-watered (blue) and water-stressed (yellow) treatments. N = 4 (±SE). Day 14 marks the beginning of the drought treatment.

hybrid (TXNM0821) having the least negative Ψ_{MD} and Ψ_{PD} for the final measurement date. Drought treatment had a minimal effect on the Ψ_{MD} and Ψ_{PD} of *V. riparia* (NY1) and hybrid (TXNM0821), as they showed the least negative values. Under drought conditions, *V. acerifolia* (9018) and *V. cinerea* (b42-34) had the lowest Ψ_{MD} values across all species. *V. vulpina* (V60-96) experienced the largest decrease in Ψ_{MD} compared to the well-watered controls. Under well-watered conditions, *V. arizonica* (b40-14) exhibited a very negative Ψ_{MD}, similar to that of the drought-stressed plants of the same species. However, the Ψ_{PD} of *V. arizonica* (b40-14) was much higher (less negative) and significantly different from that of the water-stressed plants. Similar behavior was observed for *V. aestivalis* (T52).

3.2 | Water use and biomass traits

Water use

Figure 5 (A) shows the total water use for each plant of each species and treatment over the entire experiment. As expected, there were statistically significant differences between the treatments given the nature of this experiment. However, because evaporation was the same across all pots, different species showed varying rates of water consumption under well-watered conditions. *V. arizonica* (b40-14) and *V. rupestris* (Vru42) had the highest water demands reaching a targeted soil moisture content of approximately 80%. A similar pattern was observed in the control group. Regarding the relative water cut back (with the absolute value of the control group and the relative value of drought), differences across the species were found found (data not shown). Some species experienced a higher relative cutback (*V. acerifolia* (9018) -72%; *V. aestivalis* (T52) -73%; *V. arizonica* (b40-14) -74%; *V. vulpina* (V60-96) -76%), which indicates that more severe water limitations were imposed on these plants. The hybrid (TXNM0821) had the lowest relative water cutback of -56%.

Biomass allocation

During these experiments, the drought treatment consistently led to a decrease in canopy growth, whereas the response of the roots varied. The drought treatments caused a significant reduction in canopy biomass across all species, with *V. acerifolia* (9018) and *V. arizonica* (b40-14) exhibiting the most substantial decrease compared to the control conditions (Figure 5B). The total root biomass varied across species, and no significant treatment effect was observed. However, the root biomass of most species was lower than that of the control group. *V. rupestris* (Vru42) shows the greatest reduction. Although diminished canopy growth is a distinct marker of drought stress, the ratio between roots and shoots is as a

valuable metric for evaluating carbon allocation. This is particularly relevant in the case of grapevines, where water scarcity notably affects both canopy development and berry production (Figure 5C). All species had higher shoot/root ratios for their plants under controlled conditions than under drought. The data showed significant differences across species (Figure 5D). This indicates that plants decide to reallocate their available carbon resources differently under drought conditions and prioritized root growth. However, the data showed differences across the species to which they followed this strategy. The stronger the relative increase in the root-to-shoot ratio, the more the plants focused on root growth. This is particularly the case for *V. acerifolia* (9018), *V. aestivalis* (T52), and *V. vulpina* (V60-96). When combining the information from Figure 5B, 5C, and 5D, it becomes clear that the reason for this behavior is the strong cutback in canopy growth, whereas the root biomass growth is maintained at an almost similar level, which is also indicated by the fact that no statistical differences were found. Drought stress led to a substantial reduction in canopy size (shown as the total leaf area in this study) across all species, as indicated by statistically significant differences (Figure 5E). It is worth mentioning that *V. cinerea* (b42-34) had by far the largest canopy under controlled conditions, whereas it experienced high cutback compared to the water-restricted treatment. The canopy sizes of the drought-stressed plants were similar across all species. It is worth mentioning that the only non-significant differences was found for the hybrid (TXNM0821). This species was found under well-watered conditions with relatively low canopy growth.

Biomass and water-use relationships

Biomass growth per liter of water used, often expressed as a water-use efficiency (WUE) metric, provides insight into the efficiency of a plant's water utilization in relation to its biomass production. This parameter provides information on the ability of plants to thrive and grow under water-limited conditions. Plants with higher WUE are characterized by their capacity to generate more biomass using relatively less water. This efficiency can be attributed to a combination of physiological, biochemical, and anatomical adaptations that optimize the capture, transport, and utilization of water and carbon resources. As shown in Figure 5F, there were no statistically significant differences in total leaf area to liter water used for *V. acerifolia* (9018), *V. arizonica* (b40-14), hybrid (TXNM0821), and *V. vulpina* (V60-96). Of these species, *V. arizonica* (b40-14) stood out with the highest ratio, indicating notable efficiency in utilizing the available water resources for leaf area growth. Even under water stress conditions, this species exhibited a relatively high ratio, although the reduction in leaf area expansion was more pronounced than that in some other species. Similarly, the

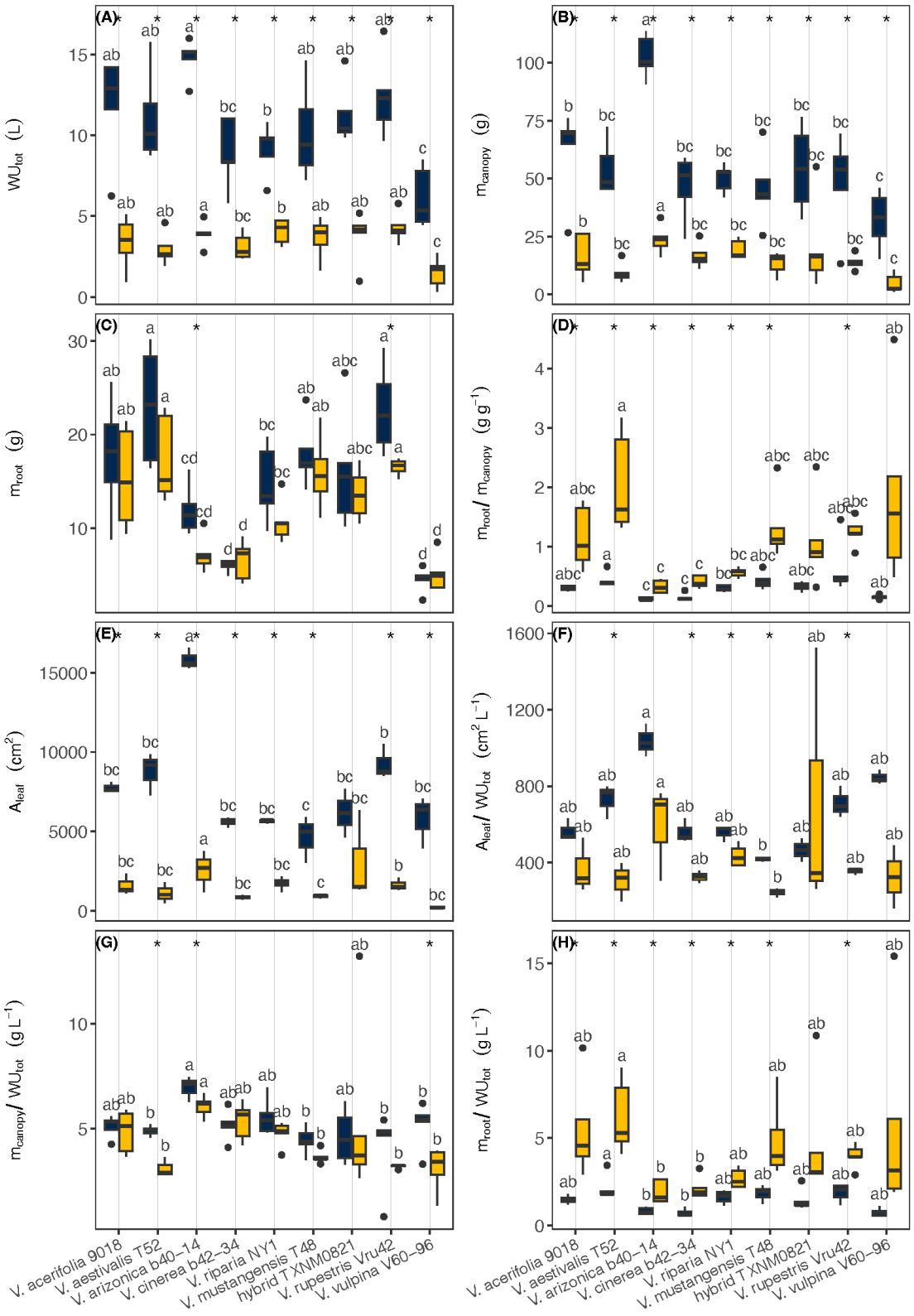

FIGURE 5 Water use and biomass traits under well-watered (blue bar) and water-stressed (yellow bar) treatments for *Vitis* accessions. (A) Total water use per plant (WU_{tot}, L), (B) Canopy biomass (m_{canopy}, g), (C) Root biomass (m_{root}, g), (D) Ratio of root biomass to canopy biomass (m_{canopy}/m_{root}, g g^{-1}), (E) Total leaf area, (A_{leaf}, cm^2), (F) Total leaf area per water used, (A_{leaf}/WU_{tot}, cm^2 L^{-1}), (G) Canopy biomass per water used, (m_{canopy}/WU_{tot}, g L^{-1}), (G) Root biomass per water used, (m_{root}/WU_{tot}, g L^{-1}).

hybrid (TXNM0821) showed a relatively high ratio under both normal and water-stress conditions, suggesting that it possesses inherent water-use efficiency traits. However, similar to *V. arizonica*, it experienced a significant reduction in leaf area under water stress conditions, indicating its adaptation to conserve water resources during periods of scarcity. Conversely, *V. vulpina* (V60-96) also displayed a relatively high cutback in the leaf area under water-stress conditions. This suggests that although it may have an efficient water utilization mechanism under normal conditions, it is less adaptable to drought stress, leading to a noticeable reduction in leaf area. The analysis of canopy biomass to water use, as depicted in Figure 5G, revealed statistically significant differences for only three plant species: *V. aestivalis* (T52), *V. arizonica* (b40-14), and *V. vulpina* (V60-96). Despite these significant differences, the overall ratio of canopy biomass to water use remained consistent across all studied species. Although no statistically significant differences were found between the two treatments, the drought treatments had higher root mass production per liter of water consumed across all species. The outstanding species with a high ratio were *V. aestivalis* (T52), *V. arizonica* (b40-14), and *V. vulpina* (V60-96).

3.3 | Plant physiological behavior

During the experiment, the major photosynthetic measurements were taken three times: at the beginning (=day 2), middle (=day 16), and final (=day 49) dates.

3.3.1 | First measurement date

The absence of statistically significant differences in the main effect of water treatment is a logical and expected outcome, given that both groups were treated equally initially, and the conditions experienced by the plant groups were consistent across all traits. The inability to measure the water potential of *V. vulpina* (V60-96) and *V. rupestris* (Vru42) owing to a lack of leaves on these plants at the beginning of the study is a practical limitation that should be noted. The observation that there were no significant outliers in physiological behavior for all traits across all species, as indicated by the groupings of Tukey letters, suggests that the studied traits remained within a relatively consistent range (Figure 6).

3.3.2 | Middle measurement date

Photosynthetic traits

When analyzing the primary effect of water treatment, it became evident that A_n decreased significantly when subjected to 14 days of water stress. This decline was not isolated, but accompanied by a similar decrease in C_i, transpiration rate (E), and g_s. Contrary to these observations, both WUE_i and WUE_{inst} exhibited an increase under water deficit conditions.

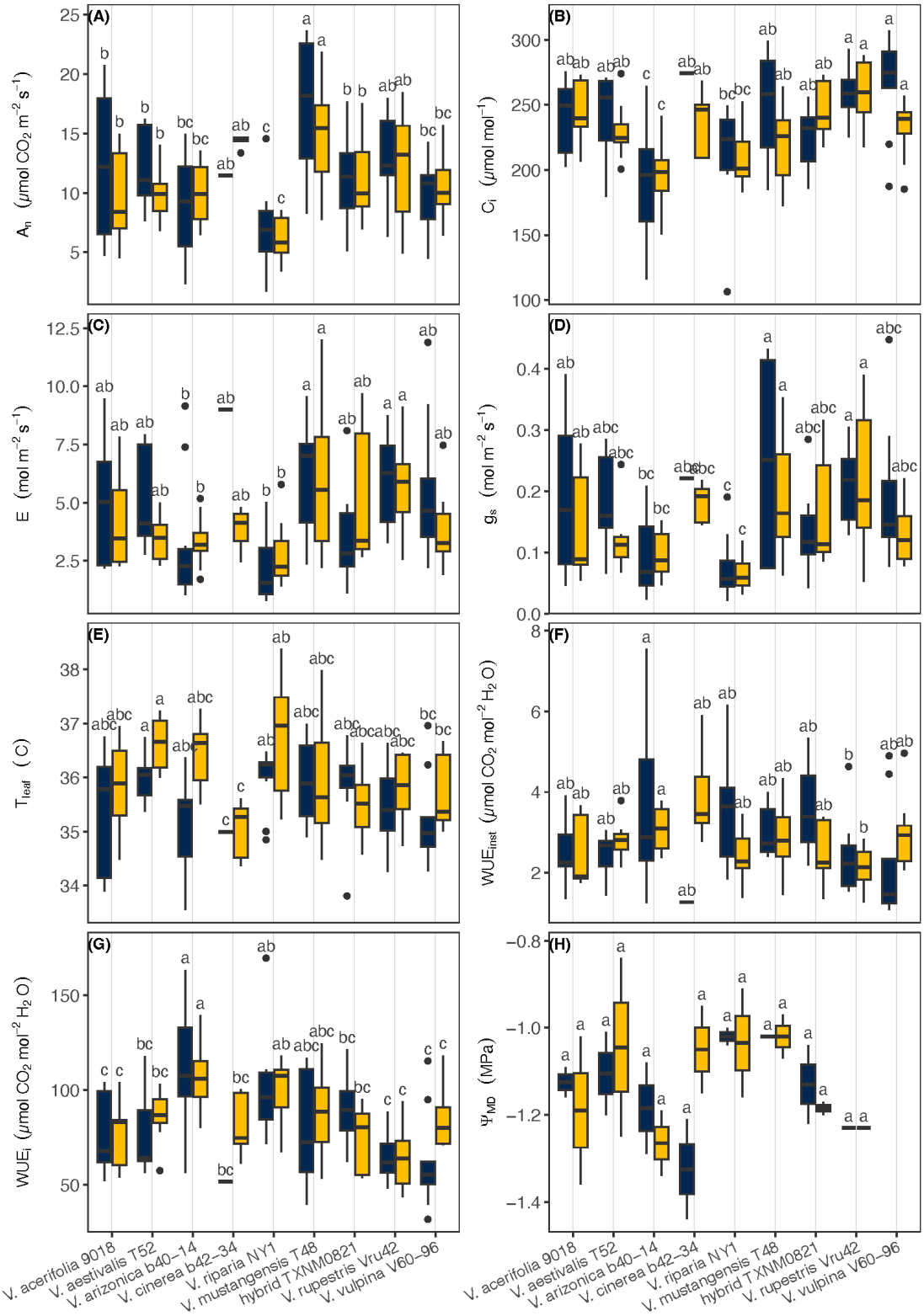

FIGURE 6 Photosynthetic traits under well-watered (blue bar) and water-stressed (yellow bar) treatments for *Vitis* accessions at first measurement date at the start of watering regimes. (A) Net assimilation rate (A_n, μmol), (B) Intercellular airspace CO_2 concentration (C_i, μmol mol s^{-1}), (C) Transpiration rate (E, mmol m^{-2} m^3 m^{-3}), (D) Stomatal conductance (g_s, mol m^{-2} s^{-1}), (E) Leaf temperature, (T_{leaf}, °C), (F) Instantaneous water use efficiency (WUE_{inst}, μmol CO_2 mol^{-1} H_2O), (G) Intrinsic water use efficiency (WUE_i, μmol CO_2 mol^{-1} H_2O), (H) Midday leaf water potential (Ψ_{MD}, MPa). N = 4 (±SE). Measurements were taken at 400 mol mol^{-1} and 1500 mol m^{-2} s^{-1} photosynthetic photon flux density.

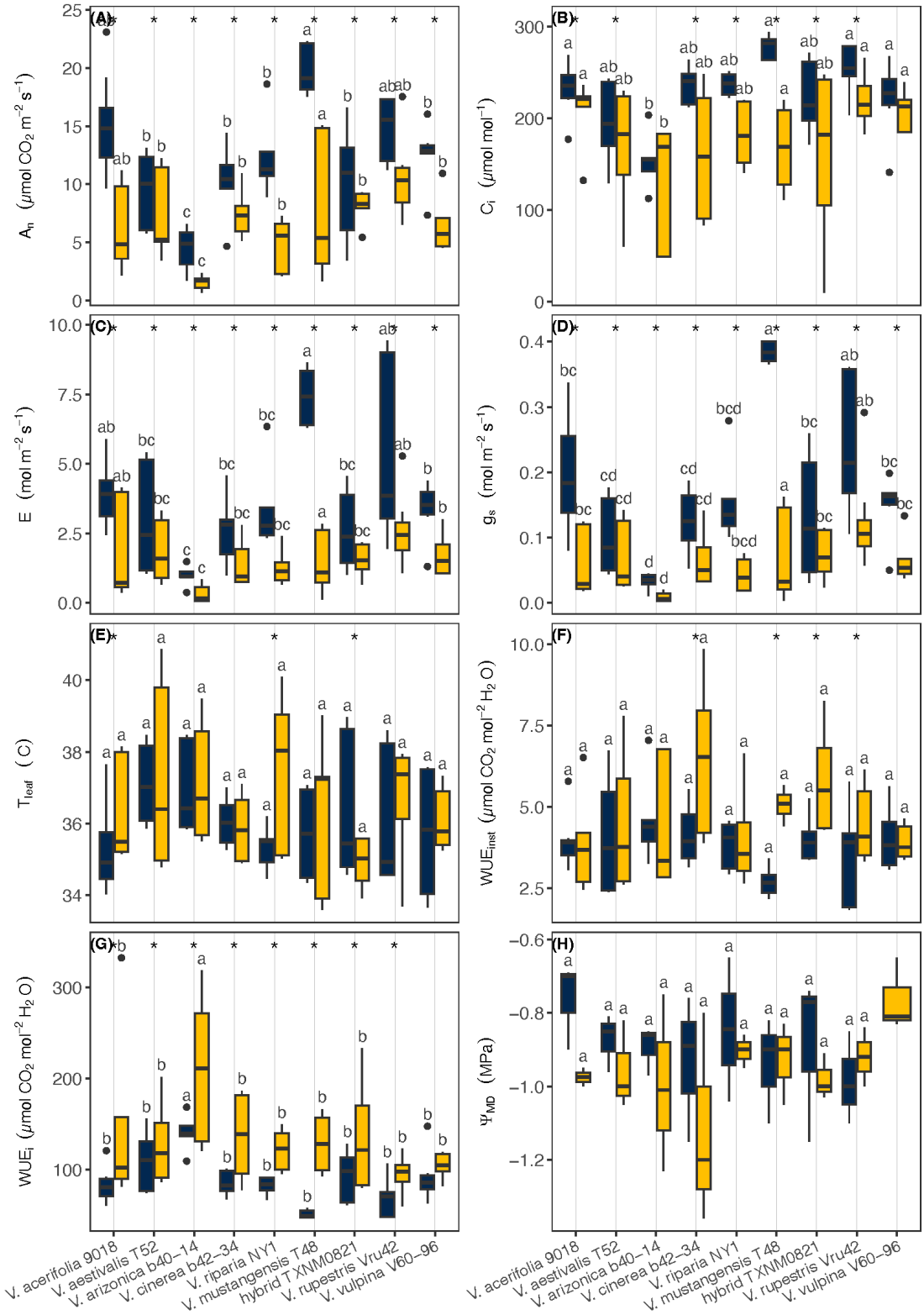

FIGURE 7 Photosynthetic traits under well-watered (blue bar) and water-stressed (yellow bar) treatments for *Vitis* accessions at the middle measurement date when leaves for segmentation were taken. (A) Net assimilation rate (A_n, μmol), (B) Intercellular airspace CO_2 concentration (C_i, μmol mol s^{-1}), (C) Transpiration rate (E, mmol m^{-2} m^3 m^{-3}), (D) Stomatal conductance (g_s, mol m^{-2} s^{-1}), (E) Leaf temperature, (T_{leaf}, °C), (F) Instantaneous water use efficiency (WUE_{inst}, μmol CO_2 mol^{-1} H_2O), (G) Intrinsic water use efficiency (WUE_i, μmol CO_2 mol^{-1} H_2O), (H) Midday leaf water potential (Ψ_{MD}, MPa). N = 4 (±SE). The measurements were taken at 400 mol mol^{-1} and 1500 mol m^{-2} s^{-1} photosynthetic photon flux density.

This implies that, despite the reduced A_n rates, the plants became more adept at utilizing the available water efficiently for photosynthesis. To thrive, plants must maintain their capacity to capture carbon. Remarkably, certain species demonstrated a better ability to sustain their photosynthetic efficiency under drought conditions than other species. Although statistically significant differences were predominantly observed between the drought and control treatments, it is noteworthy that some species maintained their photosynthetic activity while minimizing water loss. Specifically, A_n differed significantly among several species, including *V. acerifolia* (9018), *V. arizonica* (b40-14), *V. riparia* (NY1), *V. mustangensis* (T48), *V. rupestris* (Vru42), and *V. vulpina* (V60-96). Among these, *V. mustangensis* (T48) displayed the highest A_n performance under well-watered conditions. Notably, both well-watered and drought-stressed *V. arizonica* (b40-14) plants exhibited the lowest A_n and E rates, as indicated by the Tukey letters (Figure 7 (A), (C)). Under controlled conditions, *V. mustangensis* had the highest C_i, whereas *V. arizonica* (b40-14) had the lowest C_i (Figure 7 (B)). Under drought conditions, *V. acerifolia* (9018) outperformed the control plants of *V. arizonica* (b40-14). However, all species exhibited relatively similar C_i rates under water-stressed conditions, with *V. cinerea* (b42-34), *V. riparia* (NY1), and *V. mustangensis* (T48) exhibited statistically significant differences for the treatment effect. Both E and g_s displayed similar significance patterns for the treatment effect and the species *V. acerifolia* (9018), *V. arizonica* (b40-14), *V. riparia* (NY1), *V. mustangensis* (T48), and *V. vulpina* (V60-96). Additionally, *V. rupestris* (Vru42) showed a statistically significant difference in the treatment effect of g_s. The highest E and g_s values were observed for *V. rupestris* (Vru42) and *V. mustangensis* (T48) under well-watered conditions, respectively. In contrast, *V. arizonica* (b40-14) consistently performed the poorest in both traits and treatment groups.

Water-use efficiency

The concept of water-use efficiency (WUE) represents an equilibrium between production metrics such as biomass generation (measured in kilograms) or carbon dioxide assimilation (measured in moles) and the associated water costs, quantified in terms of water volume (liters) used or moles of transpired water. This equilibrium can be assessed at various spatial scales ranging from the individual leaf level to that of the entire plant or crop system. When evaluating WUE at the leaf level, it can be quantified using gas-exchange measurements or the examination of carbon isotope ratios in leaf dry matter. It is a common practice to employ instantaneous leaf gas exchange measurements over shorter time intervals. These measurements relate A_n to either g_s, a parameter referred to as WUE_i, or E, thereby defining

$_{inst}$WUE. The utilization of these two parameters, A_n/g_s and A_n/E, predominantly differentiates genetic influences from environmental effects in the context of water-use efficiency (Tomás et al., 2014b).

Statistically significant differences in WUE_{inst} were observed across species with respect to the treatment effect, specifically for *V. mustangensis* (T48) and the hybrid (TXNM0821) (Figure 7 (E)). In general, the drought treatments had higher WUE_{inst} values than the well-watered control group. It is noteworthy that WUE_{inst} was at its lowest for the well-watered plants of *V. mustangensis* (T48), even though all species and treatments were grouped with the same Tukey letter.

However, when assessing WUE_i, the pattern differed. In this case, all species and treatments were grouped similarly, except for the drought group of *V. arizonica* (b40-14), as indicated in Figure 7 (G).

Water potentials

No statistically significant differences were observed in Ψ_{MD} among the treatment groups. However, there were trends indicating that the drought-treated group generally exhibited lower water potentials than their respective control groups within the same species. Notably, for *V. vulpina* (V60-96), water potential was measured only in drought-stressed plants because of their slow growth. Among all species, the control group of *V. acerifolia* (9018) displayed the highest (least negative) water potential.

3.3.3 | Final measurement date

Photosynthetic Traits

Statistically significant differences in A_n were observed between the treatments for all species on the final measurement date. Notably, *V. arizonica* (b40-14) exhibited a pattern similar to that observed on the middle measurement date. Under well-watered conditions, the A_n rate remained comparable to that of the droughts of all other species. This trend was mirrored in E, C_i, and g_s for *V. arizonica* (b40-14). Tukey's post-hoc analysis indicated that A_n, C_i, E, and g_s were similar in all other species under drought conditions. Interestingly, not all the species displayed statistically significant differences in these parameters. *V. acerifolia* (9018) consistently maintained low C_i values under both controlled and drought conditions. Notably, the trend in C_i between the drought and control treatments was inconsistent across the species. Statistically significant species generally exhibited higher C_i values under drought treatment, whereas those without significant differences had equal or lower C_i values in drought-stressed plants. Remarkably, *V. arizonica*

exhibited a substantial increase in C_i under drought stress conditions. All species reduced their E rates to a similar level under drought conditions; however under well-watered conditions, they exhibited different E rates. For g_s, *V. mustangensis* (T48) displayed a significant reduction from the control to drought treatment. Notably, *V. arizonica* (b40-14) displayed a unique adaptation strategy, maintaining photosynthetic rates comparable to those of drought-stressed plants of other species under well-watered conditions. This suggests that *V. arizonica* (b40-14) has an inherent drought tolerance mechanism. Additionally, the diverse responses in C_i across species emphasize the complexity of water use strategies, with some species conserving CO_2 and others allowing higher C_i values under drought. The uniform reduction in transpiration rates under drought conditions suggests a common water-saving response among species, although transpiration rates under well-watered conditions vary considerably.

Water-use efficiency

WUE_{inst} showed statistically significant differences for *V. arizonica* (b40-14) and *V. mustangensis* (T48), as indicated by the Tukey letter (group c), which showed very low values. WUE_i exhibited significant differences in multiple species: *V. arizonica* (b40-14), *V. mustangensis* (T48), the hybrid (TXNM0821), and *V. rupestris* (Vru42). WUE_i, which considers the trade-off between water loss and carbon gain, displayed significant differences across several species. These variations in water-use efficiency parameters underline the diverse adaptive strategies employed by grapevines to cope with water scarcity.

3.4 | Photosynthetic capacity: CO_2 and light response curves

Inherent differences in photosynthetic capacity were observed among the accessions (Table 3). Notably, *V. aestivalis* (T52), the hybrid (NY1), and *V. vulpina* (V60-96) consistently stood out across multiple parameters, showing their remarkable photosynthetic capabilities. These three species exhibited high values for V_{cmax} and maximum rate of electron transport (J_{max}) under both well-watered and water-stressed conditions, indicating their ability to maintain robust photosynthesis and resilience even in challenging environments. However, it is crucial to recognize the diversity of responses among the *Vitis* species. *V. mustangensis* (T48) appeared to be more sensitive to water stress, as indicated by the decline in several photosynthetic parameters under drought conditions. This sensitivity suggests that this species may require more favorable water availability to sustain optimal photosynthesis. Additionally, when examining the maximum rate of triose phosphate use (*TPU*), the hybrid (NY1) demonstrated efficient utilization of triose phosphate

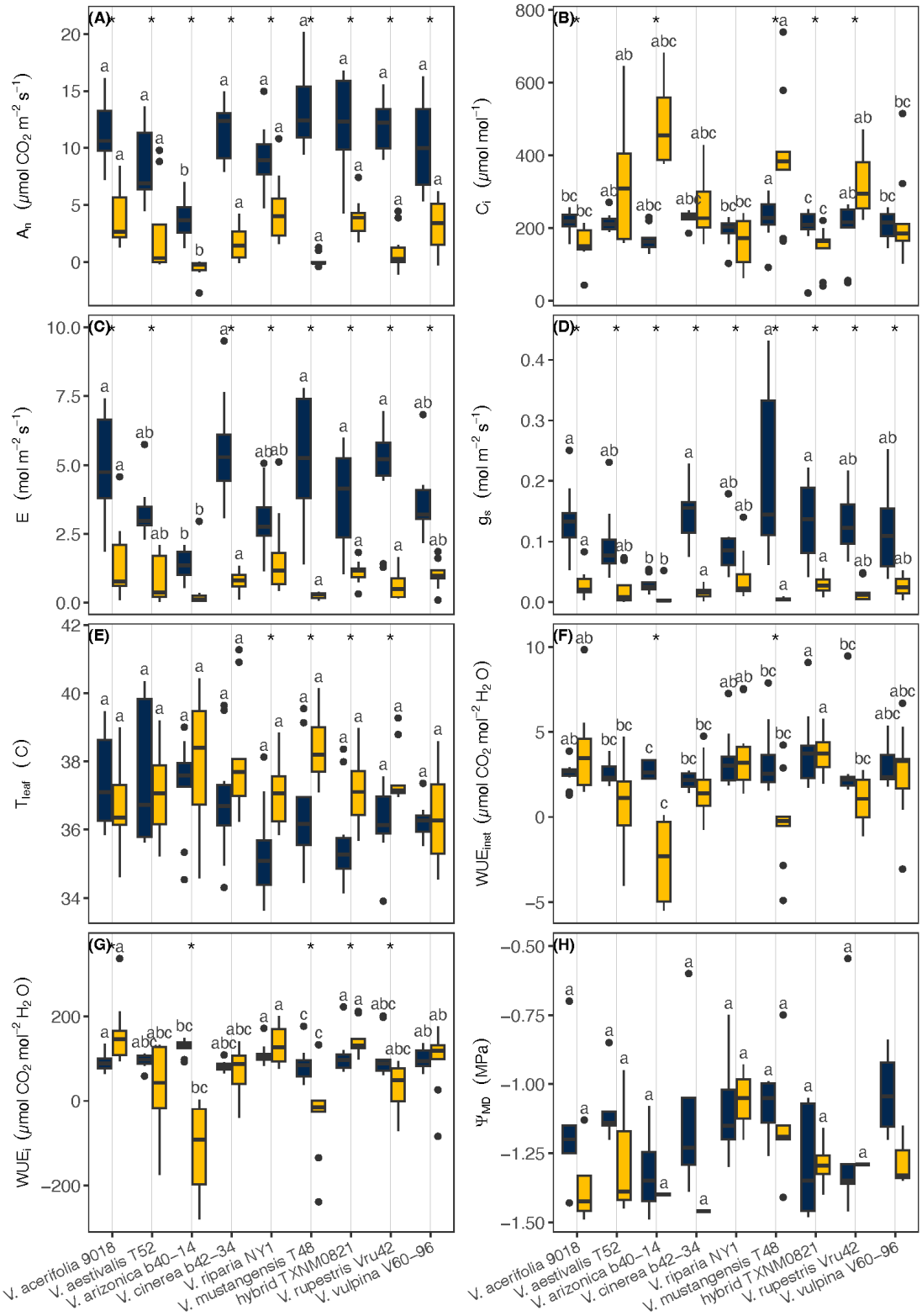

FIGURE 8 Photosynthetic traits under well-watered (blue bar) and water-stressed (yellow bar) treatments for *Vitis* accessions at the end of the experiment. (A) Net assimilation rate (A_n, μmol), (B) Intercellular airspace CO_2 concentration (C_i, μmol mol s^{-1}), (C) Transpiration rate (E, mmol m^{-2} m^3 m^{-3}), (D) Stomatal conductance (g_s, mol m^{-2} s^{-1}), (E) Leaf temperature, (T_{leaf}, °C), (F) Instantaneous water use efficiency (WUE_{inst}, μmol CO_2 mol^{-1} H_2O), (G) Intrinsic water use efficiency (WUE_i, μmol CO_2 mol^{-1} H_2O), (H) Midday leaf water potential (Ψ_{MD}, MPa). N = 4 (±SE). The measurements were taken at 400 mol mol^{-1} and 1500 mol m^{-2} s^{-1} photosynthetic photon flux density.

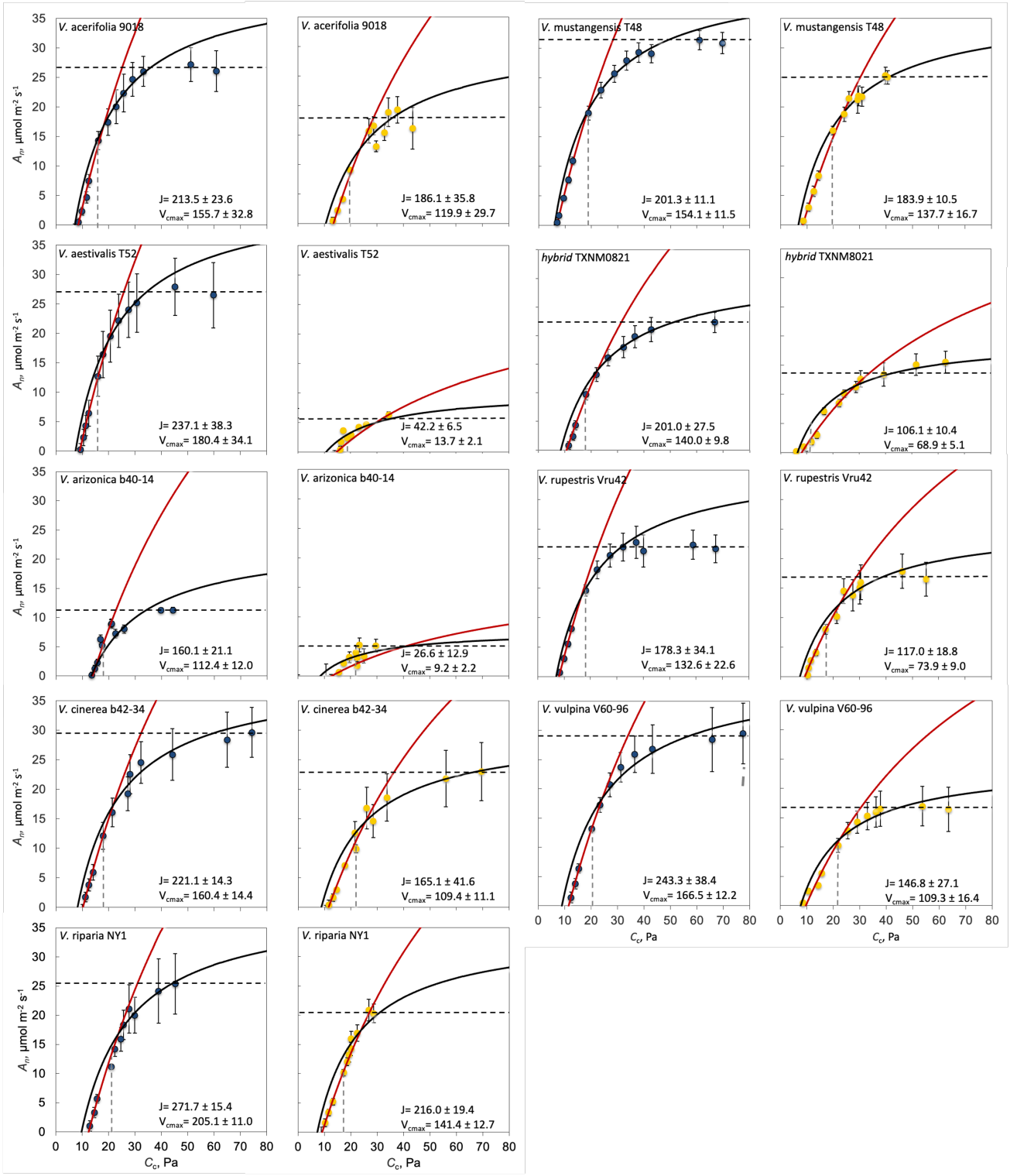

FIGURE 9 Photosynthetic CO_2 response curves were constructed using Sharkey's fitting calculator version 2.0 (Sharkey 2016), averaged for 3 replicates in *Vitis* accessions under well-watered (blue dots) and droughted (yellow) treatments. A_n-C_i-curves are shown with colored circles and error bars measured directly. A_n-C_c-curves were used to generate V_{cmax} and J, and averaged over three replicates for each accession (±SE, n=3). The assimilation rate at saturating CO_2 (A_{max}) in the triose limitation state is indicated by the dashed black horizontal line in each plot. The dashed vertical grey lines represent the C_i at ambient CO_2 (40.4 Pa), representing the limitation of g_{min} comparison with the value of the A_n-C_c-curve. The rubisco (red curves) and RuBP regeneration limitations (black curves) are shown.

TABLE 3 Photosynthetic responses of 9 *Vitis* accessions under well-watered and water-stressed conditions. (N=3, ±SE).

Species	Genotype	Control				Drought			
		V_{cmax}	*J*	*TPU*	*Rd**	V_{cmax}	*J*	*TPU*	*Rd**
V. acerifolia	9018	155.7±32.8	213.5±23.6	12.6±1.5	10.9±4.9	119.9±29.7	186.1±35.8	10.8±2.8	14.3±5.3
V. aestivalis	T52	180.4±34.1	237.1±38.3	12.9±2.8	11.7±4.8	13.7±2.1	42.3±6.5	2.9±0.8	2±2
V. arizonica	b40-14	112.4±12	161±21.1	8.3±1.9	13.6±5.9	9.2±2.2	26.6±12.9	1.6±0.7	0.6±0.6
V. cinerea	b42-34	160.4±14.3	221.1±9.2	14.9±1.1	14.5±2.2	109.4±11.1	165.1±41.6	11.3±2.9	11±3.9
V. riparia	NY1	205.1±11	271.7±15.4	16.1±0.5	22.9±2.3	141.4±12.7	216±19.4	11.5±1.5	11.4±2.9
V. mustangensis	T48	154.1±11.5	201.3±11.1	12.1±0.5	5.6±1	137.7±16.7	183.9±10.5	10.9±0.1	7.9±1.6
hybrid	TXNM0821	140±9.8	201±27.5	12.1±1.8	15.1±4.6	68.9±5.1	106.1±10.4	6.7±0.6	4.7±2.3
V. rupestris	Vru42	132.6±22.6	178.3±34.1	10.5±1.9	8±3.6	73.9±9	117±18.8	7.2±1	4.5±0.2
V. vulpina	V60-96	166.5±12.2	243.3±38.4	14.9±2.8	16.1±3.6	109.3±16.4	146.8±27.1	8.6±1.6	9.1±3.3

V_{cmax}, Maximum assimilation rate at saturating CO_2; J, Rate of electron transport; TPU, Triose Phosphate Use limitation state,; Rd, Nonphotorespiratory respiration rate.

under well-watered conditions, contributing to the overall photosynthetic process. Intriguingly, *V. acerifolia* (9018) showed a significant increase in *TPU* under water stress conditions. This adaptation may be a crucial mechanism for this species to maintain photosynthesis during periods of water scarcity, potentially contributing to its resilience. A closer look at R_d revealed the varying strategies among the *Vitis* species. *V. aestivalis* (T52) displayed relatively high R_d values under both well-watered and water-stressed conditions, indicating active respiration as part of its photosynthetic process. In contrast, *V. arizonica* (b40-14) exhibited a significant reduction in R_d under water stress conditions. This reduction may represent an energy-conservation strategy during drought stress (Figure 9).

3.5 | Anatomical traits: mesophyll width, surface, and volume parameters

Leaf porosity, defined as the extent of intercellular spaces within leaf tissue, plays a critical role in gas exchange, affecting the diffusion of CO_2 for photosynthesis and the release of O_2 and water vapor. Increased leaf porosity enhances gas diffusion efficiency, particularly CO_2 uptake, thereby improving the photosynthetic performance. This was achieved by providing a larger surface area for gas exchange, enabling better accessibility of CO_2 to the chloroplasts in the mesophyll cells. Analyzing θ_{IAS}, we noted significant differences between the drought and control treatments for two species: *V. cinerea* (b42-34) and *V. vulpina* (V60-96). Notably, *V. cinerea* (b42-34) exhibited a significant decrease in porosity under drought conditions, although it did not have the lowest θ_{IAS} among the species. Remarkably, *V. aestivalis* displayed consistently low θ_{IAS} under both well-watered and drought conditions, with well-watered plants having lower θ_{IAS}

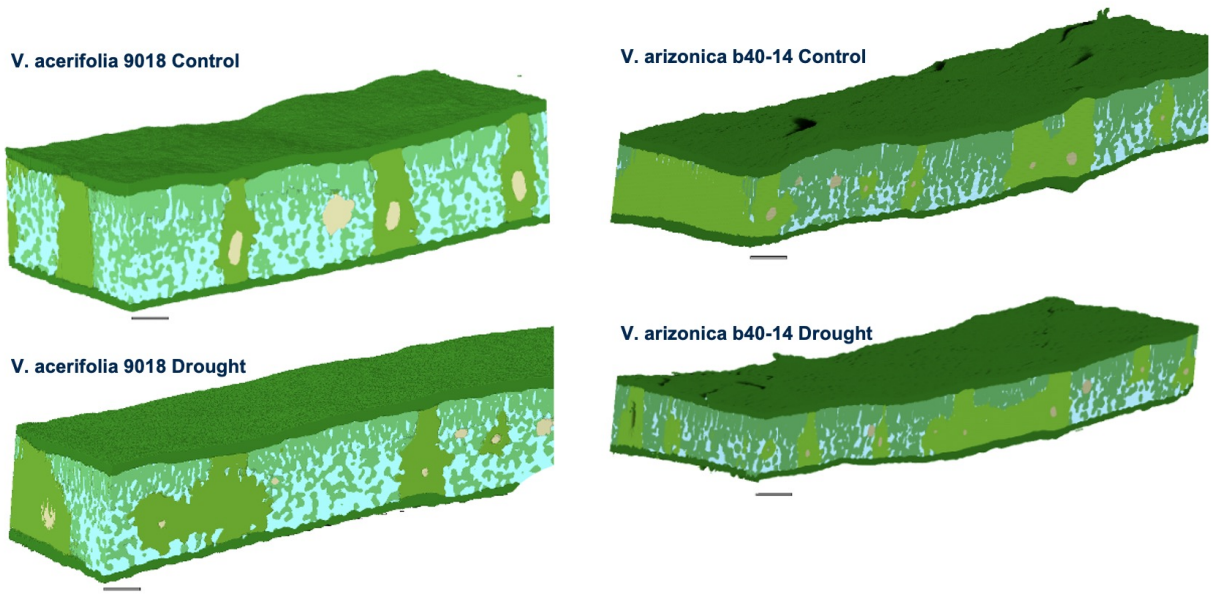

FIGURE 10 Exemplary 3D reconstruct of two *Vitis* accessions under two treatments.

than the drought-stressed plants of other species. Species with higher leaf θ_{IAS}, such as *V. riparia* (NY1), can exchange gases more efficiently, particularly CO_2, with the atmosphere. This increased gas diffusion enhances the photosynthetic efficiency. However, species with low θ_{IAS}, such as *V. aestivalis* (T52) may have limitations in CO_2 uptake.

The leaf mesophyll consists of two layers, spongy and palisade, which contribute to photosynthesis. The spongy layer below the palisade consists of loosely arranged cells with intercellular air spaces that enhance gas diffusion and facilitate gas exchange. In contrast, the palisade mesophyll consists of densely packed, vertically oriented cells that are enriched with chloroplasts and strategically positioned closer to the upper epidermis for optimal light capture.

The ratio of spongy mesophyll to palisade mesophyll varies among species and affects the photosynthetic efficiency. Under drought conditions, some species adapt by reducing the number and size of air spaces within the spongy mesophyll layer, thereby decreasing their $V_{sp\text{-}cell}/V_{pa\text{-}cell}$ratio. This structural adjustment minimizes θ_{IAS}, potentially promoting more efficient CO_2 utilization within the leaf. Examining the $V_{sp\text{-}cell}/V_{pa\text{-}cell}$ ratio, we observed statistically significant differences among four species: *V. acerifolia* (9018), *V. aestivalis* (T52), *V. riparia* (NY1), and *V. rupestris* (Vru42). Notably, *V. rupestris* (Vru42) displayed the lowest ratio in both treatments, which was lower than that of any other species. Species that reduce the $V_{sp\text{-}cell}/V_{pa\text{-}cell}$ ratio under drought conditions are likely to optimize CO_2 utilization.

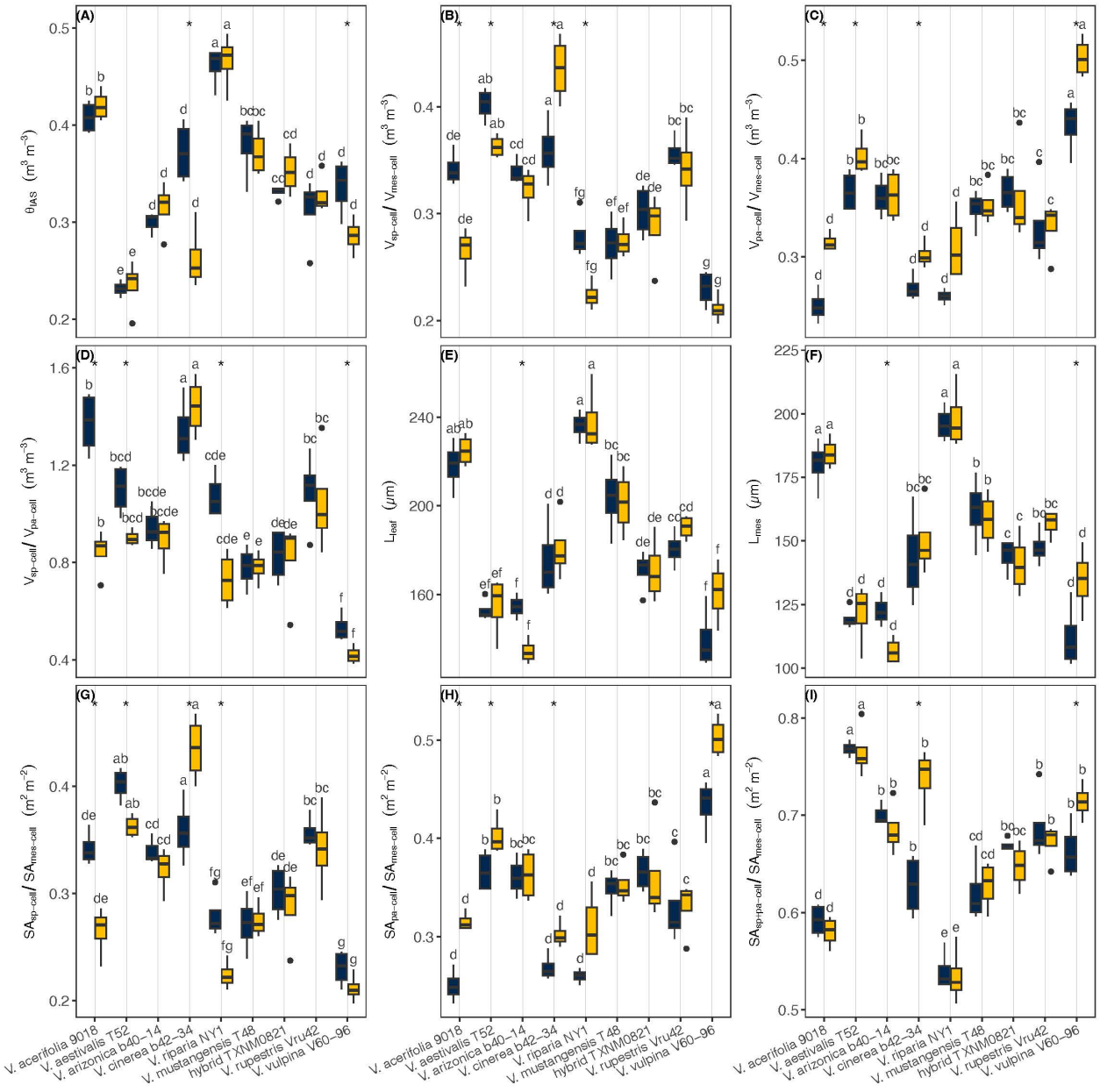

FIGURE 11 Morphological parameters under well-watered (blue bar) and water-stressed (yellow bar) treatments for *Vitis* accessions. (A) Mesophyll porosity (θ_{IAS}, $m^3\ m^{-3}$), (B) Spongy cell volume to total mesophyll cell volume ($V_{sp\text{-}cell}/\ V_{mes\text{-}cell}$, $m^3\ m^{-3}$) , (C) Palisade cell volume to total mesophyll cell volume ($V_{pa\text{-}cell}/\ V_{mes\text{-}cell}$, $m^3\ m^{-3}$), (D) Spongy cell volume to palisade cell volume, ($V_{sp\text{-}cell}/\ V_{pa\text{-}cell}$, $m^3\ m^{-3}$), (E) Leaf thickness, (L_{leaf}, µmol), (F) Mesophyll thickness, (L_{mes}, µmol, (G) Spongy cell surface area to total mesophyll surface area ($SA_{sp\text{-}cell}/\ SA_{mes\text{-}cell}$, $\mu m^2\ \mu m^{-2}$) (H) Palisade cell surface area to total mesophyll surface area ($SA_{sp\text{-}cell}/\ SA_{mes\text{-}cell}$, $\mu m^2\ \mu m^{-2}$) (I) Spongy and palisade cell surface area to total mesophyll surface area ($SA_{sp+pa\text{-}cell}/\ SA_{mes\text{-}cell}$, $\mu m^2\ \mu m^{-2}$). N= 3-4.

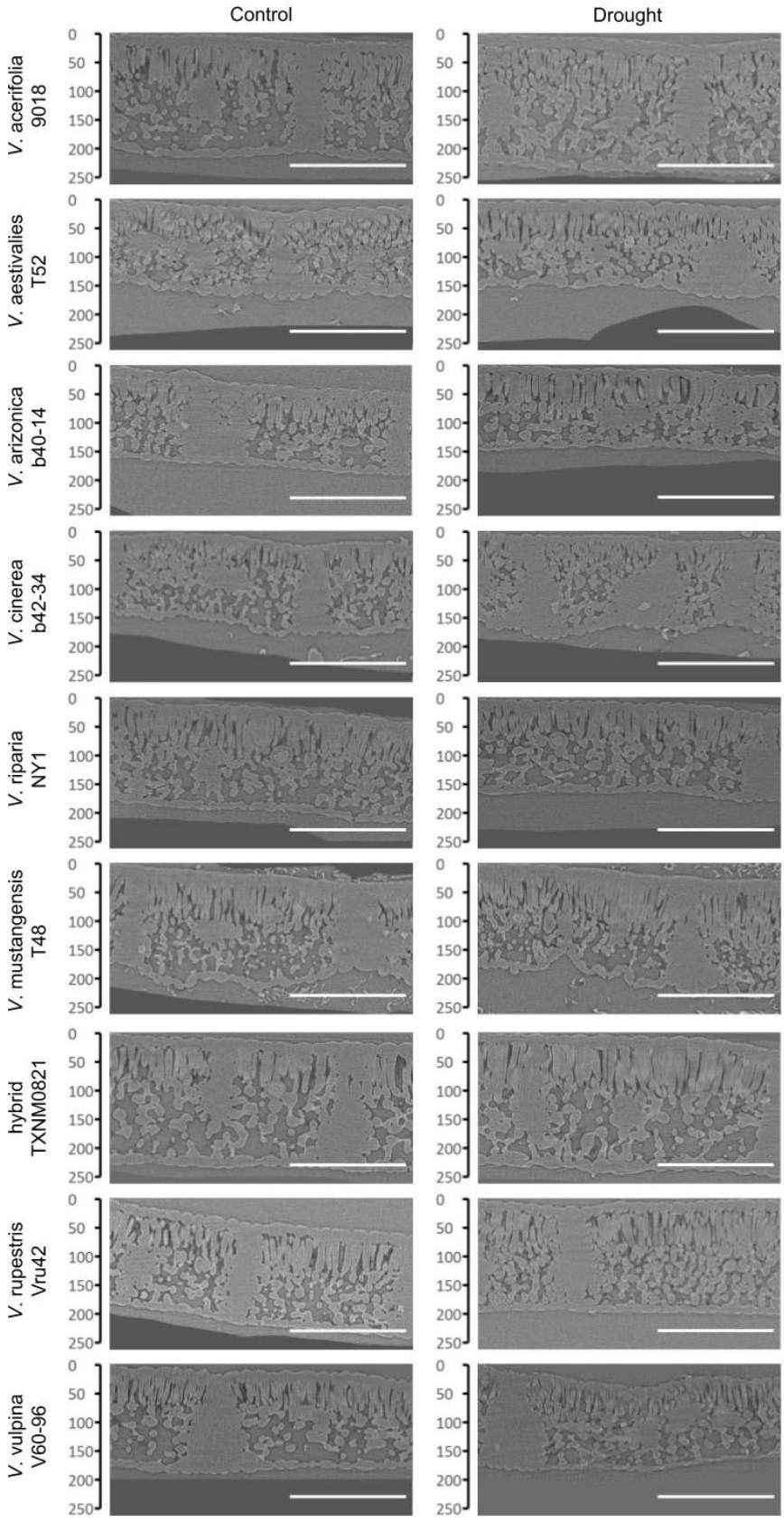

FIGURE 12 Leaf cross sections from representative scans of 9 *Vitis* accessions under well-watered and drought conditions obtained using X-ray microcomputed tomography. Bar equals 200µm.

Decreasing intercellular air spaces limits CO_2 movement within the leaf, potentially leading to more efficient CO_2 use for photosynthesis.

L_{leaf} and L_{mes} varied significantly among the species. *V. riparia* (NY1) had the widest leaves and mesophyll, whereas *V. aestivalis* (T52) and *V. arizonica* (b40-14) had narrower leaves and mesophyll. Only *V. arizonica* (b40-14) showed statistically significant differences between the control and drought treatments, with drought resulting in reduced width. Remarkably, under drought conditions, L_{leaf} of *V. rupestris* (Vru42) increased, although not significantly. However, a significant increase in L_{mes} was observed for *V. rupestris* (Vru42) under drought conditions, whereas *V. arizonica* exhibited a significant decrease (see Figure 12). Variations in L_{leaf} and L_{mes} affect the available surface area for gas exchange and light capture. Wider leaves and mesophyll, as observed in *V. riparia*, offer more space for photosynthesis. Conversely, narrower leaves, such as those of *V. aestivalis* and *V. arizonica*, may have trade-offs in terms of gas exchange and light utilization.

Analyzing $SA_{sp\text{-}cell}/\ SA_{mes\text{-}cell}$ and $SA_{pa\text{-}cell}/\ SA_{mes\text{-}cell}$, the species exhibited diverse adaptations. For example, *V. acerifolia* (9018), *V. aestivalis* (T52), and *V. riparia* (NY1) displayed statistically significant decreases in the $SA_{sp\text{-}cell}/\ SA_{mes\text{-}cell}$ ratio under drought conditions. In contrast, *V. cinerea* (b42-34) showed a substantial increase in this ratio under drought conditions, surpassing that of all other species. *V. rupestris* (Vru42) exhibited the lowest ratio in this context. However, concerning the $SA_{pa\text{-}cell}/\ SA_{mes\text{-}cell}$ ratio, *V. rupestris* (Vru42) displayed the highest ratio under drought conditions compared to the other species, with an overall increase observed for all species under drought conditions. The control plants of *V. acerifolia* (9018) exhibited a very low $SA_{pa\text{-}cell}/\ SA_{mes\text{-}cell}$ ratio, which increased significantly under drought conditions. Similar increases were observed in *V. rupestris* (Vru42), *V. aestivalis* (T52), and *V. cinerea* (b42-34). The $SA_{pa\text{-}cell+sp\text{-}cell}/\ SA_{mes\text{-}cell}$ increased significantly in *V. cinerea* (b42-34) and *V. rupestris* (Vru42) under drought conditions, whereas *V. acerifolia* (9018) and *V. riparia* (NY1) exhibited consistently low ratios across both treatment groups. Changes in $SA_{pa\text{-}cell+sp\text{-}cell}/\ SA_{mes\text{-}cell}$ reflect adjustments in the light capture and gas exchange strategies. Species such as *V. cinerea* showed increased $SA_{sp\text{-}cell}/\ SA_{mes\text{-}cell}$ under drought conditions, potentially enhancing gas diffusion. In contrast, *V. rupestris* increased $SA_{pa\text{-}cell}/\ SA_{mes\text{-}cell}$, indicating a focus on maximizing the light capture.

TABLE 4 Pearson correlation coefficients between geoclimate data.

	Lat	Long	T	MDR	Isoth.	TCV	$T_{max\text{-}WAM}$	$T_{min\text{-}CM}$	TAR	T_{WEQ}	T_{DQ}
Lat		**0.81***	**-0.83***	-0.5	**-0.79***	0.89*	-0.61	**-0.91***	**0.88***	-0.54	**-0.97***
Long	**0.81***		-0.47	**-0.81***	**-0.83***	**0.78***	-0.29	-0.54	0.59	-0.17	**-0.7***
T	**-0.83***	-0.47		0.02	0.35	-0.52	**0.93***	**0.97***	-0.66	**0.74***	**0.87***
MDR	-0.5	**-0.81***	0.02		**0.87***	**-0.68***	-0.16	0.12	-0.35	-0.07	0.4
Isoth.	**-0.79***	**-0.83***	0.35	**0.87***		**-0.95***	0.06	0.51	**-0.76***	0.16	**0.73***
TCV	**0.89***	**0.78***	-0.52	**-0.68***	**-0.95***		-0.21	**-0.7***	**0.92***	-0.3	**-0.85***
$T_{max\text{-}WAM}$	-0.61	-0.29	**0.93***	-0.16	0.06	-0.21		**0.81***	-0.36	**0.74***	**0.67***
$T_{min\text{-}CM}$	**-0.91***	-0.54	**0.97***	0.12	0.51	**-0.7***	**0.81***		**-0.83***	**0.7***	**0.94***
TAR	**0.88***	0.59	-0.66	-0.35	**-0.76***	**0.92***	-0.36	**-0.83***		-0.41	**-0.88***
T_{WEQ}	-0.54	-0.17	0.74*	-0.07	0.16	-0.3	**0.74***	**0.7***	-0.41		0.61
T_{DQ}	**-0.97***	**-0.7***	**0.87***	0.4	**0.73***	**-0.85***	**0.67***	**0.94***	**-0.88***	0.61	
T_{WAQ}	-0.52	-0.16	**0.9***	-0.32	-0.07	-0.11	**0.99***	**0.78***	-0.31	**0.71***	0.59
T_{CQ}	**-0.96***	-0.65	**0.95***	0.27	0.62	**-0.77***	**0.78***	**0.99***	**-0.84***	**0.67***	**0.98***
P	0.32	0.65	-0.1	-0.57	-0.36	0.26	-0.11	-0.08	0.02		-0.18
P_{WEM}	-0.61	-0.36	0.34	0.46	**0.76***	**-0.78***	0.05	0.5	**-0.75***	0.14	**0.67***
P_{DM}	**0.73***	**0.86***	-0.4	**-0.83***	**-0.81***	**0.72***	-0.26	-0.45	0.47	-0.38	-0.64
PCV	**-0.75***	**-0.81***	0.33	**0.87***	**0.96***	**-0.88***	0.08	0.46	-0.66	0.25	**0.69***
P_{WQ}	-0.44	-0.23	0.19	0.4	0.66	-0.65	-0.07	0.34	-0.62	-0.02	0.52
P_{DQ}	**0.68***	**0.82***	-0.34	**-0.82***	**-0.79***	**0.69***	-0.2	-0.39	0.43	-0.35	-0.58
P_{WAQ}	-0.15	-0.06	-0.13	0.42	0.54	-0.46	-0.34	0.02	-0.36	-0.2	0.23
P_{CQ}	0.6	**0.75***	-0.35	-0.64	-0.58	0.52	-0.28	-0.36	0.31	-0.39	-0.46

	T_{WAQ}	T_{CQ}	P	P_{WEM}	P_{DM}	PCV	P_{WQ}	P_{DQ}	P_{WAQ}	P_{CQ}
Lat	-0.52	**-0.96***	0.32	-0.61	**0.73***	**-0.75***	-0.44	**0.68***	-0.15	0.6
Long	-0.16	-0.65	0.65	-0.36	**0.86***	**-0.81***	-0.23	**0.82***	-0.06	**0.75***
T	**0.9***	**0.95***	-0.1	0.34	-0.4	0.33	0.19	-0.34	-0.13	-0.35
MDR	-0.32	0.27	-0.57	0.46	**-0.83***	**0.87***	0.4	**-0.82***	0.42	-0.64
Isoth.	-0.07	0.62	-0.36	**0.76***	**-0.81***	**0.96***	0.66	**-0.79***	0.54	-0.58
TCV	-0.11	**-0.77***	0.26	**-0.78***	**0.72***	**-0.88***	-0.65	**0.69***	-0.46	0.52
$T_{max\text{-}WAM}$	**0.99***	**0.78***	-0.11	0.05	-0.26	0.08	-0.07	-0.2	-0.34	-0.28
$T_{min\text{-}CM}$	**0.78***	**0.99***	-0.08	0.5	-0.45	0.46	0.34	-0.39	0.02	-0.36
TAR	-0.31	**-0.84***	0.02	**-0.75***	0.47	-0.66	-0.62	0.43	-0.36	0.31
T_{WEQ}	**0.71***	**0.67***	-0.25	0.14	-0.38	0.25	-0.02	-0.35	-0.2	-0.39
T_{DQ}	0.59	**0.98***	-0.18	**0.67***	-0.64	**0.69***	0.52	-0.58	0.23	-0.46
T_{WAQ}		**0.72***	-0.01	-0.01	-0.11	-0.06	-0.12	-0.05	-0.4	-0.16
T_{CQ}	**0.72***		-0.19	0.54	-0.58	0.58	0.38	-0.52	0.06	-0.47
P	-0.01	-0.19		0.27	**0.77***	-0.47	0.43	**0.78***	0.45	**0.88***
P_{WEM}	-0.01	0.54	0.27		-0.39	**0.71***	**0.97***	-0.37	**0.85***	-0.08
P_{DM}	-0.11	-0.58	**0.77***	-0.39		**-0.9***	-0.22	**0.99***	-0.11	**0.92***
PCV	-0.06	0.58	-0.47	**0.71***	**-0.9***		0.59	**-0.9***	0.49	**-0.71***
P_{WQ}	-0.12	0.38	0.43	**0.97***	-0.22	0.59		-0.2	**0.93***	0.11
P_{DQ}	-0.05	-0.52	**0.78***	-0.37	**0.99***	**-0.9***	-0.2		-0.12	**0.93***
P_{WAQ}	-0.4	0.06	0.45	**0.85***	-0.11	0.49	**0.93***	-0.12		0.21
P_{CQ}	-0.16	-0.47	**0.88***	-0.08	**0.92***	**-0.71***	0.11	**0.93***	0.21	

Pearson correlation coefficients between geoclimate data for the nine *Vitis* accessions. Bold indicates statistical significance at $p < 0.05$.

Abbreviations: Lat, Latitude; Long, Longitude; T, Annual Mean Temperature; MDR, Mean Diurnal Range; Isoth., Isothermality; T CV, Temperature Seasonality; $T_{max\text{-}WAM}$, Maimum Temperature of Warmest Month; $T_{min\text{-}CM}$, Minimum Temperature of Coldest Month; TAR, Temperature Annual Range; T_{WEQ}, Mean Temperature of Wettest Quarter ; T_{DQ}, Mean Temperature Driest Quarter; T_{WAQ}, Mean Temperature Warmest Quarter; T_{CQ}, Mean Temperature Coldest Quarter; P, Annual Precipitation; P_{WEM}, Precipitation of Wettest Month; P_{DM}, Precipitation of Driest Month; P CV, Precipitation Seasonality; P_{WQ}, Precipitation Wettest Quarter; P_{DQ}, Precipitation Driest Quarter; P_{WAQ}, Precipitation Warmest Quarter; P_{CQ}, Precipitation Coldest Quarter.

3.6 | Trait-climate relationships

Interactions of geoclimatic variables

The geoclimatic data (Table 4) revealed a network of relationships. Latitude and longitude displayed a robust positive correlation of 0.81, indicating that moving north or south corresponds to east or west movement. A higher annual mean temperature tends to be associated with a smaller mean diurnal range (MDR), meaning that places with more stable temperatures have less variation throughout the day. Conversely, areas with warmer peaks during the year (maximum temperature of the warmest month ($T_{max\text{-}WAM}$)) tended to experience a milder minimum temperature of the coldest month ($T_{min\text{-}CM}$), suggesting a balancing effect. Annual precipitation and mean temperature of the wettest quarter (T_{WEQ}) presented a strong negative correlation of -0.88, suggesting that regions with higher annual rainfall typically experience cooler temperatures during the wettest quarter.

Conversely, mean temperature of the driest quarter (T_{DQ}) and mean temperature of the warmest quarter (T_{WAQ}) revealed a compelling positive correlation of 0.94, highlighting that areas with warmer periods during the year also tend to have higher temperatures during the driest quarter. The annual precipitation and precipitation of the wettest quarter (P_{WQ}) demonstrated a noteworthy positive correlation of 0.77, implying that regions with more significant annual precipitation often have elevated rainfall during the wettest quarter. The precipitation of the driest quarter (P_{DQ}) and precipitation seasonality (PCV) revealed a striking negative correlation of -0.90, suggesting that areas with higher rainfall during the driest month tend to have less pronounced variations in precipitation throughout the year.

P_{DQ} and precipitation of the coldest quarter (P_{CQ}) showed a compelling positive correlation of 0.93, signifying that regions with increased rainfall during the driest quarter also experience higher precipitation during the coldest quarter. This correlation underscores the interconnectedness of seasonal precipitation patterns. Furthermore, T_{WAQ} and T_{CQ} reveal a notable positive correlation of 0.72, indicating that regions with warmer periods during the year also tend to have milder temperatures during the coldest quarter.

Effects of geoclimatic variables on physiological and anatomical parameters under well-watered conditions

latitude exhibited a strong positive correlation (0.71*) with C_i. This implies that as one moves closer to the equator (lower latitudes), there tends to be an increase in the concentration of CO_2 within plant leaf intercellular spaces, potentially indicating adaptation to varying environmental conditions. longitude (Long) also showed a substantial

positive correlation (0.70*) with C_i, suggesting that the longitudinal movement across regions, whether east or west, leads to a parallel increase in C_i. This highlights a potential connection between geographical position and CO_2 concentration within plant tissues. mean diurnal range displayed a pronounced negative correlation (-0.68*) with C_i. This suggests that regions with larger temperature fluctuations throughout the day tend to have lower CO_2 concentrations within plant leaf intercellular spaces. The isothermality (Isoth.) exhibited a strong negative correlation (-0.69*) with C_i, emphasizing the influence of temperature stability on plant CO_2 exchange processes. Regions with less diurnal temperature variations tended to exhibit higher CO_2 concentrations. temperature seasonalityand C_i were positively correlated (0.62*), indicating that areas with pronounced temperature seasonality tended to have higher CO_2 concentrations within plant leaves. J_{max} displayed a robust positive correlation (0.73*) with longitude, suggesting that longitudinal differences across regions impact the J_{max}, possibly driven by variations in climate conditions. J_{max} also showed a significant negative correlation (-0.75*) with mean diurnal range, indicating that regions with larger temperature fluctuations tend to have lower electron transport rates. V_{cmax} exhibited a strong positive correlation (0.67*) with longitude, suggesting that longitudinal variations across regions may influence V_{cmax} in photosynthesis. Ψ_{MD} showed a robust positive correlation (0.81*) with C_i, implying that higher CO_2 concentrations are associated with greater leaf water potential. Among the anatomical parameters, θ_{IAS} exhibited a negative correlation (-0.62*) with annual precipitation, suggesting that regions with higher annual precipitation tend to have lower leaf tissue θ_{IAS}. The $V_{pa\text{-}cell}/V_{mes\text{-}cell}$ ratio displayed a strong positive correlation (0.75*) with annual precipitation, indicating that areas with higher annual precipitation tended to have a larger volume proportion of mesophyll palisade cells.

Effects of geoclimatic variables on physiological and anatomical parameters under drought conditions

In 6, several significant correlations were observed between geoclimatic variables and physiological/anatomical parameters, indicating relationships between environmental conditions and plant response to drought. latitude displayed a moderate positive correlation (0.35) with photosynthetic parameters (E and A_n), indicating that as one moved closer to the equator (lower latitudes), there tends to be a positive effect on photosynthesis under drought conditions. latitude exhibited a positive correlation with Ψ_{MD} and a significant positive correlation with Ψ_{PD}, suggesting that as one moves closer to the equator, plants may experience increased water stress, leading to lower Ψ_{MD} values. longitude exhibited a relatively strong positive correlation (0.51) with photosynthetic parameters (E and A_n), suggesting that longitudinal

TABLE 5 Pearson correlation coefficients between geoclimate variables and physiological and anatomical parameters under well-watered conditions.

	Lat	Long	T	MDR	Isoth.	TCV	$T_{max\text{-}WAM}$	$T_{min\text{-}CM}$	TAR	T_{WEQ}	T_{DQ}
E	0.53	0.57	-0.26	-0.64	**-0.68***	0.6	-0.12	-0.31	0.39	-0.33	-0.55
A	0.11	0.21	0.31	-0.52	-0.56	0.46	0.53	0.14	0.29	0.21	-0.13
C_i	0.59	**0.71***	-0.31	**-0.68***	**-0.69***	0.62	-0.18	-0.36	0.41	-0.4	-0.58
g_s	0.34	0.44	0.01	-0.58	-0.63	0.55	0.2	-0.11	0.37	-0.15	-0.35
WUE_i	-0.59	**-0.7***	0.33	**0.67***	**0.68***	-0.61	0.21	0.38	-0.41	0.41	0.59
WUE_{inst}	-0.41	-0.62	0.36	0.34	0.23	-0.2	0.42	0.29	-0.06	0.41	0.31
V_{cmax}	0.46	**0.67***	-0.12	**-0.75***	**-0.71***	0.58	0.03	-0.22	0.38	0.27	-0.39
A_{max}	0.04	0.32	0.33	**-0.68***	-0.52	0.3	0.44	0.25	0.02	0.36	-0.07
J_{max}	0.5	**0.73***	-0.18	**-0.75***	**-0.7***	0.57	-0.05	-0.26	0.36	0.29	-0.43
Ψ_{MD}	-0.05	0.03	0.18	-0.35	-0.24	0.07	0.21	0.21	-0.13	0.27	-0.03
Ψ_{PD}	0.18	-0.13	-0.45	0.33	0.17	-0.08	-0.52	-0.33	0.04	-0.3	-0.2
θ_{IAS}	0.06	-0.23	-0.27	0.4	0.14	0	-0.23	-0.27	0.2	-0.06	-0.25
$V_{sp\text{-}cell}/V_{mes\text{-}cell}$	-0.49	-0.41	0.54	0.04	0.21	-0.29	0.5	0.5	-0.32	0.17	0.52
$V_{pa\text{-}cell}/V_{mes\text{-}cell}$	0.36	0.62	-0.17	-0.47	-0.34	0.25	-0.18	-0.14	0.06	-0.09	-0.18
$V_{sp\text{-}cell}/V_{pa\text{-}cell}$	-0.49	-0.59	0.43	0.29	0.3	-0.29	0.43	0.39	-0.21	0.23	0.39
L_{leaf}	-0.02	-0.46	-0.16	0.46	0.12	0.03	-0.07	-0.22	0.28	-0.15	-0.18
L_{mes}	0.05	-0.39	-0.23	0.43	0.08	0.09	-0.13	-0.29	0.34	-0.19	-0.25
$SA_{sp\text{-}cell}/SA_{mes\text{-}cell}$	-0.49	-0.41	0.54	0.04	0.21	-0.29	0.5	0.5	-0.32	0.17	0.52
$SA_{pa\text{-}cell}/SA_{mes\text{-}cell}$	0.36	0.62	-0.17	-0.47	-0.34	0.25	-0.18	-0.14	0.06	-0.09	-0.18
$SA_{pa+sp\text{-}cell}/SA_{mes\text{-}cell}$	-0.06	0.23	0.27	-0.4	-0.14	0	0.23	0.27	-0.2	0.06	0.25

	T_{WAQ}	T_{CQ}	P	P_{WEM}	P_{DM}	PCV	P_{WQ}	P_{DQ}	P_{WAQ}	P_{CQ}
E	0	-0.42	0.38	-0.59	**0.77***	**-0.83***	-0.51	**0.77***	-0.44	0.57
A	0.6	0.06	-0.04	-0.65	0.31	-0.6	**-0.68***	0.33	**-0.76***	0.07
C_i	-0.05	-0.47	0.58	-0.42	**0.83***	**-0.81***	-0.31	**0.81***	-0.23	**0.67***
g_s	0.3	-0.2	0.3	-0.55	0.61	-0.75*	-0.5	0.62	-0.49	0.43
WUE_i	0.08	0.48	-0.58	0.41	**-0.83***	**0.8***	0.31	**-0.81***	0.22	**-0.67***
WUE_{inst}	0.34	0.36	**-0.83***	-0.24	**-0.68***	0.39	-0.39	**-0.67***	-0.5	**-0.81***
V_{cmax}	0.14	-0.31	0.08	-0.5	0.43	-0.61	-0.53	0.4	-0.52	0.21
A_{max}	0.54	0.13	0.05	-0.5	0.37	-0.55	-0.59	0.37	**-0.71***	0.07
J_{max}	0.06	-0.36	0.16	-0.45	0.48	-0.59	-0.47	0.44	-0.42	0.27
Ψ_{MD}	0.28	0.13	-0.12	-0.46	0.23	-0.33	-0.52	0.24	-0.58	0
Ψ_{PD}	-0.54	-0.29	-0.11	-0.1	0.06	0.05	0.01	0.09	0.16	0.2
θ_{IAS}	-0.3	-0.19	-0.62	-0.31	-0.38	0.23	-0.38	-0.45	-0.23	-0.6
$V_{sp\text{-}cell}/V_{mes\text{-}cell}$	0.47	0.51	-0.07	0.27	-0.31	0.27	0.2	-0.26	-0.05	-0.24
$V_{pa\text{-}cell}/V_{mes\text{-}cell}$	-0.08	-0.23	**0.75***	0.11	**0.69***	-0.49	0.25	**0.72***	0.29	**0.86***
$V_{sp\text{-}cell}/V_{pa\text{-}cell}$	0.36	0.44	-0.51	0.06	-0.6	0.46	-0.07	-0.6	-0.23	**-0.7***
L_{leaf}	-0.15	-0.12	**-0.83***	-0.48	-0.49	0.21	-0.56	-0.53	-0.49	**-0.7***
L_{mes}	-0.21	-0.2	**-0.8***	-0.49	-0.46	0.18	-0.56	-0.5	-0.47	**-0.68***
$SA_{sp\text{-}cell}/SA_{mes\text{-}cell}$	0.47	0.51	-0.07	0.27	-0.31	0.27	0.2	-0.26	-0.05	-0.24
$SA_{pa\text{-}cell}/SA_{mes\text{-}cell}$	-0.08	-0.23	**0.75***	0.11	**0.69***	-0.49	0.25	**0.72***	0.29	**0.86***
$SA_{pa+sp\text{-}cell}/SA_{mes\text{-}cell}$	0.3	0.19	0.62	0.31	0.38	-0.23	0.38	0.45	0.23	0.6

Pearson correlation coefficients between the absolute values of the physiological and anatomical variables and geoclimatic data for nine *Vitis* accessions under well-watered treatment were calculated using mean values (±SE, n = 4). Bold indicates statistical significance at $p < 0.05$.

variations across regions may influence photosynthesis even during drought. mean diurnal range displayed negative correlations with most physiological parameters, indicating that greater temperature fluctuations throughout the day may adversely affect plant performance. Stabilizing temperature conditions may be favorable for plant growth and

photosynthesis. isothermality displayed a moderate negative correlation (-0.49) with the photosynthetic parameters (E and A_n), indicating that regions with less temperature variation tend to have higher photosynthetic rates during drought. temperature seasonality demonstrated a significant positive correlation (0.48) with the photosynthetic parameters (E and A_n), suggesting that areas with pronounced temperature seasonality may experience increased photosynthesis during drought. C_i was positively correlated (0.48) with longitude and (0.17) with latitude, indicating a relationship between geographical position and CO_2 concentration within plant leaf intercellular spaces during drought. g_s showed a positive correlation (0.31) with latitude and (0.48) with longitude, suggesting that geographical factors may influence stomatal conductance during drought. $WUE_i$and inst displayed negative correlations with several geoclimatic variables, implying that these parameters are sensitive to climatic conditions and may decrease under drought stress. V_{cmax}, maximum assimilation rate at saturating CO_2 (A_{max}), and J_{max} exhibited various correlations with geoclimatic variables, indicating that these photosynthetic parameters are influenced by geographical and climatic factors during drought. Porosity was positively correlated with latitude and negatively correlated with longitude, implying that geographical factors may influence leaf tissue θ_{IAS} during drought. $V_{pa\text{-}cell}/V_{mes\text{-}cell}$ exhibit a strong positive correlation (0.70) with annual precipitation, indicating that areas with higher annual precipitation tend to have a larger volume proportion of mesophyll palisade cells during drought. ($V_{sp\text{-}cell}/V_{mes\text{-}cell}$, $V_{pa\text{-}cell}/V_{mes\text{-}cell}$, and $V_{sp\text{-}cell}/V_{pa\text{-}cell}$ exhibited complex correlations with geoclimatic variables. These ratios may reflect adaptations in leaf anatomy that balance the demands of photosynthesis and water conservation.

Effects of physiological parameters under well-watered conditions

Table 7 illustrates the significant correlations among the physiological parameters under well-watered conditions. These associations reveal effective water management strategies for vines to support growth and photosynthesis.

E shows positive relationships with the key parameters A_n, C_i, g_s, WUE_i, and A_{max}. This indicates that vines tend to increase E when water is abundant. Higher E rates facilitate CO_2 uptake (A_n) and maintain optimal C_i levels while optimizing stomatal conductance. These adjustments ensure efficient gas exchange and preserve adequate Ψ_{MD}, thereby maximizing photosynthesis and growth when water is plentiful.

A_n positively correlates with various parameters, including E, g_s, and A_{max}. These associations suggest that grapevines actively enhance their photosynthesis under well-watered conditions. They increase A_n while maintaining an efficient g_s.

TABLE 6 Pearson correlation coefficients between geoclimate variables and physiological and anatomical parameters under drought conditions.

	Lat	Long	T	MDR	Isoth.	TCV	$T_{max\text{-}WAM}$	$T_{min\text{-}CM}$	TAR	T_{WEQ}	T_{DQ}
E	0.35	0.51	-0.07	-0.39	-0.49	0.48	0.12	-0.18	0.41	0.28	-0.36
A	0.33	0.36	-0.08	-0.27	-0.46	0.49	0.12	-0.22	0.48	0.05	-0.37
C_i	0.17	0.48	0.09	-0.46	-0.33	0.23	0.17	0.09	0.02	0.39	-0.12
g_s	0.31	0.48	-0.01	-0.41	-0.47	0.44	0.16	-0.11	0.33	0.24	-0.31
WUE_i	-0.04	-0.45	-0.24	0.4	0.22	-0.11	-0.28	-0.22	0.09	-0.64	-0.1
WUE_{inst}	-0.18	-0.49	-0.08	0.45	0.34	-0.24	-0.16	-0.07	-0.04	-0.4	0.13
V_{cmax}	0.39	0.48	-0.12	-0.36	-0.52	0.54	0.1	-0.26	0.52	0.18	-0.43
A_{max}	0.3	0.37	-0.05	-0.38	-0.49	0.47	0.12	-0.19	0.42	0.07	-0.37
J_{max}	0.4	0.47	-0.12	-0.38	-0.55	0.57	0.11	-0.28	0.55	0.18	-0.44
Ψ_{MD}	0.45	0.27	-0.48	-0.23	-0.34	0.31	-0.46	-0.42	0.24	-0.35	-0.5
Ψ_{PD}	**0.67***	0.47	-0.62	-0.32	-0.54	0.56	-0.5	-0.63	0.53	-0.3	**-0.75***
θ_{IAS}	0.19	-0.24	-0.42	0.47	0.09	0.11	-0.34	-0.44	0.39	-0.21	-0.37
$V_{sp\text{-}cell}/V_{mes\text{-}cell}$	-0.6	-0.36	0.65	-0.01	0.28	-0.41	0.55	0.64	-0.51	0.24	0.63
$V_{pa\text{-}cell}/V_{mes\text{-}cell}$	0.38	0.63	-0.18	-0.52	-0.38	0.28	-0.17	-0.14	0.07	0	-0.21
$V_{sp\text{-}cell}/V_{pa\text{-}cell}$	-0.6	-0.54	0.55	0.23	0.37	-0.41	0.48	0.52	-0.38	0.23	0.52
L_{leaf}	0.06	-0.36	-0.19	0.33	0	0.14	-0.07	-0.25	0.34	-0.16	-0.27
L_{leaf}	0.13	-0.3	-0.25	0.3	-0.04	0.18	-0.13	-0.31	0.38	-0.19	-0.33
$SA_{sp\text{-}cell}/SA_{mes\text{-}cell}$	-0.6	-0.36	0.65	-0.01	0.28	-0.41	0.55	0.64	-0.51	0.24	0.63
$SA_{pa\text{-}cell}/SA_{mes\text{-}cell}$	0.38	0.63	-0.18	-0.52	-0.38	0.28	-0.17	-0.14	0.07	0	-0.21
$SA_{pa+sp\text{-}cell}/SA_{mes\text{-}cell}$	-0.19	0.24	0.42	-0.47	-0.09	-0.11	0.34	0.44	-0.39	0.21	0.37

	T_{WAQ}	T_{CQ}	P	P_{WEM}	P_{DM}	P CV	P_{WQ}	P_{DQ}	P_{WAQ}	P_{CQ}
E	0.16	-0.23	-0.01	-0.44	0.24	-0.43	-0.47	0.19	-0.37	0.01
A	0.15	-0.25	-0.09	-0.54	0.22	-0.46	-0.56	0.19	-0.46	0.01
C_i	0.23	-0.01	0.37	-0.13	0.42	-0.35	-0.1	0.4	-0.04	0.31
g_s	0.21	-0.18	0.11	-0.43	0.34	-0.48	-0.43	0.31	-0.34	0.14
WUE_i	-0.33	-0.14	-0.35	-0.04	-0.29	0.24	-0.05	-0.3	-0.07	-0.32
WUE_{inst}	-0.22	0.03	-0.35	0.14	-0.41	0.35	0.12	-0.39	0.05	-0.3
V_{cmax}	0.13	-0.3	-0.1	-0.51	0.18	-0.41	-0.54	0.12	-0.43	-0.09
A_{max}	0.17	-0.22	-0.13	-0.51	0.16	-0.41	-0.58	0.11	-0.53	-0.15
J_{max}	0.14	-0.31	-0.13	-0.52	0.15	-0.4	-0.56	0.09	-0.46	-0.13
Ψ_{MD}	-0.39	-0.46	0.02	-0.53	0.48	-0.49	-0.45	0.48	-0.33	0.38
Ψ_{PD}	-0.43	**-0.67***	-0.07	**-0.72***	0.48	-0.58	-0.66	0.44	-0.45	0.24
θ_{IAS}	-0.42	-0.35	**-0.68***	-0.41	-0.38	0.19	-0.45	-0.43	-0.25	-0.55
$V_{sp\text{-}cell}/V_{mes\text{-}cell}$	0.54	0.64	0.06	0.46	-0.29	0.32	0.36	-0.26	0.07	-0.22
$V_{pa\text{-}cell}/V_{mes\text{-}cell}$	-0.07	-0.24	**0.7***	0.01	**0.71***	-0.52	0.15	**0.74***	0.21	**0.84***
$V_{sp\text{-}cell}/V_{pa\text{-}cell}$	0.42	0.56	-0.31	0.29	-0.56	0.49	0.15	-0.56	-0.07	-0.62
L_{leaf}	-0.13	-0.18	**-0.77***	-0.57	-0.37	0.08	-0.65	-0.41	-0.56	-0.63
L_{mes}	-0.19	-0.25	**-0.73***	-0.57	-0.34	0.07	-0.63	-0.38	-0.53	-0.6
$SA_{sp\text{-}cell}/SA_{mes\text{-}cell}$	0.54	0.64	0.06	0.46	-0.29	0.32	0.36	-0.26	0.07	-0.22
$SA_{pa\text{-}cell}/SA_{mes\text{-}cell}$	-0.07	-0.24	**0.7***	0.01	**0.71***	-0.52	0.15	**0.74***	0.21	**0.84***
$SA_{pa+sp\text{-}cell}/SA_{mes\text{-}cell}$	0.42	0.35	**0.68***	0.41	0.38	-0.19	0.45	0.43	0.25	0.55

Pearson correlation coefficients between the absolute values of the physiological and anatomical variables and geoclimatic data for nine *Vitis* accessions under drought treatment were calculated using mean values (±SE, n = 4). Bold indicates statistical significance at $p < 0.05$.

Additionally, these correlations indicate that grapevines optimize A_{max} when water is not limiting, thereby promoting robust growth and carbon fixation.

C_i was positively correlated with E and g_s but negatively correlated with WUE_i. These correlations demonstrate the

ability of vines to regulate internal C_i levels by adjusting transpiration and stomatal conductance for optimal CO_2 uptake when water is readily available. g_s also exhibits positive correlations with WUE_i and A_{max}. These relationships indicate that grapevines prioritize efficient gas exchange, CO_2 assimilation, and growth under well-watered conditions. Furthermore, A_{max} was positively linked to Ψ_{MD} and V_{cmax} showed a strong positive relationship with J_{max}, highlighting their interdependence in supporting photosynthetic processes.

TABLE 7 Pearson correlation coefficients between physiological parameters under well-watered conditions.

	E	A	C_i	g_s	WUE_i	WUE_{inst}	V_{cmax}	A_{max}	J_{max}	Ψ_{MD}	Ψ_{PD}
E		**0.7***	**0.94***	**0.91***	**-0.94***	-0.51	0.29	**0.67***	0.29	0.57	0.08
A	**0.7***		0.59	**0.88***	-0.57	0.07	0.3	**0.82***	0.21	0.57	-0.31
C_i	**0.94***	0.59		**0.87***	**-1***	**-0.67***	0.28	0.57	0.29	0.35	-0.1
g_s	**0.91***	**0.88***	**0.87***		**-0.86***	-0.37	0.19	**0.69***	0.14	0.48	-0.13
WUE_i	**-0.94***	-0.57	**-1***	**-0.86***		**0.68***	-0.28	-0.56	-0.29	-0.35	0.08
WUE_{inst}	-0.51	0.07	**-0.67***	-0.37	**0.68***		-0.01	0.01	-0.08	0.09	-0.15
V_{cmax}	0.29	0.3	0.28	0.19	-0.28	-0.01		0.53	**0.97***	0.18	-0.31
A_{max}	**0.67***	**0.82***	0.57	**0.69***	-0.56	0.01	0.53		0.51	**0.78***	-0.35
J_{max}	0.29	0.21	0.29	0.14	-0.29	-0.08	**0.97***	0.51		0.24	-0.23
Ψ_{MD}	0.57	0.57	0.35	0.48	-0.35	0.09	0.18	**0.78***	0.24		0.22
Ψ_{PD}	0.08	-0.31	-0.1	-0.13	0.08	-0.15	-0.31	-0.35	-0.23	0.22	

Pearson correlation coefficients between the absolute values of the physiological variables for nine *Vitis* accessions under the well-watered treatment were calculated using mean values (±SE, n = 4). Bold indicates statistical significance at $p < 0.05$.

Effects of physiological parameters under drought conditions

Table 8 presents the correlations among the physiological parameters under drought conditions, showing the species' strategies for coping with water scarcity and their impact on various physiological processes. E exhibited strong positive correlations with A_n, g_s, V_{cmax}, A_{max}, and J_{max}. These correlations indicate that grapevines intensify transpiration in response to drought stress, potentially by cooling leaves and maintaining water transport. This led to an increase in A_n, optimized g_s, and efficient water use. The positive relationship with J_{max} suggests that enhanced electron transport sustains photosynthesis under drought conditions.

C_i was positively correlated with E, A_n, g_s, WUE_i, and A_{max}. This suggests that grapevines adjust C_i levels by modifying transpiration, stomatal conductance, and photosynthesis to optimize CO_2 uptake under drought stress conditions.

g_s demonstrated strong positive correlations E, A_n, WUE_i, V_{cmax}, A_{max}, and J_{max}. This indicates that grapevines aim to maintain efficient gas exchange and photosynthetic activity under drought conditions by regulating the stomatal conductance. WUE_i showed negative correlations with E, A_n, C_i (significant), g_s, WUE_{inst}, V_{cmax}, J_{max}. These relationships

highlight a trade-off between water conservation and photosynthesis. Grapevines with higher WUE_i tended to have reduced transpiration, stomatal conductance, and photosynthesis, potentially as an adaptation to drought stress.

E was strongly positively correlated with WUE_{inst}, indicated by a correlation coefficient of 0.69*. This positive relationship suggests that, as grapevines increase their transpiration rates under drought stress, they also enhance their water-use efficiency. g_s displayed a strong positive correlation with WUE_{inst} (0.80*). This correlation implies that grapevines efficiently use available water for photosynthesis when stomata are open, allowing for gas exchange. This suggests that grapevines carefully regulate stomatal conductance to optimize their water-use efficiency, under drought conditions.

In contrast, WUE_i showed a strong negative correlation with WUE_{inst} (-0.80*). This negative relationship indicates a tradeoff between WUE_i (which represents the ratio of carbon gain to water loss within the leaf) and WUE_{inst}. Grapevines with higher WUE_i may reduce transpiration and stomatal conductance to conserve water but might limit their photosynthetic capacity in the short term.

TABLE 8 Pearson correlation coefficients between physiological parameters under drought conditions.

	E	A	C_i	g_s	WUE_i	WUE_{inst}	V_{cmax}	A_{max}	J_{max}	Ψ_{MD}	Ψ_{PD}
E		**0.9***	0.66	**0.95***	-0.52	**-0.69***	**0.96***	**0.86***	**0.92***	0.14	0.53
A	**0.9***		0.45	**0.91***	-0.26	-0.47	**0.89***	**0.87***	**0.83***	0.25	0.54
C_i	0.66	0.45		**0.78***	**-0.83***	**-1***	0.49	0.34	0.4	0.23	0.41
g_s	**0.95***	**0.91***	**0.78***		-0.58	**-0.8***	**0.86***	**0.77***	**0.78***	0.27	0.57
WUE_i	-0.52	-0.26	**-0.83***	-0.58		**0.84***	-0.3	-0.07	-0.23	-0.12	-0.16
WUE_{inst}	**-0.69***	-0.47	**-1***	**-0.8***	**0.84***		-0.51	-0.36	-0.43	-0.23	-0.43
V_{cmax}	**0.96***	**0.89***	0.49	**0.86***	-0.3	-0.51		**0.94***	**0.99***	0.01	0.47
A_{max}	**0.86***	**0.87***	0.34	**0.77***	-0.07	-0.36	**0.94***		**0.94***	0.03	0.45
J_{max}	**0.92***	**0.83***	0.4	**0.78***	-0.23	-0.43	**0.99***	**0.94***		-0.07	0.41
Ψ_{MD}	0.14	0.25	0.23	0.27	-0.12	-0.23	0.01	0.03	-0.07		**0.84***
Ψ_{PD}	0.53	0.54	0.41	0.57	-0.16	-0.43	0.47	0.45	0.41	**0.84***	

Pearson correlation coefficients between the absolute values of the physiological variables for nine *Vitis* accessions under the drought treatment were calculated using mean values (±SE, n = 4). Bold indicates statistical significance at $p < 0.05$.

Effects of anatomical parameters under well-watered conditions

Several anatomical parameters of leaf tissues exhibited various correlations under well-watered conditions. Porosity was moderately negatively correlated with $V_{sp\text{-}cell}/\ V_{mes\text{-}cell}$ (-0.5), $V_{pa\text{-}cell}/\ V_{mes\text{-}cell}$ (-0.65), $SA_{sp\text{-}cell}/\ SA_{mes\text{-}cell}$ (-0.5), and $SA_{pa\text{-}cell}/\ SA_{mes\text{-}cell}$ (-0.65). This indicates that as θ_{IAS} increased, the ratios of $V_{sp\text{-}cell}/\ V_{mes\text{-}cell}$, $V_{pa\text{-}cell}/\ V_{mes\text{-}cell}$, $SA_{sp\text{-}cell}/\ SA_{mes\text{-}cell}$, and $SA_{pa\text{-}cell}/\ SA_{mes\text{-}cell}$ tended to decrease. Conversely, θ_{IAS} is positively correlated with L_{leaf} (0.83*) and L_{mes} (0.85*), suggesting that as θ_{IAS} increases, leaf and mesophyll widths also tend to increase. The

correlation of θ_{IAS} with $SA_{pa\text{-}cell+sp\text{-}cell}$/ $SA_{mes\text{-}cell}$ is -1*, indicating a perfect inverse relationship. $V_{sp\text{-}cell}$/ $V_{mes\text{-}cell}$, which represents the ratio of $V_{sp\text{-}cell}$/ $V_{mes\text{-}cell}$, exhibits a moderate negative correlation with θ_{IAS} (-0.5). This has a strong positive correlation with $V_{pa\text{-}cell}$/ $V_{mes\text{-}cell}$ (0.74*), indicating a robust positive relationship between these two parameters. Additionally, it has strong negative correlations with $SA_{sp\text{-}cell}$/ $SA_{mes\text{-}cell}$ (-1*) and $SA_{pa\text{-}cell}$/ $SA_{mes\text{-}cell}$ (-0.86*), signifying an inverse relationship. $V_{pa\text{-}cell}$/ $V_{mes\text{-}cell}$, representing the ratio of $V_{pa\text{-}cell}$/ $V_{mes\text{-}cell}$, shows a strong negative correlation with $V_{sp\text{-}cell}$/ $V_{mes\text{-}cell}$ (-0.86*). It also displayed strong negative correlations with θ_{IAS} (-0.65) and $SA_{pa\text{-}cell}$/ $SA_{mes\text{-}cell}$ (-0.81*), indicating that as $V_{pa\text{-}cell}$/ $V_{mes\text{-}cell}$ increased, θ_{IAS} and $SA_{pa\text{-}cell}$/ $SA_{mes\text{-}cell}$ tended to decrease. $V_{sp\text{-}cell}$/ $V_{pa\text{-}cell}$ has a moderate negative correlation with θ_{IAS} (0.2) and positive correlations with $V_{sp\text{-}cell}$/ $V_{mes\text{-}cell}$ (0.74*) and $V_{pa\text{-}cell}$/ $V_{mes\text{-}cell}$ (0.45). Leaf width (L_{leaf}) and L_{mes} were strongly positively correlated (0.99*), indicating that as leaf width increased, the mesophyll width also tended to increase. Both parameters are strongly negatively correlated with θ_{IAS}, $V_{sp\text{-}cell}$/ $V_{mes\text{-}cell}$, $V_{pa\text{-}cell}$/ $V_{mes\text{-}cell}$, $SA_{sp\text{-}cell}$/ $SA_{mes\text{-}cell}$, and $SA_{pa\text{-}cell}$/ $SA_{mes\text{-}cell}$, suggesting that, as L_{leaf} and L_{mes} increase, these parameters tend to decrease.

TABLE 9 Pearson correlation coefficients between anatomical parameters under well-watered conditions.

	θ_{IAS}	$V_{sp\text{-}cell}$/ $V_{mes\text{-}cell}$	$V_{pa\text{-}cell}$/ $V_{mes\text{-}cell}$	$V_{sp\text{-}cell}$/ $V_{pa\text{-}cell}$	L_{Leaf}	L_{mes}	$SA_{sp\text{-}cell}$/ $SA_{mes\text{-}cell}$	$SA_{pa\text{-}cell}$/ $SA_{mes\text{-}cell}$	$SA_{pa+sp\text{-}cell}$/ $SA_{mes\text{-}cell}$
θ_{IAS}		-0.5	-0.65	0.2	**0.83***	**0.85***	-0.5	-0.65	**-1***
$V_{sp\text{-}cell}$/ $V_{mes\text{-}cell}$	-0.5		-0.33	**0.74***	-0.12	-0.14	**1***	-0.33	0.5
$V_{pa\text{-}cell}$/ $V_{mes\text{-}cell}$	-0.65	-0.33		**-0.86***	**-0.8***	**-0.81***	-0.33	**1***	0.65
$V_{sp\text{-}cell}$/ $V_{pa\text{-}cell}$	0.2	**0.74***	**-0.86***		0.44	0.45	**0.74***	**-0.86***	-0.2
L_{Leaf}	**0.83***	-0.12	**-0.8***	0.44		**0.99***	-0.12	**-0.8***	**-0.83***
L_{mes}	**0.85***	-0.14	**-0.81***	0.45	**0.99***		-0.14	**-0.81***	**-0.85***
$SA_{sp\text{-}cell}$/ $SA_{mes\text{-}cell}$	-0.5	**1***	-0.33	**0.74***	-0.12	-0.14		-0.33	0.5
$SA_{pa\text{-}cell}$/ $SA_{mes\text{-}cell}$	-0.65	-0.33	**1***	**-0.86***	**-0.8***	**-0.81***	-0.33		0.65
$SA_{pa+sp\text{-}cell}$/ $SA_{mes\text{-}cell}$	**-1***	0.5	0.65	-0.2	**-0.83***	**-0.85***	0.5	0.65	

Pearson correlation coefficients between the absolute values of the anatomical variables for nine *Vitis* accessions under the well-watered treatment using mean values (±SE, n = 4). Bold indicates statistical significance at $p < 0.05$.

Effects of anatomical parameters under drought conditions

Under drought conditions, a new set of correlations was observed among the anatomical parameters, leading to significant changes in the relationships between these variables. First, θ_{IAS} exhibits strong negative correlations with L_{leaf} (0.9*) and L_{mes} (0.91*), indicating that as θ_{IAS} decreases under drought stress, leaf and mesophyll widths tend to increase. This suggests a potential adaptation mechanism by which the leaves become narrower to reduce water loss. Second, the

ratio of $V_{sp\text{-}cell}/ V_{mes\text{-}cell}$ is strongly positively correlated with $V_{pa\text{-}cell}/ V_{mes\text{-}cell}$ (0.83*), implying that, as the proportion of $V_{sp\text{-}cell}/ V_{mes\text{-}cell}$ increases, the proportion of $V_{pa\text{-}cell}/ V_{mes\text{-}cell}$ also tends to increase under drought conditions. This could be a response to optimizing the resource allocation within the leaves. Third, the inverse relationship between $V_{sp\text{-}cell}/ V_{pa\text{-}cell}$ and $V_{pa\text{-}cell}/ V_{mes\text{-}cell}$ continues to be significant under drought conditions (-0.79*). This indicates that the balance between $V_{sp\text{-}cell}/ V_{pa\text{-}cell}$ remains an important aspect of leaf anatomy even when water is limited. Furthermore, L_{leaf} and L_{mes} were highly positively correlated (0.99*), demonstrating a strong association between these two parameters under drought stress. This suggests that leaves tend to maintain a consistent proportion of leaf and mesophyll widths, even when experiencing water scarcity. Finally, the $SA_{pa\text{-}cell+sp\text{-}cell}/ SA_{mes\text{-}cell}$ ratio has a strong inverse relationship with θ_{IAS} (-1*). This implies that, as the combined $SA_{pa\text{-}cell+sp\text{-}cell}/ SA_{mes\text{-}cell}$ decreases, θ_{IAS} tends to increase significantly under drought conditions.

TABLE 10 Pearson correlation coefficients between anatomical parameters under drought conditions.

	θ_{IAS}	$V_{sp\text{-}cell}/ V_{mes\text{-}cell}$	$V_{pa\text{-}cell}/ V_{mes\text{-}cell}$	$V_{sp\text{-}cell}/ V_{pa\text{-}cell}$	L_{leaf}	L_{mes}	$SA_{sp\text{-}cell}/ SA_{mes\text{-}cell}$	$SA_{pa\text{-}cell}/ SA_{mes\text{-}cell}$	$SA_{pa+sp\text{-}cell}/ SA_{mes\text{-}cell}$
θ_{IAS}		-0.56	-0.57	-0.03	**0.9***	**0.91***	-0.56	-0.57	**-1***
$V_{sp\text{-}cell}/ V_{mes\text{-}cell}$	-0.56		-0.36	**0.83***	-0.29	-0.31	**1***	-0.36	0.56
$V_{pa\text{-}cell}/ V_{mes\text{-}cell}$	-0.57	-0.36		**-0.79***	**-0.72***	**-0.72***	-0.36	**1***	0.57
$V_{sp\text{-}cell}/ V_{pa\text{-}cell}$	-0.03	**0.83***	**-0.79***		0.22	0.22	**0.83***	**-0.79***	0.03
L_{leaf}	**0.9***	-0.29	**-0.72***	0.22		**0.99***	-0.29	**-0.72***	**-0.9***
L_{mes}	**0.91***	-0.31	**-0.72***	0.22	**0.99***		-0.31	**-0.72***	**-0.91***
$SA_{sp\text{-}cell}/ SA_{mes\text{-}cell}$	-0.56	**1***	-0.36	**0.83***	-0.29	-0.31		-0.36	0.56
$SA_{pa\text{-}cell}/ SA_{mes\text{-}cell}$	-0.57	-0.36	**1***	**-0.79***	**-0.72***	**-0.72***	-0.36		0.57
$SA_{pa+sp\text{-}cell}/ SA_{mes\text{-}cell}$	**-1***	0.56	0.57	0.03	**-0.9***	**-0.91***	0.56	0.57	

Pearson correlation coefficients between the absolute values of theanatomical variables for 9 *Vitis* accessions under the drought treatment using mean values (±SE, n = 4). Bold indicates statistical significance at $p < 0.05$.

Effects of anatomical parameters on physiological parameters under well-watered conditions

Under well-watered conditions, the transpiration rate exhibited a strong negative correlation with $V_{sp\text{-}cell}/ V_{mes\text{-}cell}$, with a coefficient of approximately -0.52. This suggests that a higher proportion of spongy cells in the mesophyll is associated with reduced transpiration. A_n showed interesting correlations. It had a strong negative correlation with $V_{sp\text{-}cell}/ V_{mes\text{-}cell}$ (approximately -0.52), indicating that a higher proportion of spongy cells in the mesophyll is linked to lower A_n rates. However, it had a weak positive correlation with the ratio of $V_{pa\text{-}cell}/ V_{mes\text{-}cell}$, at approximately 0.41, suggesting that a greater proportion of palisade cells in the mesophyll may positively affect photosynthesis. g_s was strongly negatively correlated with $V_{sp\text{-}cell}/ V_{mes\text{-}cell}$, with a coefficient of approximately -0.38. This implies that

a higher proportion of spongy cells in the mesophyll is associated a with reduced stomatal conductance. Ψ_{MD} was significantly negatively correlated with various anatomical parameters. It is negatively correlated with $V_{sp\text{-}cell}/ V_{mes\text{-}cell}$, $V_{sp\text{-}cell}/ V_{pa\text{-}cell}$, $SA_{sp\text{-}cell}/ SA_{mes\text{-}cell}$, and $SA_{pa\text{-}cell}/ SA_{mes\text{-}cell}$, with coefficients ranging from -0.27 to -0.34. WUE_{inst} had a strong positive correlation with the ratio of $V_{pa\text{-}cell}/ V_{mes\text{-}cell}$ at approximately 0.82.

TABLE 11 Pearson correlation coefficients between anatomical and physiological parameters under well-watered conditions.

	θ_{IAS}	$V_{sp\text{-}cell}/ V_{mes\text{-}cell}$	$V_{pa\text{-}cell}/ V_{mes\text{-}cell}$	$V_{sp\text{-}cell}/ V_{pa\text{-}cell}$	L_{leaf}	L_{mes}	$SA_{sp\text{-}cell}/ SA_{mes\text{-}cell}$	$SA_{pa\text{-}cell}/ SA_{mes\text{-}cell}$	$SA_{pa+sp\text{-}cell}/ SA_{mes\text{-}cell}$
E	0.04	-0.52	0.41	-0.56	-0.02	-0.03	-0.52	0.41	-0.04
A_n	0.14	-0.15	-0.01	-0.05	0.24	0.21	-0.15	-0.01	-0.14
C_i	-0.02	-0.49	0.45	-0.57	-0.16	-0.14	-0.49	0.45	0.02
g_s	0.04	-0.38	0.29	-0.4	0.05	0.03	-0.38	0.29	-0.04
WUE_i	0.01	0.51	-0.46	0.58	0.16	0.14	0.51	-0.46	-0.01
WUE_{inst}	0.33	0.5	**-0.8***	**0.82***	0.62	0.6	0.5	**-0.8***	-0.33
V_{cmax}	-0.17	-0.06	0.24	-0.17	-0.2	-0.15	-0.06	0.24	0.17
A_{max}	0.12	-0.18	0.03	-0.06	0.04	0.02	-0.18	0.03	-0.12
J_{max}	-0.13	-0.17	0.29	-0.24	-0.26	-0.21	-0.17	0.29	0.13
Ψ_{MD}	0.27	-0.34	0.01	-0.13	0.15	0.11	-0.34	0.01	-0.27
Ψ_{PD}	0.05	-0.44	0.33	-0.49	0.03	0	-0.44	0.33	-0.05

Pearson correlation coefficients between the absolute values of the physiological and anatomical variables for nine *Vitis* accessions under the well-watered treatment using mean values (±SE, n = 4). Bold indicates statistical significance at $p < 0.05$.

Effects of anatomical parameters on physiological parameters under drought conditions

Under drought conditions, the transpiration rates exhibited several notable correlations. It had a moderate positive correlation with θ_{IAS} (0.36), suggesting that a higher θ_{IAS} in leaf tissue is associated with increased transpiration. Additionally, the transpiration rate showed a moderate negative correlation with $V_{sp\text{-}cell}/ V_{mes\text{-}cell}$ at -0.50, implying that a higher proportion of spongy cells in the mesophyll was linked to reduced transpiration. A_n also displayed significant correlations under drought stress. It had a moderate positive correlation with θ_{IAS} (0.46), indicating that a higher θ_{IAS} is associated with increased photosynthesis. However, A_n exhibited a strong negative correlation with $V_{sp\text{-}cell}/ V_{mes\text{-}cell}$ (-0.51), suggesting that a higher proportion of spongy cells in the mesophyll was associated with lower A_n rates. C_i showed a significant positive correlation with the ratio of $V_{pa\text{-}cell}/ V_{mes\text{-}cell}$ at 0.49. This suggests that a greater proportion of palisade cells in the mesophyll is associated with higher intercellular CO_2 concentration. Ψ_{MD} displayed a strong negative correlation with various anatomical parameters under drought conditions. It is negatively correlated with $V_{sp\text{-}cell}/ V_{mes\text{-}cell}$, $V_{sp\text{-}cell}/ V_{pa\text{-}cell}$, $SA_{sp\text{-}cell}/ SA_{mes\text{-}cell}$, and $SA_{pa\text{-}cell}/ SA_{mes\text{-}cell}$, with coefficients ranging from -0.18

to -0.76*. These correlations indicate that a higher spongy cell volume, a higher ratio of spongy cells to palisade cells, and higher ratios of the surface area of spongy mesophyll and palisade cells to total mesophyll are associated with reduced Ψ_{MD} under drought stress. WUE_{inst} had a strong negative correlation with e $V_{sp\text{-}cell}/ V_{mes\text{-}cell}$ at -0.67*. This implies that a higher proportion of spongy cells in the mesophyll is associated with increased water-use efficiency under drought conditions. Ψ_{PD} exhibited a strong negative correlation with $V_{sp\text{-}cell}/ V_{mes\text{-}cell}$ at -0.83*. This indicates that a higher proportion of spongy cells in the mesophyll is assiciated with reduced Ψ_{PD} under drought stress.

TABLE 12 Correlations between anatomical and physiological parameters under drought conditions.

	θ_{IAS}	$V_{sp\text{-}cell}/ V_{mes\text{-}cell}$	$V_{pa\text{-}cell}/ V_{mes\text{-}cell}$	$V_{sp\text{-}cell}/ V_{pa\text{-}cell}$	L_{leaf}	L_{mes}	$SA_{sp\text{-}cell}/ SA_{mes\text{-}cell}$	$SA_{pa\text{-}cell}/ SA_{mes\text{-}cell}$	$SA_{pa+sp\text{-}cell}/ SA_{mes\text{-}cell}$
E	0.36	-0.5	0.09	-0.29	0.27	0.28	-0.5	0.09	-0.36
A	0.46	-0.51	-0.01	-0.3	0.43	0.42	-0.51	-0.01	-0.46
C_i	-0.04	-0.45	0.49	-0.41	-0.16	-0.14	-0.45	0.49	0.04
g_s	0.29	-0.56	0.22	-0.4	0.21	0.22	-0.56	0.22	-0.29
WUE_i	0.32	0.32	**-0.67***	0.49	0.48	0.48	0.32	**-0.67***	-0.32
WUE_{inst}	0.01	0.47	-0.48	0.43	0.15	0.13	0.47	-0.48	-0.01
V_{cmax}	0.45	-0.39	-0.12	-0.11	0.41	0.43	-0.39	-0.12	-0.45
A_{max}	0.43	-0.22	-0.27	0.06	0.49	0.51	-0.22	-0.27	-0.43
J_{max}	0.44	-0.3	-0.19	-0.02	0.42	0.45	-0.3	-0.19	-0.44
Ψ_{MD}	0.18	**-0.7***	0.49	**-0.76***	0.15	0.14	-0.7*	0.49	-0.18
Ψ_{PD}	0.49	**-0.83***	0.27	-0.66	0.41	0.44	**-0.83***	0.27	-0.49

Pearson correlation coefficients between the absolute values of the physiological and anatomical variables for nine *Vitis* accessions under the drought treatment using mean values (±SE, n = 4). Bold indicates statistical significance at $p < 0.05$.

4 | DISCUSSION

A significant environmental constraint for plant development and crop yield is a soil water deficit, as water is a crucial element for plant growth, driving several physiological processes such as photosynthesis, nutrient uptake, and transpiration (Boyer, 1982). *Vitis* species can grow over a wide range of biogeoclimatic conditions including extreme temperature and low precipitation(Tomás et al., 2014b). This suggests that they have developed morphological and physiological adaptation mechanisms to tolerate drought (Bohnert et al., 1995).

In this work, physiological and morphological characteristics that differ among species and levels of water availability were identified and strategies of grapevines to tolerate water stress were explored. These results provide a first understanding of the responses of these nine *Vitis* species to water stress and relating their behavior to their habitats in various climatic conditions.

In this potted dry-down experiment, the control and drought conditions were confirmed by the soil moisture values. Major physiological measurements were taken three times during the experiment, leaves were taken for X-ray micro computed tomography imaging and segmentation of leaf and mesophyll traits and most plants were harvested for root and canopy biomass at the end of the experiment. The consistent response of reduced pot water content across all *Vitis* species under drought conditions reflects the universal challenge that water stress poses to plants. The drought-induced water stress of this experiment triggered a range of responses, including stomatal closure, reduced transpiration rates, and alterations in root growth dynamics. Although individual species varied in the degree and speed of these responses, the fundamental need to conserve water resources remained a shared trait. When subjected to water stress, plants exhibit a range of responses including stomatal closure, reduced transpiration rates, and alterations in root growth dynamics. While the timing and magnitude of these responses varied among species, only some species showed significant increase in water use efficiency.

4.1 | Water potentials

Drought reduced water potential (Ψ_{MD} and Ψ_{PD}) in most species. During the initial stages of the experiment, when water was already withheld for 5 days to induce dry-down, certain species exhibited a more pronounced decline in water potential compared to other species. This initial variation in Ψ_{PD} response could be attributed to the species-specific

sensitivity to water scarcity. As the experiment progressed, the initially severe decline in water potential for some species seemed to plateau, showing a less negative water potential towards the end of the experiment, 35 days after the treatment started. This leveling off may suggest an acclimation or adjustment phase in response to prolonged water stress (Flexas et al., 2009). However, for Ψ_{MD} this trend did not show. Ψ_{MD} is measured at a time when transpiration rates are typically at their peak due to maximum sunlight and heat and plants experience the highest water stress. Ψ_{PD} is measured when stomata are mostly closed and before the plants begin active transpiration. Therefore, it is assumed that the plants experience a relative equilibrium with the soil water status (Santesteban et al., 2019). Therefore, the discrepancy between the trends of $\Psi_{PD}$and Ψ_{MD} during the experiment might be due to different plant responses at different times of the day. Additionally, existing literature considers Ψ_{MD} to be less reliable as an indicator of a plant's water status compared to Ψ_{PD} (Rienth and Scholasch, 2019). *V. riparia* (NY1), *V. mustangensis* (T48), and the hybrid (TXNM0821) showed minimal change in water potential over time and maintained their water potential higher, despite water deficit compared to their controls. In particular, *V. cinerea* (b42-34) and *V. vulpina* (V60-96) showed a significant decrease in water potential under drought conditions.

Interestingly, all species experienced a decline in midday water potential under well-watered conditions over the time of the experiment. This could be attributed to the higher water demand for growth. Leaf expansion leads to a higher water loss through transpiration and the higher demand to sustain their turgor pressure can result in a decrease in Ψ_{MD} (Boyer, 1968). However, for Ψ_{PD} an increase was observed. This experiment was conducted in November, which marks the transition from fall to winter in California. Day length, temperature, and other environmental factors can change during this period, potentially affecting plant responses. Although this experiment took place in a greenhouse, changing environmental conditions may also contribute to the observed differences. Bohnert et al. (1995) states, that while the sensitivity and response of species to water potential decreases caused by drought vary, it can be assumed that all plants possess the encoded ability for stress perception, signaling, and response. This variation in different levels of water potential decreases under drought-treated plants was also observed in this study.

According to Deloire et al. (2020), vines are subjected to moderate to severe water deficit if Ψ_{PD} is between -0.5MPa and -0.8MPa, and severe to extreme water deficit (=stress) if it is below -0.8MPa. These thresholds may vary based on the plant's growth stage or the duration of water scarcity; however they provide a general indication of when a plant experiences water stress under field conditions. In this study, all the water-stressed plants had a Ψ_{PD} less than -0.75MPa,

confirming that they were under water stress. It is worth mentioning that the hybrid (TXNM0821) had a less negative water potential compared to the other plants under water stress, despite the fact that the drought-treated plants had the same soil moisture content as the plants of other species. Less negative Ψ with similar soil water content is suggesting more stomatal closure, less transpiration and likely compensating photosynthesis with closing stomata. When looking at the figures 7, 8, and 9, it is interesting that A_{n} and g_{s} slightly decreased for TXNM0821, and WUE_{i} and WUE_{inst} both showed an increase or tend to increase under drought (compared to their control). Furthermore, stomata response controls leaf temperature. This suggests that the hybrid (TXNM0821) sustains its hydraulics and photosynthetic capacity among the highest of all species under stress by partial stomata closure.

A study found that certain cultivars of *Vitis vinifera* varied in their regulation of stomatal aperture in response to drought. Isohydric species maintain a consistent water potential in water-stressed plants, similar to well-watered plants, or their plant water status will not drop below a certain value, showing more sensitive control compared to anisohydric plants (Schultz, 2003). It is possible that some of the species studied could be classified as isohydric. However, it is noted that using the binary system to classify different species oversimplifies their responses (Levin et al., 2020), as some species are able to adjust their stomatal response based on changes in soil moisture (Domec and Johnson, 2012; Collins et al., 2010). However, the explanation for anisohyric or isohydric plant behavior is not solely due to stomatal control (Scharwies and Tyerman, 2017; Chaumont and Tyerman, 2014). Therefore, further investigation into the hydraulic conductance of root and xylem networks is necessary to accurately classify the species studied based on their iso-/anisohydric behavior.

4.2 | Biomass

Variations in water use and biomass allocation among species highlight the importance of selecting drought-tolerant varieties for grapevine cultivation in arid and water-scarce regions. However, there is a lack of information on the role of root systems in drought tolerance compared to above-ground responses (Alsina et al., 2010). Furthermore, the mechanisms by which plants allocate carbon to different tissues are not fully understood (Comas et al., 2005). Water limitation decreased canopy growth in all species but most significantly in *V. arizonica* (b40-14). Additionally, water limitation led to the greatest decrease in root growth in *V. arizonica* (b40-14) and *V. rupestris* (Vru42). When plants experience water deficits, their root growth slows, and there are significant apoplastic barriers that block hydraulic pathways (Steudle, 2000). Adjusting root-to-shoot ratios is a central concept highlighted in literature that allows plants

to alter their resource allocation in response to available water resources (Fort et al., 2017; Lambers and Poorter, 1992). As the root-to-shoot ratio was lower for plants under well-watered conditions, this indicates the reallocation of available carbon resources towards roots or the limitation water stress imposes in canopy growth. This can be a crucial adaptation strategy for the survival in dry conditions (Richards, 1983). It is worth mentioning that the species that showed a significant increase in the shoot-to-root ratio also showed a significant decrease in water potential under drought conditions. This is particularly the case for *V. acerifolia* (9018) and *V. vulpina* (V60-96). These species exhibited lower canopy growth but more consistent root growth than other species under drought conditions. The research by Southey (2017) found that the root system of a vine is well balanced with its canopy size, meaning that larger canopies are accompanied by larger root systems. Interestingly, in the present study, species were found to produce a much larger canopy-to-root ratio under well-watered conditions than other species, indicating that they focus more on canopy growth than on roots. This trend has also been observed under drought conditions. Species with higher root growth had lower canopy growth than the other species. This not only shows under well-watered conditions but is also interesting under drought stress, when it is crucial to explore the soil for available water and having more roots can be very beneficial. Zhu (2002) states that slower growth is an adaptation strategy to low resource availability focusing root development. While fast-growing species may out compete others during high water availability, slower species may develop long-term strategies by investing in enduring organs (Ouédraogo et al., 2013) to build an extensive root system to deal better with the dry growing season of drought events (Bauerle et al., 2008). It should be noted that the composite structure of the roots also affect the regulation of water uptake (Steudle, 2000), which was not investigated in this study. Iacono et al. (1998) even mentions that the characteristics of the root system affect the rate of photosynthesis of grapevine leaves. However, from a viticulture perspective, canopy growth is also important because leaf area is critical for photosynthesis and carbohydrate production. A finding by Blois et al. (2023) also states that when incorporating wild genotypes into breeding programs, they undergo assessments of their agronomic performance, as higher growth rate is a crucial factor in viticulture. *V. arizonica* (b40-14) and *V. rupestris* (Vru42) may be less suitable for drier and warmer regions because of their higher water demand, whereas *V. acerifolia* (9018) and *V. aestivalis* (T52) can be suitable candidate species with greater drought tolerance capacity. Their native habitat showed a relatively high annual mean temperature, a high maximum temperature of the warmest month and lower annual precipitation compared to the other species investigated (Table 2). Drought-induced response and regulation of biomass allocation into shoot and root are associated with

adaptation to the habitat of origin (Oleksyn et al., 2000). Species from drier environment prioritize root growth to support water access through deeper soil, while species from wetter habitats focus on a balanced shoot-root growth ratio to maximize photosynthesis.

4.3 | Photosynthetic Parameters

Plants often respond to water limitation by closing their stomata to minimize transpiration and mitigate water vapor loss (Flexas et al., 2002). The closure of stomata is crucial because it prevents excess water loss through transpiration, which could otherwise result in substantial pressure drops between the soil and leaves, leading to increasingly negative water potentials (Gambetta et al., 2020). The observed reduction in stomatal conductance was consistent across all the species in this study. The interconnectedness of carbon and water physiology in plants is evident owing to the inevitable water vapor loss from the leaves when stomata open to facilitate the uptake of CO_2 from the atmosphere. Significant decline in A_n for all *Vitis* species in this study indicate the negative impacts of drought on photosynthesis through impaired CO_2 capture and biochemical activity in parallel with increased water loss under high evaporative demand. These findings align with the well-established concept that water stress often leads to reduced photosynthetic activity (Tomás et al., 2014b,a). Notably, *V. arizonica* (b40-14) stands out for its low photosynthetic rates compared to those of other species under well-watered and water-stressed conditions. This poor performance suggest a lack of developed drought tolerance mechanisms within this species. Under drought conditions, all species showed a common water-saving response, with reduced transpiration rates. However, their transpiration rates under well-watered conditions vary considerably, indicating species-specific strategies for water use efficiency. Stomatal conductance also varied among species, with *V. mustangensis* (T48) displaying the highest significant reduction under drought conditions compared to their control. This suggests that some species are more sensitive to water stress, and may require optimal water availability to sustain photosynthesis. Variation in stomatal regulation across species under drought conditions has also been reported in the literature (Costa et al., 2012). Inherent differences in photosynthetic capacity were observed among the accessions, with *V. aestivalis* (T52), Hybrid (NY1), and *V. vulpina* (V60-96), indicating their robust photosynthetic capabilities even under water-stressed conditions. This underscores the importance of the genetic diversity within genus *Vitis*. However, what sets some species apart is their ability to adapt and maintain or increase their WUE_i under water deficit conditions as observed in this study. This is a common adaptation strategy under water-stressed conditions. In this study, it was observed that on the middle measurement date, the drought-stressed plants exhibited higher WUE_i (Flexas et al., 2010).

However, there was variation in WUE_i changes over the period of experiments. *V. arizonica* (b40-14), *V. mustangensis* (T48), and *V. rupestris* showed more decrease in WUE_i after 35 days under drought, whereas *V. acerifolia* (9018) and the hybrid (TXNM0821) maintained their WUE_i higher during the same time. Those differences could be explained by natural genetic variation across these genotypes (Flexas et al., 2010), as previously described in *Arabidopsis* Masle et al. (2005). Despite the lower A_n, *V. acerifolia* (9018) and the hybrid (TXNM0821) managed to make more efficient use of the limited water resources available for photosynthesis. Species with high WUE likely possess adaptations that enhance their ability to efficiently capture, transport, and utilize water and carbon resources. These adaptations could include traits such as reduced stomatal conductance, improved water transport mechanisms, or efficient photosynthetic pathways, and, under drought conditions, may result in ongoing productivity. A greater WUE under drought conditions may result in continued productivity (Passioura, 2015; Tomás et al., 2014b) The findings concerning WUE_{inst} indicate that certain species, such as the hybrid (TXNM0821) and *V. acerifolia* (9018), displayed significant differences in their responses to the drought treatment. Notably, drought-stressed plants exhibited higher WUE_{inst} values than their well-watered counterparts, suggesting that under water stress conditions, these species became more efficient in utilizing water for photosynthesis. All these responses observed at the leaf level should be scaled up to the canopy level for a whole-plant performance analysis under water stress, as WUE is related not only to stomatal control and leaf structure but also to many other traits such as biochemical signals and diffusive properties (Costa et al., 2016; Tomás et al., 2014a). This study also highlights the diversity in the C_i responses among species. Some species conserve CO_2 by maintaining low C_i values under both controlled and drought conditions, whereas others exhibit higher C_i values under drought conditions. *V. arizonica* (b40-14), in particular, displays a substantial increase in C_i under drought conditions, indicating a distinct approach to water and CO_2 management. Leaf conductance is strongly positively correlated with the photosynthesis rate, and therefore imposes a strong limitation (Tomás et al., 2014a).

4.4 | Climatic variables and inherent functional diversity

The observed differences in physiological responses between species might result from variations in leaf anatomical traits, which can affect the area of diffusion of CO_2 and the effective diffusion path length (Tomás et al., 2014a). Peguero-Pina et al. (2012) previously reported a correlation between mesophyll porosity and mesophyll conductance in two *Abies* species. According to Koundouras et al. (2008), physiological and morphological tolerance to drought may reflect adaptation potentials for drier conditions. Even under the greenhouse conditions with moderate stress intensity,

the shorter duration of the experiment and the fact that leaves were taken for X-ray imaging shortly after the dry-down, morphological changes, that could drive physiological responses, were observed in this study. Further anatomical adaptations may require more acclimation through extending the duration of the experiment or intensifying drought stress. According to Patakas et al. (2003), photosynthesis is affected by palisade and spongy mesophyll thickness, intercellular air space, and the surface of mesophyll cells exposed to intercellular air spaces per unit leaf area. In this study, was indeed correlated with these parameters, significantly WUE_i to spongy parenchyma cell volume. A study investigating forest species found similar results, mentioning a great genetic variability of those traits across species and drought affecting leaf photosynthetic capacity and anatomic traits linked with light harvesting, water exchange, and CO_2 (Khan et al., 2022). In sugarcane, decreased leaf thickness has been found to be an important marker for drought tolerance as it is beneficial for transpiration (Taratima et al., 2020, 2019). In the present study, no clear trend was observed and the variation in thickness could be related to thickness variation among replications instead of a treatment-induced effect. However, leaf thickness was positively correlated with the major physiological traits, meaning that as leaf thickness decreased, these parameters decreased as well.

Response under well-watered conditions

Latitude and longitude exhibited strong positive correlations with C_i (0.59). This suggests that as one moves closer to the equator (lower latitudes) or longitudinally across regions (east or west), there tends to be an increase in the concentration of CO_2 within the plant leaf intercellular spaces. This intriguing finding may indicate an adaptation to varying environmental conditions driven by geographical factors, implying that certain regions may naturally favor higher CO_2 concentrations within leaves, potentially influencing the A_n rates. Mean Diurnal Range displayed a significant negative correlation with C_i (-0.68*). Regions with larger daily temperature fluctuations tended to have lower C_i. This relationship might occur due to the impact of temperature on g_s which has a strong negative correlation (-0.58) with mean diurnal range. Higher temperatures could lead to increased stomatal closure (lower g_s) as a protective mechanism to conserve water, reducing the entry of CO_2 into the leaf. However, temperature seasonality and C_i were positively correlated (0.62), suggesting that areas with pronounced temperature seasonality over the year tend to have higher CO_2 concentrations within plant leaves. Higher photosynthesis in species from high TCV habitats was related to their greater C_i and CO_2 diffusion inside leaves. While larger daily temperature fluctuations might lead to reduced CO_2

concentrations within plant leaves due to altered stomatal behavior, certain species from environments with higher seasonal temperature variability might possess adaptations that enable them to maintain higher CO_2 concentrations and better CO_2 diffusion inside leaves. J_{max} exhibited a robust positive correlation with longitude, indicating that longitudinal differences across regions impact the electron transport rate. Among the anatomical parameters, Ψ_{MD} exhibited a robust positive correlation with C_i. Higher CO_2 concentrations were associated with greater leaf water potential, highlighting the interconnectedness of physiological and anatomical traits in response to geoclimatic variables.

Response under drought conditions

Latitude displayed a moderate positive correlation with photosynthetic parameters (E (0.35) and A_n (0.33)) under drought conditions, implying that moving closer to the equator may positively affect photosynthesis even in water-limited environments. This suggests that certain geographical regions may naturally promote better photosynthetic performance under drought stress. longitude exhibited a relatively strong positive correlation with photosynthetic parameters (E (0.51) and A_n (0.36)) under drought, indicating that longitudinal variations across regions may have a significant influence on photosynthesis even during water scarcity. Mean diurnal range displayed negative correlations with most physiological parameters under drought except for the two WUE. This suggests that regions with greater temperature fluctuations throughout the day may have adverse effects on plant performance during drought stress. Temperature stability emerges as a crucial factor for maintaining photosynthetic activity in arid conditions. Several other climatic variables, such as isothermality and temperature seasonality exhibited correlations with photosynthetic parameters, emphasizing the influence of climatic conditions on photosynthesis during drought.

4.5 | Drought-induced changes in photosynthetic capacity related to structural and functional changes

Several significant differences in correlations between anatomical and physiological parameters exist between drought and control conditions. Drought conditions often led to stronger correlations, particularly negative ones, between anatomical parameters related to cell proportions in the mesophyll and physiological parameters like transpiration, photosynthesis, water potential, and water-use efficiency. These differences highlight how plant leaf anatomy adapts and influences physiological responses under water stress to cope with water scarcity, ultimately affecting their performance and survival. The species with lower diffusion resistance (e.g. higher θ_{IAS}) benefit from a higher CO_2 diffusion capacity, and exhibit inherently higher performance and biochemical activities (i.e., V_{cmax}). Although leaves with higher θ_{IAS}

tended to have higher transpiration rates E, they had higher photosynthesis rates A_n as well. Comparing A_n-C_i and A_n-C_c curves provides insights into the limitations imposed by diffusion on photosynthesis associated with the drawdown of CO_2 from intercellular airspace (C_i) to the chloroplast (C_c). Species from higher latitudes, higher longitudes and higher temperature seasonality exhibit enhanced performance through increasing V_{cmax} at low CO_2 concentrations, estimated by A_n response to C_c, when RuBisCO is limiting A_n (Figure 9, Table 6). This might be connected to increased resources allocation towards RuBisCO activity (Niinemets et al., 2009; Sharkey et al., 2007), indicating enhanced A_n and greater CO_2 diffusion ability, at lower CO_2 concentrations (Momayyezi et al., 2022b). Greater maximum electron transport rate (J_{max}), determined using the A_n-C_c curve where RuBP-regeneration constrains A_n, was linked to higher θ_{IAS} and increased enzymatic activity during CO_2 fixation and the formation of carbohydrates (e.g., Calvin cycle). This association was observed in species originating from regions with higher latitudes and longitudes, greater temperature variability, and lower variability in precipitation patterns. A_{max} was strongly associated to V_{cmax} and J_{max} (Table 8), supporting greater biochemical and diffusional capacity for species from higher latitudes and longitudes, regions with less precipitation seasonality and higher temperature seasonality which have leaves with more porosity, less spongy mesophyll but more palisade mesophyll. More temperature seasonality lead to higher photosynthesis performance. As longitude increased, palisade mesophyll increased as well. However, there was a strong correlation between palisade mesophyll and both annual precipitation and the driest month's precipitation, indicating that leaves accumulated more palisade mesophyll in regions with higher rainfall. This increase in palisade mesophyll also corresponded to a larger surface area. Plants with more palisade perform less as they show a lower carboxylation capacity. Moreover, areas with higher precipitation tended to have thinner leaves and lower mesophyll porosity possibly affecting diffusion. Therefore, thicker leaves were associated with higher photosynthesis. This study revealed a negative correlation between palisade mesophyll and intrinsic water use efficiency. Understanding the factors affecting water use efficiency becomes particularly challenging due to the simultaneous decrease in A_n and g_s, illustrating the complexity of this trait. These anatomical characteristics in regions with more rainfall resulted in an overall reduced physiological and biochemical performance. Consequently, it is not surprising that species thriving in drier conditions aren't commonly found in the wettest habitats. However, A_n and WUE_i benefited from a higher θ_{IAS}. C_i exhibited a positive correlation with the ratio of $V_{pa\text{-}cell}$/ $V_{mes\text{-}cell}$ suggesting that a higher proportion of palisade cells in the mesophyll is associated with increased C_i levels. This highlights the intricate relationship between anatomical characteristics and physiological plant responses.

Therefore, maintaining a balance between spongy and palisade mesophyll is crucial for optimal plant performance. The results show a strong negative correlation between water potentials and spongy mesophyll. More spongy mesophyll leads to a more negative Ψ_{PD} and lower photosynthetic performance. This relationship was previously observed by Binks et al. (2016), suggesting that thinner spongy mesophyll and higher Ψ_{PD} might indicate enhanced resilience to drought. This study also found a positive association between higher Ψ_{PD} and various photosynthetic parameters as well as a less spongy mesophyll leading to higher photosynthetic performance under drought. *Vitis* leaves with higher spongy mesophyll volume (e.g., less porosity at spongy mesophyll) show lower midday and pre-dawn water potentials (Table 12). Consistent with previous findings, leaves with less porous spongy mesophyll exhibit lower hydraulic conductance, particularly under elevated temperatures and during dehydration (Sack et al., 2015). Dense spongy mesophyll increases hydraulic resistance (i.e., decreases water potential) due to reduced cell-to-cell connectivity, thereby slowing water movement in the liquid phase (Buckley et al., 2015).

It should be pointed out that generalizations regarding results from this study are the result of an individual species' and genotype above- and below-ground response to water deficits. In a commercial vineyard, the grafted scion would have its own response to water deficits. Furthermore, under conditions of climate change, grapevine reproductive growth is not solely influenced by water stress but also depends on various factors, including grapevine cultivars and other environmental factors such as CO_2 levels and temperature (Kizildeniz et al., 2015). Additionally, it is important to acknowledge that many studies investigating the impact of water stress on photosynthesis have been conducted over brief time frames and in controlled environments. Consequently, translating these findings into field conditions throughout the growing season proved to be a complex task (Grassi and Magnani, 2005). However, understanding the mechanisms underlying variations in drought tolerance among grapevine genotypes serves two main purposes. First, it helps in selecting the appropriate plant material for specific climate and production conditions, thereby promoting sustainability. Second, it allows to identify the key traits responsible for these differences, improving the design of methods to develop new drought-resistant grapevine varieties. It is important to remember that grapevines are long-lived crops that can be produced for many decades in changing environments. Collectively, these findings highlight the intricate interplay between geoclimatic variables and plant physiological and anatomical responses. They underscore the significance of geographical location, temperature stability, and other climatic factors in shaping plant adaptation to well-watered and drought conditions.

5 | CONCLUSION

The findings of this study highlight the diverse responses of North American *Vitis* species to drought stress, with implications for their potential use in viticulture, particularly in regions with limited water resources. Grapevine responses to water stress are integrated across physiological, biochemical, and genetic levels. In summary, the present study investigated the responses of various grapevine species to extended water stress, encompassing a wide range of physiological and growth parameters. The results revealed the diverse strategies employed by these species to adapt to the limited water availability. Our results show that water-limiting conditions altered biomass allocation patterns and reduced the overall canopy growth. We also show that water stress consistently led to a reduction in photosynthetic activity, affecting A_{n}, $\mathrm{C_i}$, E, and g_{s}. However, the species separated in their relative functional responses to and ability tolerate water stress. Some species demonstrated remarkable adaptability, maintaining their photosynthetic capacity even under water-deficit conditions. This resilience suggests the natural capacity to balance carbon capture and water conservation. Leaf water potentials, reflecting the plant's hydration status, generally exhibited lower values in drought-stressed groups than in well-watered groups, with *V. acerifolia* (9018) emerging as the species with the highest water potential. Photosynthetic capacity in *Vitis* accessions was associated with leaf anatomical and biochemical components. More water use-efficient species under drought had particular leaf anatomy including thinner leaves with less palisade volume from drier habitats (with less mean palisade), supported by their higher photosynthetic performance (e.g. V_{cmax}, A_{max}, WUE_{i}). Overall, this study underscores the importance of understanding species-specific responses to water stress as this knowledge is vital for sustainable vineyard practices in the face of a changing climate. These findings also emphasize the potential of certain species such as *V. acerifolia* (9018) to contribute to the resilience of vineyards under water-limited conditions. Further research is neccesary to explore the underlying mechanisms of adaptation and opportunities for crossbreeding to enhance drought tolerance in cultivated grapevine varieties and rootstocks. Anatomical adaptations and geoclimatic origins are particularly crucial.

REFERENCES

Alsina, M. M., D. R. Smart, T. Bauerle, F. de Herralde, C. Biel, C. Stockert, C. Negron, and R. Save, 2010: Seasonal changes of whole root system conductance by a drought-tolerant grape root system. *Journal of Experimental Botany*, **62**, no. 1, 99–109, doi:10.1093/jxb/erq247.
URL https://doi.org/10.1093/jxb/erq247

Arnold, C. and A. Schnitzler, 2020: Ecology and genetics of natural populations of north american vitis species used as rootstocks in european grapevine breeding programs. *Frontiers in Plant Science*, doi:10.3389/fpls.2020.00866.

Bartlett, M., G. Sinclair, G. Fontanesi, T. Knipfer, M. A. Walker, and A. Mcelrone, 2021: Root pressure-volume curve traits capture rootstock drought tolerance. *Annals of botany*, **129**, doi:10.1093/aob/mcab132.

Bauerle, T. L., D. R. Smart, W. L. Bauerle, C. Stockert, and D. M. Eissenstat, 2008: Root foraging in response to heterogeneous soil moisture in two grapevines that differ in potential growth rate. *New Phytologist*, **179**, no. 3, 857–866, doi:https://doi.org/10.1111/j.1469-8137.2008.02489.x.
URL https://nph.onlinelibrary.wiley.com/doi/abs/10.1111/j.1469-8137.2008.02489.x

Binks, O., P. Meir, L. Rowland, A. C. L. da Costa, S. S. Vasconcelos, A. A. R. de Oliveira, L. Ferreira, and M. Mencuccini, 2016: Limited acclimation in leaf anatomy to experimental drought in tropical rainforest trees. *Tree Physiology*, **36**, no. 12, 1550–1561, doi:10.1093/treephys/tpw078.
URL https://doi.org/10.1093/treephys/tpw078

Blois, L., M. d. Miguel, P. Bert, N. Girollet, N. Ollat, B. Rubio, V. Segura, K. P. Voss-Fels, J. Schmid, and E. Marguerit, 2023: Genetic structure and first genome-wide insights into the adaptation of a wild relative of grapevine, vitis berlandieri. *Evolutionary Applications*, doi:10.1111/eva.13566.

Bohnert, H. J., D. E. Nelson, and R. G. Jensen, 1995: Adaptations to Environmental Stresses. *The Plant Cell*, **7**, no. 7, 1099–1111, doi:10.1105/tpc.7.7.1099.
URL https://doi.org/10.1105/tpc.7.7.1099

Boyer, J. S., 1968: Relationship of Water Potential to Growth of Leaves 1. *Plant Physiology*, **43**, no. 7, 1056–1062, doi:10.1104/pp.43.7.1056.
URL https://doi.org/10.1104/pp.43.7.1056

— 1982: Plant productivity and environment. *Science*, **218**, no. 4571, 443–448, doi:10.1126/science.218.4571.443.
URL https://www.science.org/doi/abs/10.1126/science.218.4571.443

Briscoe Runquist, R. D., A. J. Gorton, J. B. Yoder, N. J. Deacon, J. J. Grossman, S. Kothari, M. P. Lyons, S. N. Sheth, P. Tiffin, and D. A. Moeller, 2020: Context dependence of local adaptation to abiotic and biotic environments: A quantitative and qualitative synthesis. *The American Naturalist*, **195**, no. 3, 412–431, doi:10.1086/707322, pMID: 32097038.
URL https://doi.org/10.1086/707322

Buckley, T. N., G. P. John, C. Scoffoni, and L. Sack, 2015: How Does Leaf Anatomy Influence Water Transport outside the Xylem? . *Plant Physiology*, **168**, no. 4, 1616–1635, doi:10.1104/pp.15.00731.
URL https://doi.org/10.1104/pp.15.00731

Chaumont, F. and S. D. Tyerman, 2014: Aquaporins: Highly Regulated Channels Controlling Plant Water Relations. *Plant Physiology*, **164**, no. 4, 1600–1618, doi:10.1104/pp.113.233791.
URL https://doi.org/10.1104/pp.113.233791

Chaves, M. M., O. Zarrouk, R. Francisco, J. M. Costa, T. Santos, A. P. Regalado, M. L. Rodrigues, and C. M. Lopes, 2010: Grapevine under deficit irrigation: hints from physiological and molecular data. *Annals of Botany*, **105**, no. 5, 661–676, doi:10.1093/aob/mcq030.
URL https://doi.org/10.1093/aob/mcq030

Collins, M., S. Fuentes, and E. W. R. Barlow, 2010: Partial rootzone drying and deficit irrigation increase stomatal sensitivity to vapour pressure deficit in anisohydric grapevines. *Functional Plant Biology*, doi:10.1071/fp09175.

Comas, L. H., L. J. Anderson, R. M. Dunst, A. N. Lakso, and D. M. Eissenstat, 2005: Canopy and environmental control of root dynamics in a long-term study of concord grape. *New Phytologist*, **167**, no. 3, 829–840, doi:https://doi.org/10.1111/j.1469-8137.2005.01456.x.
URL https://nph.onlinelibrary.wiley.com/doi/abs/10.1111/j.1469-8137.2005.01456.x

Cortés, A. J. and F. López-Hernández, 2021: Harnessing crop wild diversity for climate change adaptation. *Genes*, **12**, no. 5, doi:10.3390/genes12050783.
URL https://www.mdpi.com/2073-4425/12/5/783

Costa, J., M. Ortuño, C. M. Lopes, and M. M. Chaves, 2012: Grapevine varieties exhibiting differences in stomatal response to water deficit. *Functional Plant Biology*, doi:10.1071/fp11156.

Costa, J., M. Vaz, J. Escalona, R. Egipto, C. Lopes, H. Medrano, and M. Chaves, 2016: Modern viticulture in southern europe: Vulnerabilities and strategies for adaptation to water scarcity. *Agricultural Water Management*, **164**, 5–18, doi:https://doi.org/10.1016/j.agwat.2015.08.021, enhancing plant water use efficiency to meet future food production.
URL https://www.sciencedirect.com/science/article/pii/S0378377415300858

Deloire, A., A. Pellegrino, and S. Rogiers, 2020: A few words on grapevine leaf water potential. *IVES Technical Reviews, vine and wine*, doi:10.20870/IVES-TR.2020.3620.

Domec, J.-C. and D. M. Johnson, 2012: Does homeostasis or disturbance of homeostasis in minimum leaf water potential explain the isohydric versus anisohydric behavior of Vitis vinifera L. cultivars? *Tree Physiology*, **32**, no. 3, 245–248, doi:10.1093/treephys/tps013.
URL https://doi.org/10.1093/treephys/tps013

Dry, N., 2007: *Grapevine rootstocks: selection and management for South Australian vineyards*. Lythrum Press.

Fick, S. E. and R. J. Hijmans, 2017: Worldclim 2: new 1-km spatial resolution climate surfaces for global land areas. *International Journal of Climatology*, **37**, no. 12, 4302–4315, doi:https://doi.org/10.1002/joc.5086.
URL https://rmets.onlinelibrary.wiley.com/doi/abs/10.1002/joc.5086

Flexas, J., M. Barón, J. Bota, J.-M. Ducruet, A. Gallé, J. Galmés, M. Jiménez, A. Pou, M. Ribas-Carbó, C. Sajnani, M. Tomàs, and H. Medrano, 2009: Photosynthesis limitations during water stress acclimation and recovery in the drought-adapted Vitis hybrid Richter-110 (V. berlandieri×V. rupestris). *Journal of Experimental Botany*, **60**, no. 8, 2361–2377, doi:10.1093/jxb/erp069.
URL https://doi.org/10.1093/jxb/erp069

Flexas, J., J. Bota, J. Escalona, B. Sampol, and H. Medrano, 2002: Effects of drought on photosynthesis in grapevines under field conditions: An evaluation of stomatal and mesophyll limitations. *Functional Plant Biology - FUNCT PLANT BIOL*, **29**, doi:10.1071/PP01119.

Flexas, J., J. Galmés, A. Gallé, J. Gulías, A. Pou, M. Ribas-Carbi, M. Tomàs, and H. Medrano, 2010: Improving water use efficiency in grapevines: potential physiological targets for biotechnological improvement. *Australian Journal of Grape and Wine Research*, **16**, no. s1, 106–121, doi:https://doi.org/10.1111/j.1755-0238.2009.00057.x.

URL https://onlinelibrary.wiley.com/doi/abs/10.1111/j.1755-0238.2009.00057.x

Fort, K., J. Fraga, D. Grossi, and M. A. Walker, 2017: Early measures of drought tolerance in four grape rootstocks. *Journal of the American Society for Horticultural Science*, **142**, 36–46, doi:10.21273/JASHS03919-16.

Gambetta, G. A., J. C. Herrera, S. Dayer, Q. Feng, U. Hochberg, and S. D. Castellarin, 2020: The physiology of drought stress in grapevine: towards an integrative definition of drought tolerance. *Journal of Experimental Botany*, **71**, no. 16, 4658–4676, doi:10.1093/jxb/eraa245.

URL https://doi.org/10.1093/jxb/eraa245

Granett, J., B. Bisabri-Ershadi, and J. Carey, 1983: Life tables of phylloxera on resistant and susceptible grape rootstocks. *Entomologia Experimentalis et Applicata*, **34**, no. 1, 13–19, doi:https://doi.org/10.1111/j.1570-7458.1983.tb03284.x.

URL https://onlinelibrary.wiley.com/doi/abs/10.1111/j.1570-7458.1983.tb03284.x

Grassi, G. and F. Magnani, 2005: Stomatal, mesophyll conductance and biochemical limitations to photosynthesis as affected by drought and leaf ontogeny in ash and oak trees. *Plant, Cell & Environment*, **28**, no. 7, 834–849, doi:https://doi.org/10.1111/j.1365-3040.2005.01333.x.

URL https://onlinelibrary.wiley.com/doi/abs/10.1111/j.1365-3040.2005.01333.x

Hatfield, J. L. and C. Dold, 2019: Water-use efficiency: Advances and challenges in a changing climate. *Frontiers in Plant Science*, **10**, doi:10.3389/fpls.2019.00103.

URL https://www.frontiersin.org/articles/10.3389/fpls.2019.00103

Iacono, F., A. Buccella, and E. Peterlunger, 1998: Water stress and rootstock influence on leaf gas exchange of grafted and ungrafted grapevines1research conducted partly with the financial support of the italian consiglio nazionale delle ricerche, special project raisa, sub-project 2.1. *Scientia Horticulturae*, **75**, no. 1, 27–39, doi:https://doi.org/10.1016/S0304-4238(98)00113-7.

URL https://www.sciencedirect.com/science/article/pii/S0304423898001137

IPCC, 2022: Global warming of 1.5°c: Special report on impacts of global warming of 1.5°c above pre-industrial levels in context of strengthening response to climate change, sustainable development, and efforts to eradicate poverty. doi:10.1017/9781009157940.

Kaltenbach, M., 2023: Code repository: Master thesis. *GitHub repository*.

URL https://github.com/forrestellab/vitisdrought/tree/324d956962d627fe291fdc6b69e66a2216588e49/MS_Kaltenbach

Keller, M., 2010: Managing grapevines to optimise fruit development in a challenging environment: a climate change primer for viticulturists. *Australian Journal of Grape and Wine Research*, **16**, no. s1, 56–69, doi:https://doi.org/10.1111/j.1755-0238.2009.00077.x.

URL https://onlinelibrary.wiley.com/doi/abs/10.1111/j.1755-0238.2009.00077.x

Khan, A., F. Shen, L. Yang, W. Xing, and B. Clothier, 2022: Limited acclimation in leaf morphology and anatomy to experimental drought in temperate forest species. *Biology*, **11**, no. 8, 1186, doi:10.3390/biology11081186.

URL http://dx.doi.org/10.3390/biology11081186

Kikkert, J. R., M. R. Thomas, and B. I. Reisch, 2001: *Grapevine Genetic Engineering*, Springer Netherlands, Dordrecht. 393–410.

URL https://doi.org/10.1007/978-94-017-2308-4_15

Kizildeniz, T., I. Mekni, H. Santesteban, I. Pascual, F. Morales, and J. Irigoyen, 2015: Effects of climate change including elevated co2 concentration, temperature and water deficit on growth, water status, and yield quality of grapevine (vitis vinifera l.) cultivars. *Agricultural Water Management*, **159**, 155–164, doi:https://doi.org/10.1016/j.agwat.2015.06.015.

URL https://www.sciencedirect.com/science/article/pii/S0378377415300299

Koundouras, S., I. T. Tsialtas, E. Zioziou, and N. Nikolaou, 2008: Rootstock effects on the adaptive strategies of grapevine (vitis vinifera l. cv. cabernet–sauvignon) under contrasting water status: Leaf physiological and structural responses. *Agriculture, Ecosystems & Environment*, **128**, no. 1, 86–96, doi:https://doi.org/10.1016/j.agee.2008.05.006.

URL https://www.sciencedirect.com/science/article/pii/S0167880908001448

Lambers, H. and H. Poorter, 1992: Inherent variation in growth rate between higher plants: A search for physiological causes and ecological consequences. *Advances in Ecological Research*, **23**, 187–261, doi:10.1016/S0065-2504(03)34004-8.

Larcher, W., 2003: *Physiological plant ecology: ecophysiology and stress physiology of functional groups*. Springer Science & Business Media.

Lasky, J. R., D. L. Des Marais, J. K. McKay, J. H. Richards, T. E. Juenger, and T. H. Keitt, 2012: Characterizing genomic variation of arabidopsis thaliana: the roles of geography and climate. *Molecular Ecology*, **21**, no. 22, 5512–5529, doi:https://doi.org/10.1111/j.1365-294X.2012.05709.x.

URL https://onlinelibrary.wiley.com/doi/abs/10.1111/j.1365-294X.2012.05709.x

Levin, A. D., L. E. Williams, and M. A. Matthews, 2020: A continuum of stomatal responses to water deficits among 17 wine grape cultivars (vitis vinifera). *Functional Plant Biology*, doi:10.1071/fp19073.

Masle, J., S. Gilmore, and G. Farquhar, 2005: The erecta gene regulates plant transpiration efficiency in arabidopsis. *Nature*, **436**, 866–70, doi:10.1038/nature03835.

Momayyezi, M., A. M. Borsuk, C. R. Brodersen, M. E. Gilbert, G. Théroux-Rancourt, D. A. Kluepfel, and A. J. McElrone, 2022a: Desiccation of the leaf mesophyll and its implications for co2 diffusion and light processing. *Plant, Cell & Environment*, **45**, no. 5, 1362–1381, doi:https://doi.org/10.1111/pce.14287.

URL https://onlinelibrary.wiley.com/doi/abs/10.1111/pce.14287

Momayyezi, M., D. A. Rippner, F. V. Duong, P. V. Raja, P. J. Brown, D. A. Kluepfel, J. M. Earles, E. J. Forrestel, M. E. Gilbert, and A. J. McElrone, 2022b: Structural and functional leaf diversity lead to variability in photosynthetic capacity across a range of juglans regia genotypes. *Plant, Cell & Environment*, **45**, no. 8, 2351–2365, doi:https://doi.org/10.1111/pce.14370.

URL https://onlinelibrary.wiley.com/doi/abs/10.1111/pce.14370

Morano, L. D. and M. A. Walker, 1995: Soils and plant communities associated with three vitis species. *The American Midland Naturalist*, **134**, no. 2, 254–263.

URL http://www.jstor.org/stable/2426296

Niinemets, , A. Díaz-Espejo, J. Flexas, J. Galmés, and C. R. Warren, 2009: Role of mesophyll diffusion conductance in constraining potential photosynthetic productivity in the field. *Journal of Experimental Botany*, **60**, no. 8, 2249–2270, doi:10.1093/jxb/erp036.

URL https://doi.org/10.1093/jxb/erp036

Oleksyn, J., R. Zytkowiak, P. Karolewski, P. B. Reich, and M. G. Tjoelker, 2000: Genetic and environmental control of seasonal carbohydrate dynamics in trees of diverse Pinus sylvestris populations. *Tree Physiology*, **20**, no. 12, 837–847, doi:10.1093/treephys/20.12.837.

URL https://doi.org/10.1093/treephys/20.12.837

Ollat, N., L. Bordenave, J. P. Tandonnet, J. M. Bourisquot, and E. Marguerit, 2016: Grapevine rootstocks: origins and perspectives.

URL https://api.semanticscholar.org/CorpusID:89435528

Ollat, N., E. Marguerit, M. de Miguel, A. Coupel-Ledru, S. J. Cookson, C. van Leeuwen, P. Vivin, P. Gallusci, V. Segura, and E. Duchêne, 2023: Moving towards grapevine genotypes better adapted to abiotic constraints. *Vitis (Special Issue)*, **62**, 67–76, doi:https://doi.org/10.5073/vitis.2023.62.special-issue.67-76.

Ouédraogo, D.-Y., F. Mortier, S. Gourlet-Fleury, V. Freycon, and N. Picard, 2013: Slow-growing species cope best with drought: evidence from long-term measurements in a tropical semi-deciduous moist forest of central africa. *Journal of Ecology*, **101**, no. 6, 1459–1470, doi:https://doi.org/10.1111/1365-2745.12165.

URL https://besjournals.onlinelibrary.wiley.com/doi/abs/10.1111/1365-2745.12165

Padgett-Johnson, M., L. Williams, and M. Walker, 2003: Vine water relations, gas exchange, and vegetative growth of seventeen vitis species grown under irrigated and nonirrigated conditions in california. *Journal of the American Society for Horticultural Science jashs*, **128**, no. 2, 269 – 276, doi:10.21273/JASHS.128.2.0269.

URL https://journals.ashs.org/jashs/view/journals/jashs/128/2/article-p269.xml

Pap, D., A. J. Miller, J. P. Londo, and L. G. Kovács, 2015: Population structure of vitis rupestris, an important resource for viticulture. *American Journal of Enology and Viticulture*, **66**, no. 4, 403–410, doi:10.5344/ajev.2015.15012.

URL https://www.ajevonline.org/content/66/4/403

Passioura, J. B., 2015: The yield of crops in relation to drought. *Physiology and Determination of Crop Yield*, doi:10.2134/1994.physiologyanddetermination.c23.

Patakas, A., G. Kofidis, and A. M. Bosabalidis, 2003: The relationships between co2 transfer mesophyll resistance and photosynthetic efficiency in grapevine cultivars. *Scientia Horticulturae*, doi:10.1016/s0304-4238(02)00201-7.

Peguero-Pina, J. J., J. Flexas, J. Galmés, Niinemets, D. Sancho-Knapik, G. Barredo, D. Villarroya, and E. Gil-Pelegrín, 2012: Leaf anatomical properties in relation to differences in mesophyll conductance to co₂and photosynthesis in two related mediterraneanabiesspecies. *Plant Cell & Environment*, doi:10.1111/j.1365-3040.2012.02540.x.

Riaz, S., D. Pap, J. Uretsky, V. Laucou, J.-M. Boursiquot, L. Kocsis, and M. Andrew Walker, 2019: Genetic diversity and parentage analysis of grape rootstocks. *Theoretical and Applied Genetics*, **132**, 1847–1860.

Richards, D., 1983: *The Grape Root System*, John Wiley & Sons, Ltd, chapter 3. 127–168.

URL https://onlinelibrary.wiley.com/doi/abs/10.1002/9781118060728.ch3

Rienth, M. and T. Scholasch, 2019: State-of-the-art of tools and methods to assess vine water status. *OENO One*, **53**, doi:10.20870/oeno-one.2019.53.4.2403.

Rippner, D. A., P. V. Raja, J. M. Earles, M. Momayyezi, A. Buchko, F. V. Duong, E. J. Forrestel, D. Y. Parkinson, K. A. Shackel, J. L. Neyhart, and A. J. McElrone, 2022: A workflow for segmenting soil and plant x-ray computed tomography images with deep learning in google's colaboratory. *Frontiers in*

Plant Science, **13**, doi:10.3389/fpls.2022.893140.

URL https://www.frontiersin.org/articles/10.3389/fpls.2022.893140

RStudio Team, 2020: Rstudio: Integrated development environment for r.

URL http://www.rstudio.com/

Sack, L., C. Scoffoni, D. M. Johnson, T. N. Buckley, and T. J. Brodribb, 2015: The anatomical determinants of leaf hydraulic function. *Functional and Ecological Xylem Anatomy*, 255–271, doi:10.1007/978-3-319-15783-2_10.

Santesteban, L., C. Miranda, D. Marín, B. Sesma, D. Intrigliolo, J. Mirás-Avalos, J. Escalona, A. Montoro, F. de Herralde, P. Baeza, P. Romero, J. Yuste, D. Uriarte, J. Martínez-Gascueña, J. Cancela, V. Pinillos, M. Loidi, J. Urrestarazu, and J. Royo, 2019: Discrimination ability of leaf and stem water potential at different times of the day through a meta-analysis in grapevine (vitis vinifera l.). *Agricultural Water Management*, **221**, 202–210, doi:https://doi.org/10.1016/j.agwat.2019.04.020.

URL https://www.sciencedirect.com/science/article/pii/S037837741831802X

Scharwies, J. D. and S. D. Tyerman, 2017: Comparison of isohydric and anisohydric vitis vinifera l. cultivars reveals a fine balance between hydraulic resistances, driving forces and transpiration in ripening berries. *Functional Plant Biology*, doi:10.1071/fp16010.

Schultz, H., 2000: Climate change and viticulture: A european perspective on climatology, carbon dioxide and uv-b effects. *Australian Journal of Grape and Wine Research*, **6**, no. 1, 2–12, doi:https://doi.org/10.1111/j.1755-0238.2000.tb00156.x.

URL https://onlinelibrary.wiley.com/doi/abs/10.1111/j.1755-0238.2000.tb00156.x

— 2003: Differences in hydraulic architecture account for near-isohydric and anisohydric behavior of two field-grown vitis vinifera l. cultivars during drought. *Plant, Cell Environment*, **26**, 1393 – 1405, doi:10.1046/j.1365-3040.2003.01064.x.

Serra, I., A. Strever, P. Myburgh, and A. Deloire, 2014: Review: the interaction between rootstocks and cultivars (vitis viniferal.) to enhance drought tolerance in grapevine. *Australian Journal of Grape and Wine Research*, **20**, no. 1, 1–14, doi:https://doi.org/10.1111/ajgw.12054.

URL https://onlinelibrary.wiley.com/doi/abs/10.1111/ajgw.12054

Serrano, A. S., J. Martínez-Gascueña, G. L. Alonso, C. Cebrián-Tarancón, M. D. Carmona, A. Mena, and J. L. Chacón-Vozmediano, 2022: Agronomic response of 13 spanish red grapevine (vitis vinifera l.) cultivars under drought conditions in a semi-arid mediterranean climate. *Agronomy*, **12**, no. 10, doi:10.3390/agronomy12102399.

URL https://www.mdpi.com/2073-4395/12/10/2399

Sharkey, T. D., 2016: What gas exchange data can tell us about photosynthesis. *Plant, Cell & Environment*, **39**, no. 6, 1161–1163, doi:https://doi.org/10.1111/pce.12641.

URL https://onlinelibrary.wiley.com/doi/abs/10.1111/pce.12641

Sharkey, T. D., C. J. Bernacchi, G. D. Farquhar, and E. L. Singsaas, 2007: Fitting photosynthetic carbon dioxide response curves for c3 leaves. *Plant, Cell & Environment*, **30**, no. 9, 1035–1040, doi:https://doi.org/10.1111/j.1365-3040.2007.01710.x.

URL https://onlinelibrary.wiley.com/doi/abs/10.1111/j.1365-3040.2007.01710.x

Southey, J. M., 2017: Root distribution of different grapevine rootstocks on a relatively saline soil. *South African Journal of Enology and Viticulture*, doi:10.21548/13-1-2189.

Steudle, E., 2000: Water uptake by roots: effects of water deficit. *Journal of Experimental Botany*, **51**, no. 350, 1531–1542, doi:10.1093/jexbot/51.350.1531.
URL https://doi.org/10.1093/jexbot/51.350.1531

Taratima, W., T. Ritmaha, N. Jongrungklang, P. Maneerattanarungroj, and N. Kunpratum, 2020: Effect of stress on the leaf anatomy of sugarcane cultivars with different drought tolerance (saccharum officinarum, poaceae). *Revista De Biología Tropical*, doi:10.15517/rbt.v68i4.41031.

Taratima, W., T. Ritmaha, N. Jongrungklang, S. Raso, and P. Maneerattanarungroj, 2019: Leaf anatomical responses to drought stress condition in hybrid sugarcane leaf (saccharum officinarum 'kk3'). *Malaysian Applied Biology*.
URL https://api.semanticscholar.org/CorpusID:228264397

Théroux-Rancourt, G., J. M. Earles, M. E. Gilbert, M. A. Zwieniecki, C. K. Boyce, A. J. McElrone, and C. R. Brodersen, 2017: The bias of a two-dimensional view: comparing two-dimensional and three-dimensional mesophyll surface area estimates using noninvasive imaging. *New Phytologist*, **215**, no. 4, 1609–1622, doi:https://doi.org/10.1111/nph.14687.
URL https://nph.onlinelibrary.wiley.com/doi/abs/10.1111/nph.14687

Théroux-Rancourt, G., M. R. Jenkins, C. R. Brodersen, A. McElrone, E. J. Forrestel, and J. M. Earles, 2020: Digitally deconstructing leaves in 3d using x-ray microcomputed tomography and machine learning. *Applications in Plant Sciences*, **8**, no. 7, e11380, doi:https://doi.org/10.1002/aps3.11380.
URL https://bsapubs.onlinelibrary.wiley.com/doi/abs/10.1002/aps3.11380

Tomás, M., H. Medrano, E. Brugnoli, J. Escalona, S. Martorell, A. Pou, M. Ribas-Carbó, and J. Flexas, 2014a: Variability of mesophyll conductance in grapevine cultivars under water stress conditions in relation to leaf anatomy and water use efficiency. *Australian Journal of Grape and Wine Research*, **20**, no. 2, 272–280, doi:https://doi.org/10.1111/ajgw.12069.
URL https://onlinelibrary.wiley.com/doi/abs/10.1111/ajgw.12069

Tomás, M., H. Medrano, J. M. Escalona, S. Martorell, A. Pou, M. Ribas-Carbó, and J. Flexas, 2014b: Variability of water use efficiency in grapevines. *Environmental and Experimental Botany*, **103**, 148–157, doi:https://doi.org/10.1016/j.envexpbot.2013.09.003, response to abiotic stresses of plants of Mediterranean-type ecosystems.
URL https://www.sciencedirect.com/science/article/pii/S009884721300124X

Zhu, J., 2002: Salt and drought stress signal transduction in plants. *Annual Review of Plant Biology*, doi:10.1146/annurev.arplant.53.091401.143329.

SUPPLEMENTARY DATA

TABLE S 1 *Vitis* species and genotypes used in study, coordinates of the collection location and climate data of their native habitat.

Genotype	Species	Lat	Long	T	MDR	Isoth.	TCV	$T_{max-WAM}$	T_{min-CM}	TAR	T_{WEQ}	T_{DQ}
9018	acerifolia	34.0083	-100.282	16.5	15	38	853.6	35.8	-3.5	39.3	25.2	5.2
T52	aestivalis	30.6327	-97.6772	19.2	12.4	38	705	35	2.5	32.5	23.1	10.9
b40-14	arizonica	27.4525	-107.712	15.5	18.1	59	438.6	30.6	0	30.6	20.3	14.9
b42-34	cinerea	25.1085528	-99.8062	22.1	13.9	48	516	35.9	7.1	28.8	25.7	15.1
T48	mustangensis	30.7592	-98.7003	18.8	14.5	41	720.9	35.6	0.7	34.9	22.9	9.1
NY1	riparia	43.841723	-73.387025	7.2	12.3	29	996.8	27.8	-13.6	41.4	18.4	-5
TXNM0821	hybrid (*V. riparia* x *V. arizonica*)	35.6689	-105.3361	6.7	16.8	47	667.1	25.2	-10.5	35.7	14.8	-0.4
Vru42	rupestris	37.76774	-90.3835	12.4	13.1	34	892.4	31.4	-6.9	38.3	12.4	0.4
V60-96	vulpina	40.380579	-75.032293	10.7	11.7	32	877	29.5	-6.8	36.3	21	-0.8

Genotype	Species	T_{WAQ}	T_{CQ}	P	P_{WEM}	P_{DM}	PCV	P_{WQ}	P_{DQ}	P_{WAQ}	P_{CQ}
9018	acerifolia	27.3	5.2	565	83	17	49	213	61	191	61
T52	aestivalis	27.9	9.8	837	114	43	31	278	163	182	163
b40-14	arizonica	20.9	9.9	891	226	10	92	549	45	503	128
b42-34	cinerea	28.2	15.1	849	180	19	68	393	65	297	65
T48	mustangensis	27.7	9.1	701	101	30	35	240	113	179	113
NY1	riparia	19.5	-6.3	919	104	53	18	275	172	273	178
TXNM0821	hybrid (*V. riparia* x *V. arizonica*)	15.5	-1.5	526	100	21	60	251	69	244	69
Vru42	rupestris	23.6	0.4	1105	117	62	18	330	215	290	215
V60-96	vulpina	21.9	-0.8	1172	117	75	12	329	254	325	254

Geoclimate data for 9 *Vitis* accessions. Bold indicates significance at $p < 0.05$.

Abbreviations: Lat, Latitude; Long, Longitude; AMT, Annual Mean Temperature; MDR, Mean Diurnal Range; Isoth., Isothermality; T CV, Temperature Seasonality; $T_{max-WAM}$, Maximum Temperature of Warmest Month; T_{min-CM}, Minimum Temperature of Coldest Month; TAR, Temperature Annual Range; T_{WEQ}, Mean Temperature of Wettest Quarter ; T_{DQ}, Mean Temperature Driest Quarter; T_{WAQ}, Mean Temperature Warmest Quarter; T_{CQ}, Mean Temperature Coldest Quarter; P, Annual Precipitation; P_{WEM}, Precipitation of Wettest Month; P_{DM}, Precipitation of Driest Month; P CV, Precipitation Seasonality; P_{WQ}, Precipitation Wettest Quarter; P_{DQ}, Precipitation Driest Quarter; P_{WAQ}, Precipitation Warmest Quarter; P_{CQ}, Precipitation Coldest Quarter.

TABLE S 2 Analysis of variance (ANOVA) of the main and effects and interaction effects of biomass parameters.

W_{tot}	Df	Sum Sq	Mean Sq	F value	Pr(>F)
Species	8	190.62	23.83	6.90	0.0000
Treatment	1	1185.13	1185.13	343.43	0.0000
Species:Treatment	8	75.90	9.49	2.75	0.0105
Residuals	72	248.46	3.45		
m_{root}					
Species	8	2472.51	309.06	20.19	0.0000
Treatment	1	189.05	189.05	12.35	0.0008
Species:Treatment	8	123.61	15.45	1.01	0.4370
Residuals	71	1086.91	15.31		
m_{canopy}					
Species	8	11517.80	1439.73	9.54	0.0000
Treatment	1	35240.26	35240.26	233.45	0.0000
Species:Treatment	8	5090.45	636.31	4.22	0.0004
Residuals	71	10717.60	150.95		
m_{canopy}/m_{root}					
Species	8	9.85	1.23	4.49	0.0002
Treatment	1	14.35	14.35	52.41	0.0000
Species:Treatment	8	6.47	0.81	2.95	0.0067
Residuals	70	19.17	0.27		
A_{leaf}					
Species	8	170261040.39	21282630.05	16.57	0.0000
Treatment	1	504391871.13	504391871.13	392.75	0.0000
Species:Treatment	8	113942174.82	14242771.85	11.09	0.0000
Residuals	34	43664316.54	1284244.60		
A_{leaf}/W_{tot}					
Species	8	868752.48	108594.06	2.80	0.0170
Treatment	1	809854.47	809854.47	20.88	0.0001
Species:Treatment	8	545712.14	68214.02	1.76	0.1204
Residuals	34	1318795.55	38788.10		
m_{canopy}/W_{tot}					
Species	8	63.61	7.95	4.48	0.0002
Treatment	1	12.28	12.28	6.91	0.0105
Species:Treatment	8	16.35	2.04	1.15	0.3409
Residuals	71	126.07	1.78		
m_{root}/W_{tot}					
Species	8	76.59	9.57	2.64	0.0136
Treatment	1	172.49	172.49	47.57	0.0000
Species:Treatment	8	41.01	5.13	1.41	0.2058
Residuals	71	257.45	3.63		

TABLE S 3 Analysis of variance (ANOVA) of the main and effects and interaction effects of morphological parameters.

θ_{IAS}	Df	Sum Sq	Mean Sq	F value	Pr(>F)
Species	8	0.29	0.04	58.67	0.0000
Treatment	1	0.00	0.00	3.44	0.0691
Species:Treatment	8	0.03	0.00	5.99	0.0000
Residuals	53	0.03	0.00		
$V_{sp\text{-}cell}/ V_{mes\text{-}cell}$					
Species	8	0.22	0.03	53.92	0.0000
Treatment	1	0.01	0.01	10.78	0.0018
Species:Treatment	8	0.03	0.00	7.14	0.0000
Residuals	53	0.03	0.00		
$V_{pa\text{-}cell}/ V_{mes\text{-}cell}$					
Species	8	0.23	0.03	43.23	0.0000
Treatment	1	0.01	0.01	21.89	0.0000
Species:Treatment	8	0.01	0.00	2.58	0.0185
Residuals	53	0.04	0.00		
$V_{sp\text{-}cell}/ V_{pa\text{-}cell}$					
Species	8	4.06	0.51	36.78	0.0000
Treatment	1	0.32	0.32	23.10	0.0000
Species:Treatment	8	0.62	0.08	5.59	0.0000
Residuals	53	0.73	0.01		
L_{leaf}					
Species	8	66426.22	8303.28	58.19	0.0000
Treatment	1	173.76	173.76	1.22	0.2748
Species:Treatment	8	1805.38	225.67	1.58	0.1527
Residuals	53	7562.90	142.70		
L_{mes}					
Species	8	49419.50	6177.44	54.73	0.0000
Treatment	1	159.13	159.13	1.41	0.2404
Species:Treatment	8	1661.75	207.72	1.84	0.0899
Residuals	53	5981.99	112.87		
$SA_{sp\text{-}cell}/ SA_{mes\text{-}cell}$					
Species	8	0.22	0.03	53.92	0.0000
Treatment	1	0.01	0.01	10.78	0.0018
Species:Treatment	8	0.03	0.00	7.14	0.0000
Residuals	53	0.03	0.00		
$SA_{pa\text{-}cell}/ SA_{mes\text{-}cell}$					
Species	8	0.23	0.03	43.23	0.0000
Treatment	1	0.01	0.01	21.89	0.0000
Species:Treatment	8	0.01	0.00	2.58	0.0185
Residuals	53	0.04	0.00		
$SA_{pa\text{-}cell+sp\text{-}cell}/ SA_{mes\text{-}cell}$					
Species	8	0.29	0.04	58.67	0.0000
Treatment	1	0.00	0.00	3.44	0.0691
Species:Treatment	8	0.03	0.00	5.99	0.0000
Residuals	53	0.03	0.00		

TABLE S 4 Analysis of variance (ANOVA) of the main and effects and interaction effects of physiological parameters for first measurement date.

A_n	Df	Sum Sq	Mean Sq	F value	Pr(>F)
Species	8	907.64	113.46	7.44	0.0000
Treatment	1	18.55	18.55	1.22	0.2723
Species:Treatment	8	66.68	8.34	0.55	0.8197
Residuals	129	1968.39	15.26		
C_i					
Species	8	57021.23	7127.65	7.40	0.0000
Treatment	1	1426.42	1426.42	1.48	0.2258
Species:Treatment	8	11710.63	1463.83	1.52	0.1564
Residuals	129	124246.30	963.15		
g_s					
Species	8	0.31	0.04	5.13	0.0000
Treatment	1	0.01	0.01	1.86	0.1745
Species:Treatment	8	0.04	0.01	0.70	0.6895
Residuals	127	0.95	0.01		
E					
Species	8	172.54	21.57	4.23	0.0002
Treatment	1	4.86	4.86	0.95	0.3307
Species:Treatment	8	57.68	7.21	1.42	0.1959
Residuals	129	657.00	5.09		
T_{leaf}					
Species	8	16.19	2.02	3.12	0.0030
Treatment	1	6.84	6.84	10.56	0.0015
Species:Treatment	8	6.95	0.87	1.34	0.2291
Residuals	127	82.29	0.65		
WUE_i					
Species	8	18.51	2.31	2.29	0.0249
Treatment	1	1.19	1.19	1.18	0.2791
Species:Treatment	8	19.43	2.43	2.41	0.0187
Residuals	129	130.12	1.01		
WUE_{inst}					
Species	8	26676.68	3334.58	7.11	0.0000
Treatment	1	276.55	276.55	0.59	0.4441
Species:Treatment	8	4655.32	581.91	1.24	0.2811
Residuals	127	59590.06	469.21		
Ψ_L					
Species	7	16.56	2.37	1.04	0.4503
Treatment	1	0.20	0.20	0.09	0.7710
Species:Treatment	7	9.11	1.30	0.57	0.7666
Residuals	13	29.58	2.28		

TABLE S 5 Analysis of variance (ANOVA) of the main and effects and interaction effects of physiological parameters for middle measurement date.

A_n	Df	Sum Sq	Mean Sq	F value	Pr(>F)
Species	8	937.10	117.14	10.74	0.0000
Treatment	1	804.40	804.40	73.78	0.0000
Species:Treatment	8	268.14	33.52	3.07	0.0041
Residuals	92	1003.11	10.90		
C_i					
Species	8	61859.49	7732.44	3.98	0.0005
Treatment	1	54152.39	54152.39	27.85	0.0000
Species:Treatment	8	21896.41	2737.05	1.41	0.2047
Residuals	87	169166.89	1944.45		
g_s					
Species	8	0.30	0.04	10.63	0.0000
Treatment	1	0.28	0.28	78.03	0.0000
Species:Treatment	8	0.16	0.02	5.53	0.0000
Residuals	91	0.33	0.00		
E					
Species	8	121.32	15.17	8.08	0.0000
Treatment	1	114.53	114.53	61.01	0.0000
Species:Treatment	8	55.41	6.93	3.69	0.0009
Residuals	92	172.72	1.88		
T_{leaf}					
Species	8	28.60	3.57	1.44	0.1923
Treatment	1	3.18	3.18	1.28	0.2607
Species:Treatment	8	21.73	2.72	1.09	0.3759
Residuals	84	208.60	2.48		
WUE_i					
Species	8	26.74	3.34	1.90	0.0707
Treatment	1	17.90	17.90	10.15	0.0020
Species:Treatment	8	25.23	3.15	1.79	0.0901
Residuals	87	153.38	1.76		
WUE_{inst}					
Species	8	61000.84	7625.10	4.72	0.0001
Treatment	1	47837.14	47837.14	29.61	0.0000
Species:Treatment	8	11820.57	1477.57	0.91	0.5083
Residuals	89	143771.01	1615.40		
Ψ_L					
Species	8	21.60	2.70	1.13	0.3700
Treatment	1	8.96	8.96	3.75	0.0614
Species:Treatment	7	8.50	1.21	0.51	0.8217
Residuals	33	78.88	2.39		

TABLE S 6 Analysis of variance (ANOVA) of the main and effects and interaction effects of physiological parameters for final measurement date.

A_n	Df	Sum Sq	Mean Sq	F value	Pr(>F)
Species	8	445.50	55.69	7.06	0.0000
Treatment	1	2785.80	2785.80	353.03	0.0000
Species:Treatment	8	338.58	42.32	5.36	0.0000
Residuals	155	1223.12	7.89		
C_i					
Species	8	309726.00	38715.75	5.48	0.0000
Treatment	1	130690.86	130690.86	18.50	0.0000
Species:Treatment	8	471524.52	58940.56	8.34	0.0000
Residuals	152	1073962.70	7065.54		
g_s					
Species	8	0.08	0.01	3.91	0.0003
Treatment	1	0.43	0.43	159.33	0.0000
Species:Treatment	8	0.10	0.01	4.61	0.0000
Residuals	157	0.42	0.00		
E					
Species	8	63.73	7.97	4.58	0.0000
Treatment	1	401.26	401.26	230.88	0.0000
Species:Treatment	8	75.99	9.50	5.47	0.0000
Residuals	157	272.86	1.74		
T_{leaf}					
Species	8	48.30	6.04	3.01	0.0037
Treatment	1	28.48	28.48	14.18	0.0002
Species:Treatment	8	38.30	4.79	2.38	0.0189
Residuals	155	311.32	2.01		
WUE_i					
Species	8	138.94	17.37	4.82	0.0000
Treatment	1	55.48	55.48	15.39	0.0001
Species:Treatment	8	137.85	17.23	4.78	0.0000
Residuals	152	548.12	3.61		
WUE_{inst}					
Species	8	163981.62	20497.70	6.07	0.0000
Treatment	1	45317.21	45317.21	13.41	0.0003
Species:Treatment	8	283476.43	35434.55	10.49	0.0000
Residuals	154	520393.51	3379.18		
Ψ_{LWP}					
Species	7	50.83	7.26	1.45	0.2079
Treatment	1	14.49	14.49	2.89	0.0954
Species:Treatment	7	16.76	2.39	0.48	0.8458
Residuals	48	240.41	5.01		